THE ROLES OF MUSE1 AND MUSE15 IN PLANT INNATE IMMUNITY

by

Xiaoou Dong

B.Sc., The University of Hong Kong, 2010

A THESIS SUBMITTED IN PARTIAL FULFILMENT OF
THE REQUIREMENTS FOR THE DEGREE OF

DOCTOR OF PHILOSOPHY

in

The Faculty of Graduate and Postdoctoral Studies

(Botany)

THE UNIVERSITY OF BRITISH COLUMBIA

(Vancouver)

July 2016

Abstract

Nucleotide-binding leucine-rich repeat (NLR) immune receptors play crucial roles in pathogen recognition and defense activation in animals and plants. The immune responses mediated by NLR proteins are tightly regulated in plants so that the host effectively responds to pathogen attack without experiencing autoimmunity. However, the mechanisms underlying this regulation are not fully understood. To better understand this process, a mutant *snc1*-enhancing (MUSE) forward genetic screen was performed in model plant *Arabidopsis thaliana*. This thesis describes the identification and characterization of two genes encoding negative regulators of defense responses, *MUSE1* and *MUSE15*, respectively.

MUSE1 encodes a previously uncharacterized RING domain protein exhibiting E3 ubiquitin ligase activity. It has a close paralog in the *Arabidopsis* genome, which is MUSE2. Albeit both *muse1* and *muse2* single mutants are wild type (WT)-like, the *muse1 muse2* double knockout mutant displays severe autoimmunity, suggesting their overlapping functions in regulating defense. Through epistatic analysis, it was found that the autoimmunity of *muse1 muse2* is fully dependent on SNC1, suggesting that MUSE1 and MUSE2 are specifically involved in the regulation of SNC1-mediated immunity. Genetic and biochemical analyses excluded SNC1, bHLH84 and MOS10 from being potential ubiquitination substrates of MUSE1 and MUSE2, and offered clues to the identity of the substrates of MUSE1 and MUSE2. These findings add to the growing list of characterized E3 ubiquitin ligases involved in the stringent regulation of NLR-mediated immunity.

MUSE15 encodes ADR1-L1, which belongs to the ADR1 helper NLR family. Previous studies have demonstrated that the ADR1 family is required for defense mediated by multiple sensor NLRs. Unexpectedly, loss of *ADR1-L1* enhances immunity-related phenotypes in multiple autoimmune mutants including *snc1*, *cpr1*, *bal* and *lsd1*. This immunity-enhancing effect is not mediated by increased SNC1 protein stability, nor is it fully dependent on the accumulation of defense hormone salicylic acid (SA). Transcriptional analysis revealed an up-regulation of *ADR1* and *ADR1-L2* in the *adr1-L1* background, which may over-compensate the loss of *ADR1-L1*, leading to stronger defense responses. The complex regulation within the ADR1 family extends our knowledge on the interplay among helper NLRs.

Preface

The work described in this thesis is the culmination of research from September 2010 through April 2016. It consists of two separate yet related research projects corresponding to Chapter 2 and Chapter 3.

Chapter 2 - **Two E3 ubiquitin ligases with overlapping functions, MUSE1 and MUSE2, negatively regulate SNC1-mediated plant immunity** was based on the following unpublished manuscript:

Oliver Xiaoou Dong, Kaeli C. M. Johnson, Yuxiang Wu, Yan Huang, Shitou Xia, Xuejin Chen, Yuelin Zhang and Xin Li

- **O.X.D.** and X.L. designed the experiments. **O.X.D.** performed most of the described experiments. Y.W. performed the crude mapping of *muse1-1*. K.C.M.J., Y.H., S.X. and X.C mapped and identified five additional mutant alleles of *muse1*. O.D. and X.L. wrote the manuscript.

Chapter 3 - **TNL-mediated immunity in Arabidopsis requires complex regulation of the redundant *ADR1* gene family** was modified from the following published manuscript:

[†]Oliver Xiaoou Dong, [†]Meixuezi Tong, Vera Bonardi, Farid El Kasmi, Virginia Woloshen, Lisa K. Wünsch, Jeffery L. Dangl and Xin Li. (2016). TNL-mediated immunity in Arabidopsis requires complex regulation of the redundant *ADR1* gene family. *New Phytologist*. 10.1111/nph.13821. Edited by Ken Shirasu.

- **O.X.D.**, M.T., X.L., V. B. and J.L.D. designed the experiments. **O.X.D.** and M.T. performed most of the described experiments. V.W. characterized and mapped *muse15-2*. V.B., F.E.K. and L.K.W. generated the *lsd1-2 adr1-L1* mutant and combinatory mutants between autoimmune mutants and *adr* triple. **O.X.D.**, J.L.D. and X.L. wrote the manuscript. All authors reviewed and edited the manuscript.
- [†]These authors contributed equally to this work.

Table of contents

List of figures

List of abbreviations

35S	a strong plant-specific promoter, originally isolated from cauliflower mosaic virus
a.a.	amino acid
ABA	abscisic acid
ABI1	ABA INSENSITIVE 1
ABRC	Arabidopsis Biological Resource Center
ACRE276	*Avr9/Cf-9 Rapidly Elicited gene 276*, an E3 ubiquitin ligase in tobacco
ACT1	*Actin 1*
ACT7	*Actin 7*
ADP	adenosine diphosphate
ADR1	ACTIVATED DISEASE RESISTANCE 1, a member of the ADR1 helper NLR family
ADR1-L1	ADR1-LIKE 1, a member of the ADR1 helper NLR family
ADR1-L2	ADR1-LIKE 2, a member of the ADR1 helper NLR family
Ala	alanine
ANOVA	analysis of variance
APC	Anaphase Promoting Complex
ATP	adenosine triphosphate
AtUBC8	*Arabidopsis thaliana* UBIQUITIN CONJUGATING ENZYME 8
ATXR7	ARABIDOPSIS TRITHORAX-RELATED7
Avr	avirulence
Avr9	an avirulence effector from *Cladosporium fulvum*
AvrB	Avirulence protein B; an avirulence effector from *Pseudomonas syringae* pv. *Glycinea*
Avr-Pia	an avirulence effector from *Magnaporthe oryzae*
Avr-Pita	an avirulence effector from *Magnaporthe oryzae*
AvrPtoB	an avirulence effector from *Pseudomonas syringae* pv. *tomato*
AvrRpm1	an avirulence effector from *Pseudomonas syringae* pv. *maculicola*

AvrRps4	an avirulence effector from *Pseudomonas syringae* pv. *pisi*
AvrRpt2	an avirulence effector from *Pseudomonas syringae* pv. *tomato*
BAK1	BRI1-ASSOCIATED RECEPTOR KINASE
bHLH84	basic Helix-Loop-Helix 84, a transcription factor in *Arabidopsis thaliana*
BLAST	Basic Local Alignment Search Tool
bon1	*bonzai1*, an autoimmune mutants
bp	base pair
BTB	BR-C, ttk and bab; a common structural domain often involved in protein-protein interaction
CaRING1	*Capsicum annuum* RING1; an E3 ubiquitin ligase in pepper
CBB	Coomassie Brilliant Blue
CC	coiled-coil
CC_R	RPW8-like CC domain
cDNA	complementary DNA
CeBiP	Chitin Elicitor Binding Protein
CERK1	CHITIN ELICITOR RECEPTOR KINASE 1
cfu	colony-forming unit
ChIP-Seq	chomatin immunoprecipitation-sequencing
Chr.	chromosome
chs1	*chilling sensitive 1*, autoimmune mutant of a TIR-NB protein
chs2	*chilling sensitive 2*, autoimmune mutant of a TNL protein
chs3	*chilling sensitive 3*, autoimmune mutant of a TNL with LIM domain
CHYR1	CHY ZINC-FINGER AND RING PROTEIN 1, a RING E3 ligase regulating stomata closure
CNL	coiled-coil NLR protein
COI1	CORONATINE INSENSITIVE 1
Col-0	Columbia-0; an *Arabidopsis thaliana* ecotype; also referred to as wild type in this thesis
CPR1	*CONSTITUTIVE EXPRESSER OF PR GENES 1*
CUL	CULLIN

DDB	UV-DAMAGED DNA-BINDING PROTEIN
DNA	deoxyribonucleic acid
DUB	deubiquitinating enzyme
E1	ubiquitin-activating enzyme
E2	ubiquitin-conjugating enzyme
E2F	a transcription factor family which plays a central role in the regulation of cell cycle progression
E3	ubiquitin ligase
E4	ubiquitin conjugation factor
EBF	EIN3-BINDING F BOX PROTEIN
EDS1	ENHANCED DISEASE SUSCEPTIBILITY 1
eds5	*enhanced disease susceptibility 5*
EDTA	ethylenediaminetetraacetic acid
EFR	EF-TU RECEPTOR
EF-Tu	bacterial Elongation Factor Tu
EIN3	ETHYLENE-INSENSITIVE3, a transcription factor downstream ethylene signalling
EMS	ethyl methanesulfonate; a chemical mutagen
ETI	effector-triggered immunity
Exo70B2	EXOCYST SUBUNIT EXO70 FAMILY PROTEIN B2
flg22	a 22-amino acid sequence of the conserved N-terminal part of flagellin
FLS2	FLAGELLIN-SENSITIVE 2
FW	fresh weight
GA	gibberellic acid
GFP	green fluorescent protein
Glu	glutamate
GST	Glutathione S-transferase
H.a.	*Hyaloperonospora arabidopsidis*
HA	hemagglutinin; an epitope tag with amino acid sequence YPYDVPDYA
HaRxL44	an effector from *Hyaloperonospora arabidopsidis* containing RxLR motif

HECT	Homologous to the E6-AP Carboxyl Terminus; a domain found in HECT-class E3 ubiquitin protein ligases
His	6xHis-tag; an epitope tag often used in recombinant protein purification
HR	hypersensitive response
hrcC-	A type-III secretion-deficient mutant strain of *Pseudomonas syringae* pv. *tomato* DC3000
HSP90	HEAT SHOCK PROTEIN 90, a chaperone protein family
IP-MS	immunoprecipitation-mass spectrum
JA	jasmonic acid
JAZ	JASMONATE-ZIM-DOMAIN PROTEIN
KAc	potassium acetate
kb	kilo-base pair
kDa	kilo-Dalton
L6	a TNL disease resistance protein in *Linum usitatissimum*
LB	lysogeny broth
LeETR4	*Lycopersicon esculentum ETHYLENE RESPONSE 4*, one ethylene receptor gene in tomato
L*er*	Landsberg *erecta*
LHY	LATE ELONGATED HYPOCOTYL
LIM	A protein structural domain that mediate protein-protein interactions, named after their initial discovery in the proteins Lin11, Isl-1 & Mec-3
LPS	lipopolysaccharide
LRR	leucine-rich repeat
lsd1	*lesion simulating disease 1*, an autoimmune mutant exhibiting spontaneous cell death
Lys	lysine
MAP	Mitogen-Activated Protein
MED19a	MEDIATOR SUBUNIT 19a
$MgCl_2$	magnesium chloride
MLA10	*Mildew A10*, encodes a CNL in barley (*Hordeum vulgare*)
MOS	Modifier of *snc1*
MS	Murashige and Skoog; a plant growth medium

MUSE	Mutant, *snc1*-enhancing
NaAc	sodium acetate
NAC1	NAC DOMAIN CONTAINING PROTEIN 1
NB	nucleotide-binding
ARC	adaptor shared by APAF-1, R proteins, and CED-4
NB-LRR	nucleotide-binding, leucine-rich repeat
NDR1	NON-RACE SPECIFIC DISEASE RESISTANCE 1, a key defense component required by CNLs in Arabidopsis
NLR	nucleotide-binding domain leucine-rich repeat protein
NLS	nuclear-localization signal
npr1	*nonexpresser of PR genes 1*
NR	ethylene receptor gene in tomato
NRG1	N REQUIREMENT GENE 1, a CC_R-NB-LRR protein in tobacco, whose function is required by TNL N
NSERC	Natural Sciences and Engineering Research Council of Canada
Nup88	nucleoporin 88kDa, also known as MOS7
OD	optical density
OsCERK1	*Oryza sativa* ELICITOR RECEPTOR KINASE 1
OsRLCK185	*Oryza sativa* RECEPTOR-LIKE CYTOPLASMIC KINASE 185
P.s.m.	*Pseudomonas syringae* pv. *maculicola*
P.s.t.	*Pseudomonas syringae* pv. *tomato*
PAD4	PHYTOALEXIN DEFICIENT 4
PAMP	pathogen-associated molecular pattern
PCR	polymerase chain reaction
PGN	Peptidoglycan
PIN2	PIN-FORMED 2, an auxin efflux carrier in *Arabidopsis thaliana*
Pi-ta	a CNL in *Oryza sativa*
PME	pectin methylesterases
PR	pathogenesis-related
Pro	proline
PRR	pattern recognition receptor

PTI	PAMP-triggered immunity
PUB	PLANT U-BOX
pv	pathovar
qRT-PCR	quantitative reverse transcriptase PCR
R gene	*Resistance* gene
RAR1	REQUIRED FOR MLA12 RESISTANCE 1, a co-chaperone which forms complex with Hsp90
RBX	RING BOX PROTEIN
RGA4	R-GENE ANALOG 4; a CNL in *Oryza sativa*
RIN4	RPM1-INTERACTING PROTEIN 4
RING	Really Interesting New Gene
RING1	encodes a RING finger domain protein
RIPK	receptor interacting protein kinase
RLK	receptor-like kinase
RLP	receptor-like protein
RNA	ribonucleic acid
ROS	Reactive oxygen species
RPM1	RESISTANCE TO *P. SYRINGAE* PV. *MACULICOLA* 1, a CNL
RPP2	RECOGNITION OF *PERONOSPORA PARASITICA* 2, a TNL
RPP4	RECOGNITION OF *PERONOSPORA PARASITICA* 4, a TNL
RPP5	RECOGNITION OF *PERONOSPORA PARASITICA* 5, a TNL
RPS2	RESISTANT TO *P. SYRINGAE* 2, a CNL
RPS4	RESISTANT TO *P. SYRINGAE* 4, a TNL
RPW8	RESISTANCE TO POWDERY MILDEW 8, a untypical CNL, defining member of the CC_R-NB-LRR proteins
RRS1	RESISTANT TO *RALSTONIA SOLANACEARUM* 1, a TNL with WRKY domain
R-SNARE	R-Soluble NSF Attachment Protein Receptor; a family of proteins mediating vesicle fusion
RT-PCR	reverse transcriptase PCR
Rx	RESISTANCE AGAINST POTATO VIRUS X, a CNL
SA	salicylic acid
SCF	SKP1-CULLIN-F-box

SD	standard deviation
SDS	sodium dodecyl sulphate
SDS-PAGE	sodium dodecyl sulfate polyacrylamide gel electrophoresis
SGT1	SUPPRESSOR OF G2 ALLELE OF SKP1, a co-chaperone complexing with Hsp90
SINAT5	an Arabidopsis homologue of the SINA (SEVEN IN ABSENTIA)
SIZ1	SAP (scaffold attachment factor, acinus, PIAS), and Miz1 (Msx2-interacting zinc finger)
SKP1	SUPPRESSOR OF KINETOCHORE PROTEIN 1, a common component of the SCF E3 ubiquitin ligase complex
SLY1	SLEEPY1; an F-box protein that is involved in GA signaling
SNC1	SUPPRESSOR OF *NPR1*, CONSTITUTIVE, 1, a TNL
snc2	*suppressor of npr1, constitutive, 2*, autoimmune mutant of an RLP
SNC4	SUPPRESSOR OF *NPR1*, CONSTITUTIVE, 4, an RLK
SpRing	a RING E3 ligase in *Solanum pimpinellifolium*
SWI/SNF	SWItch/Sucrose Non-Fermentable; is a nucleosome remodeling complex
SYD	SPLAYED; a SWI2/SNF2-like protein
T-DNA	transfer DNA
TIR	Toll/interleukin-1 receptor
TIR1	TRANSPORT INHIBITOR RESPONSE 1
TNL	Toll/interleukin-1 receptor NLR protein
TPR1	TOPLESS-RELATED 1, a transcriptional co-repressor
TRAF	TNF receptor associated factors
TTSS	Type III secretion system
Ub	ubiquitin
UBC	E2 ubiquitin-conjugating enzyme
UTR	untranslated region
VAMP	VESICLE-ASSOCIATED MEMBRANE PROTEIN
WT	wild type
Y2H	yeast two-hybrid

Acknowledgements

I offer my deep gratitude to my supervisor, Dr. Xin Li, for the constant encouragement and inspiration she gave me during my Ph.D. studies. I would also like to thank my committee members Dr. George Haughn, Dr. Jim Kronstad and Dr. Fred Sack, who have kindly spent their time in the past six years in tracking my progress and providing valuable feedback on my research.

The research discussed in this thesis was financially supported by the Natural Sciences and Engineering Research Council of Canada (NSERC), the Michael Smith Laboratories, the UBC Four-Year Fellowship and the UBC Department of Botany William Cooper Endowment Fund.

I greatly appreciate the collaborations with all current and past members from the Li Lab and the Zhang Lab. It was a truly memorable experience to have shared my passion in genetics with my congenial lab mates. I would express my special gratitude to Dr. Fang Xu and Dr. Yu Ti Cheng, both of whom have acted as my role models in science.

I appreciate the insightful discussions on designing and performing experiment offered by Dr. Yuelin Zhang, Dr. Jeffery Dangl, Dr. Vera Bonardi, Dr. Hugo Germain, Dr. Kerstin Kirchsteiger, Dr. Ning Zheng, Dr. Mark Estelle and Dr. Weiman Xing. I also thank Dr. Yuelin Zhang, Dr. Qi Xie, Dr. Xingwang Deng, Dr. Shuhua Yang and The Arabidopsis Biological Resource Centre (ABRC) for generously sharing essential experimental materials.

Dedicated to my beloved parents,

Weihong Sun & Yufan Dong,

for their ever-lasting support
throughout my years of education

1. Introduction

1.1 Plant immunity

In nature, plants are constantly surrounded by a broad spectrum of microbial pathogens. Nevertheless, for a given plant host, few types of pathogens can cause diseases. This is largely because of the existence of three major tiers of defense mechanisms in plants (Dangl and Jones, 2001; Chisholm et al., 2006; Jones and Dangl, 2006). Firstly, physical and chemical barriers prevent a majority of potential pathogens from accessing plant cells (Underwood, 2012; Serrano et al., 2014). Secondly, specialized plasma membrane-localized receptors recognize conserved molecular patterns associated with pathogens and trigger downstream defense activation (Macho and Zipfel, 2014). Thirdly, a collection of highly specific intracellular receptors perceive pathogen-derived effector molecules and trigger more robust defense (Bernoux et al., 2011a; Cui et al., 2015; Li et al., 2015). Equipped with such a multilayered immune system, plants are capable of successfully defending themselves against attacks by pathogens in most cases to prevent diseases (Figure 1.1).

1.1.1 Physical and chemical barriers

Preformed rigid structures in plants serve as the first obstacle to microbial pathogens. The hydrophobic cuticle layer coats the surface of aerial plant organs, preventing many prospective microbial pathogens from reaching the interior of a plant host (Serrano et al., 2014). At the cellular level, the rigid cell wall acts as an additional layer of protection for individual plant cells. In addition, plant cells are able to actively reinforce the cell wall through the deposition of callose beneath sites of pathogen detection, forming thickened structures called papillae (Jacobs et al., 2003).

Besides physical barriers, plants synthesize and secrete diverse secondary metabolites with antimicrobial properties, a process usually enhanced in response to attempted

infection by plant pathogens (Bednarek, 2012). For instance, the indole-type phytochemical camalexin in Arabidopsis has been shown to play a crucial role in defense against bacterial and oomycete pathogens (Glazebrook and Ausubel, 1994; Glazebrook et al., 1997).

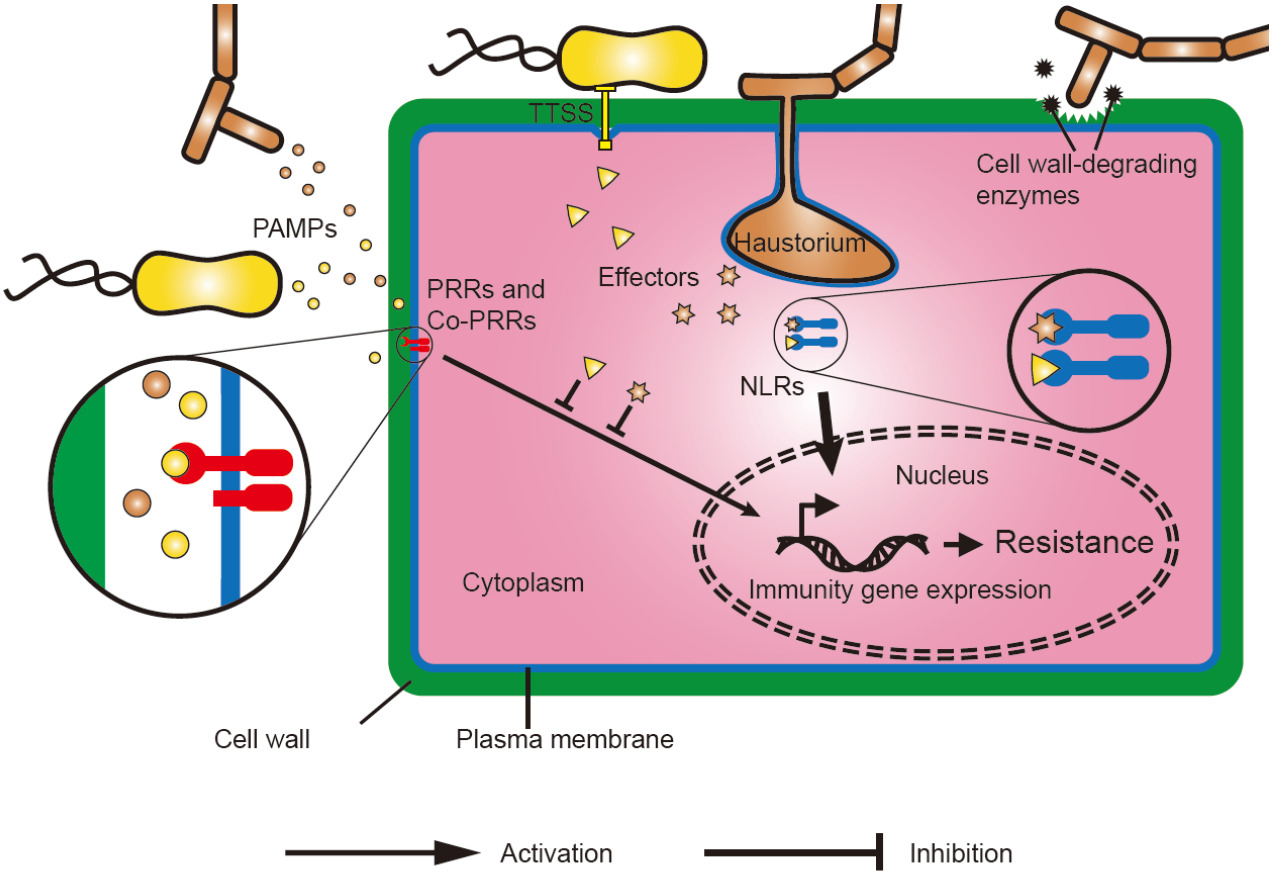

Figure 1.1 The plant immune system.

A schematic diagram illustrating the activation of defense responses within a plant cell. TTSS, type III secretion system; PAMP, pathogen-associated molecular pattern; PRR, pattern-recognition receptor; NLR, nucleotide-binding domain leucine-rich repeat protein.

1.1.2 PAMP-triggered immunity (PTI)

In order to overcome the physical barriers of plant hosts, many successful pathogens have evolved strategies to gain access to the plasma membrane. For example, necrotrophic pathogens often produce wall-degrading enzymes to deconstruct the cell wall, whereas

biotrophic pathogens often rely on penetration or secretory structures such as appressoria or secretion systems to penetrate the physical barriers (Mendgen and Hahn, 2002; Cunnac et al., 2009).

Pathogens usually possess conserved molecular patterns referred to as pathogen-associated molecular patterns (PAMPs). PAMPs are common molecular features shared by microbial plant pathogens across species. Several examples of known PAMPs are flagellin, lipopolysaccharides (LPS), and peptidoglycans (PGNs) from bacteria and chitin from fungi (Monaghan and Zipfel, 2012). Pathogens that overcome the host physical barriers come in proximity to the host protoplasts, often exposing their PAMPs to the corresponding host receptors termed pattern-recognizing receptors (PRRs) on the plasma membrane (Nicaise et al., 2009; Macho and Zipfel, 2014). Upon PAMP recognition, PRRs activate intracellular signal transduction pathways, usually via Mitogen-Activated Protein (MAP) kinase cascades, to turn on downstream defense responses (Tena et al., 2001).

One well-studied PRR in Arabidopsis is FLAGELLIN-SENSITIVE 2 (FLS2), a receptor-like kinase (RLK) with an extracellular leucine-rich repeat (LRR) domain, a transmembrane domain and an intracellular kinase domain (Gomez-Gomez and Boller, 2000). The ligand of FLS2 is flg22, a 22-amino acid peptide from the N-terminus of PAMP flagellin. Upon flg22 treatment, FLS2 triggers a series of phosphorylation events, eventually leading to cellular defense responses. The *fls2* mutants fail to perceive the bacterial elicitor flagellin and thus exhibit enhanced disease susceptibility (Gomez-Gomez and Boller, 2000).

PRRs often function together with co-receptors to transduce signal (Macho and Zipfel, 2014). The chitin receptor Chitin Elicitor Binding Protein (CeBiP) in rice, for example, lacks an intracellular signalling domain (Kaku et al., 2006). Upon chitin perception, CeBiP dimerize and recruits its co-receptor CHITIN ELICITOR RECEPTOR KINASE 1 (OsCERK1), an RLK, to form a protein complex, which is required to trigger cellular anti-fungal defense responses (Shimizu et al., 2010). OsCERK1 is also involved in the perception of PGN by directly interacting with and phosphorylating RECEPTOR-LIKE CYTOPLASMIC KINASE 185

(OsRLCK185). (Yamaguchi et al., 2013). In Arabidopsis, RLK BRI1-ASSOCIATED RECEPTOR KINASE 1 (BAK1) functions as an essential co-receptor for multiple PRRs including FLS2 and EF-TU RECEPTOR (EFR), the receptors of PAMP flg22 and elongation factor (EF)-Tu, respectively (Chinchilla et al., 2007).

The downstream defense responses triggered by PRRs usually include the expression of pathogenesis related (*PR*) genes, callose deposition, stomata closure and the accumulation of defense hormone salicylic acid (SA) (Dodds and Rathjen, 2010). Defense activated through this pathway is often referred to as PAMP-triggered immunity (PTI). Although relatively quick, PTI is weak and often fails to prevent successful pathogens from further colonization (Jones and Dangl, 2006).

1.1.3 Effector-triggered immunity (ETI)

1.1.3.1 Pathogens use effectors to suppress host defense

Over the evolutionary history, an "arms race" exists between plant hosts and plant pathogens (Jones and Dangl, 2006). Plant hosts have evolved defense mechanisms to prevent the development of diseases while successful pathogens have evolved strategies to interfere with defense mechanisms in their corresponding hosts. One of the strategies that is often employed by pathogens is the production and delivery of immunity-suppressing molecules termed effectors (Kamoun, 2007; Cunnac et al., 2009).

Bacterial pathogens are often able to assemble syringe-like secretion structures to transfer effectors. Filamentous pathogens usually form specialized infection structures known as appressoria, which penetrate through cuticles and cell walls. This allows the subsequent development of haustoria, invaginated feeding structures in close contact with the host plasma membrane.

For example, tomato bacterial speck pathogen *Pseudomonas syringae* pv. *tomato* (*P.s.t.*) DC3000 injects effector protein AvrPtoB into the host cells via the type III secretion system (Gohre et al., 2008; Xin and He, 2013). AvrPtoB is an E3 ubiquitin ligase that promotes the ubiquitination and degradation of the PRRs FLS2 and CERK1 in Arabidopsis, thus impairing the host's ability to perceive the corresponding PAMPs (Gohre et al., 2008; Gimenez-Ibanez et al., 2009). Filamentous pathogen *Hyaloperonospora arabidopsidis* (*H.a.*), the causal agent of Downy Mildew in Arabidopsis, secretes the effector HaRxL44 into host cells. HaRxL44 localizes to the nucleus and interacts with the defense component MEDIATOR SUBUNIT 19a (MED19a), leading to its degradation (Caillaud et al., 2013).

Besides protein degradation, effectors may also interfere with host defense through cleavage of host proteins (Shao et al., 2003), protection of PAMPs from host recognition (van den Burg et al., 2006), suppression of stomatal immunity (Lozano-Duran et al., 2014) or other mechanisms (Jones and Dangl, 2006).

1.1.3.2 Plant NLRs perceive effectors and trigger robust defense

As an additional layer of defense, plant resistance (R) proteins recognize their cognate effectors secreted by pathogens and trigger robust defense responses (Chisholm et al., 2006). Hence, effectors that are successfully detected by host R proteins confer disease resistance in the host, and thus are often referred to as avirulence (Avr) proteins. Both *Avr* genes and *R* genes are highly polymorphic as a result of the intense "arms race" between pathogens and their plant hosts (Meyers et al., 2003; Jones and Dangl, 2006). This specific genetic interaction between *Avr* genes and *R* genes was first described by Flor in a classic gene-for-gene model: the matching recognition between the products of a single *Avr* gene from the pathogen and a single *R* gene from the plant host determines the outcome of a certain plant-pathogen interaction (Flor, 1971). Successful recognition of Avr proteins by R proteins often leads to programmed cell death at the site of Avr detection, a process known as the hypersensitive response (HR), increased expression of defense genes and the accumulation of SA (Dangl et al., 2013). If a pathogen strain expresses one

or more *Avr* genes whose products can be recognized by the corresponding R proteins in a specific host, this pathogen is considered avirulent to that host strain. Conversely, a pathogen strain without effectors that are specifically recognized by any R protein in a certain host is considered virulent to that host strain.

The majority of the *R* genes that have been cloned so far encode nucleotide-binding (NB) leucine-rich repeats proteins (NLRs) (Li et al., 2015). NLRs display considerable structural diversity, yet their biological functions are highly similar across plant species (Maekawa et al., 2011a). Based on the two major variant forms at the N terminus, NLRs can be classified into Toll interleukin receptor (TIR) NLRs (TNLs), and coiled-coil (CC) NLRs (CNLs). Genetic analyses in Arabidopsis have revealed that the function of TNLs is strongly dependent on defense components ENHANCED DISEASE SUSCEPTIBILITY 1 (EDS1) and PHYTOALEXIN DEFICIENT 4 (PAD4), whereas that of CNLs often relies on NON-RACE SPECIFIC DISEASE RESISTANCE 1 (NDR1) to function (Aarts et al., 1998). Therefore, at least two distinct signal transduction pathways exist downstream of NLR-mediated defense in *Arabidopsis*.

In some cases, NLRs perceive Avr proteins through direct intermolecular recognition. For example, rice CNL Pi-ta perceives Avr-Pita from rice blast fungus *Magnaporthe grisea* through physical interaction, which leads to resistance to pathogen strains expressing Avr -Pita (Jia et al., 2000). Alternatively, NLRs may perceive Avrs indirectly through detecting the modification of host targets caused by Avrs. Effector perception by guarding host proteins enables a single NLR to recognize multiple structurally diverse Avrs modifying the same targets in the host. For example, Arabidopsis CNL RESISTANCE TO *P. SYRINGAE* PV. *MACULICOLA* 1 (RPM1) guards its interacting protein RPM1-INTERACTING PROTEIN 4 (RIN4) against two sequence-unrelated type III effectors AvrRpm1 and AvrB, both of which manipulate the activity of RIN4 by inducing its phosphorylation by receptor interacting protein kinase (RIPK). Upon AvrRpm1 or AvrB-induced phosphorylation of RIN4, RPM1 is activated and triggers downstream immune responses (Mackey et al., 2002; Chung et al., 2011).

1.1.3.3. Regulation of NLRs

As important components of strong defense in plants, NLRs are under tight regulation at multiple levels to ensure effective immune responses without causing autoimmunity, which usually incurs a fitness cost.

Most NLR-encoding genes are expressed at relatively low levels (Li et al., 2015), yet the regulation of transcription of *NLR* genes plays a crucial role in controlling their defense output. For example, ARABIDOPSIS TRITHORAX-RELATED 7 (ATXR7), an H3K4 methyl transferase, epigenetically regulates the expression of TNL-encoding genes *SNC1* and *RECOGNITION OF PERONOSPORA PARASITICA 4* (*RPP4*). In mutant *atxr7*, the expression of both *SNC1* and *RPP4* is decreased and the disease resistance to pathogen *H.a.* is severely compromised (Xia et al., 2013).

Post-transcriptional regulation also plays important roles in fine-tuning *NLR* expression. It has been shown that Arabidopsis MODIFIER OF SNC1, 4 (MOS4) and MODIFIER OF SNC1, 12 (MOS12) are both required for the proper splicing of *TNL* genes *RESISTANT TO P. SYRINGAE 4* (*RPS4*) and *SNC1*, as loss-of-function mutants *mos4* or *mos12* exhibit altered splicing patterns of TNLs (Xu et al., 2012). Both *mos4* and *mos12* mutants show enhanced disease susceptibility to virulent and avirulent pathogens, suggesting that proper splicing of TNLs is essential to their function (Xu et al., 2012).

Importantly, NLR-mediated defense is under regulation through protein stability control, consistent with the reported correlation between the levels of NLR proteins and the strength of defense responses triggered by these NLRs (Xu et al., 2014a). As an example, Arabidopsis *CONSTITUTIVE EXPRESSER OF PR GENES 1* (*CPR1*) encodes an F-box protein, a subunit of an E3 ubiquitin ligase (Cheng et al., 2011; Gou et al., 2012). CPR1 physically interacts with multiple NLRs including RESISTANT TO *PSEUDOMONAS SYRINGAE* 2 (RPS2) and SNC1, and mediates their ubiquitination and subsequent degradation (Cheng et al., 2011). Knockout mutant *cpr1* over-accumulates SNC1 protein and exhibits autoimmune

phenotypes (Cheng et al., 2011; Gou et al., 2012). On the contrary, overexpressing *CPR1* leads to enhanced disease susceptibility to virulent pathogen *P.s.t.* DC3000 and avirulent pathogen strains *P.s.t.* DC3000 *AvrRpt2*, which produces the cognate effector of RPS2 (Cheng et al., 2011; Gou et al., 2012). Another example of stability control of NLR involves the heat shock protein 90 family (HSP90s) in Arabidopsis. Loss-of-function mutations in HSP90.2 and HSP90.3 lead to increased accumulation of multiple NLRs including SNC1, RPS2 and RPS4 and cause autoimmunity (Huang et al., 2014a). On the other hand, studies have revealed that Arabidopsis HSP90s and their co-chaperones SUPPRESSOR OF G2 ALLELE OF SKP1 (SGT1) and REQUIRED FOR MLA12 RESISTANCE 1 (RAR1) are required for the proper folding of a number of NLRs, a process essential to the function of these NLRs (Shirasu, 2009). These studies on HSP90s suggest a dual role of chaperones in maintaining NLR homeostasis.

The current model states that NLRs are normally kept in an inactive state by intramolecular interactions among different domains. Such conformation is disrupted upon Avr recognition, usually accompanied by an exchange of ADP for ATP at the nucleotide-binding domain, leading to the activation of downstream defense signaling (Padmanabhan and Dinesh-Kumar, 2014). For example, structure-function studies of the potato CNL RESISTANCE AGAINST POTATO VIRUS X (Rx) showed that the intramolecular interaction between the NB and the LRR domain keeps the receptor in an inactive state (Rairdan and Moffett, 2006) and that the overexpression of NB domain without the constraint of LRR causes elicitor-independent programmed cell death (Rairdan et al., 2008).

Emerging evidence indicates that balanced nuclear-cytosolic distribution of NLRs is indispensable for effective defense triggered by some NLRs. Studies on the interaction between Arabidopsis defense regulator EDS1 and NLR RPS4 have demonstrated that forced localization of RPS4 to either the nucleus or the cytosol results in compartment-specific defense branches, suggesting that the coordination of subcellular localization of NLRs is essential in balancing multiple aspects of defense output (Heidrich et al., 2011). Arabidopsis *MODIFIER OF SNC1, 7* (*MOS7*) encodes nucleoporin Nup88, which is involved

in nucleocytoplasmic trafficking. A study of the *mos7* mutant suggests that proper nuclear accumulation of NLR SNC1 is required for its defense outputs (Cheng et al., 2009).

1.1.3.4 Interplay among NLRs

Increasing evidence suggests that multiple NLRs often function together in triggering defense responses (Griebel et al., 2014). Genetic dependence among NLRs has been reported in multiple studies. In some cases, NLRs dimerize or oligomerize with each other as part of their activation process.

Two examples of NLRs that self-associate to form oligomers are TNL L6 in flax (Bernoux et al., 2011b) and CNL MLA10 in barley (Maekawa et al., 2011b). In both cases, the N-terminal domains of the NLRs are capable of homodimerization, which is required for immune signaling. Different NLRs may physically interact as well, as in the case of Arabidopsis TNLs RPS4 and RESISTANT TO *RALSTONIA SOLANACEARUM* 1 (RRS1), which form heterodimer through the N terminal TIR domains (Williams et al., 2014). Additionally, this association was required for the formation of a signalling-competent receptor complex for effector perception (Williams et al., 2014). By contrast, rice NLR RGA5 forms heterodimer through its CC domain with NLR R-GENE ANALOG 4 (RGA4) to restrict RGA4-triggered cell death (Cesari et al., 2014). This restriction is relieved upon binding of Avr-Pia to R-GENE ANALOG 5 (RGA5), which results in cell death activation (Cesari et al., 2013).

The majority of plant NLRs identified thus far fit the canonical gene-for-gene definition of R proteins, which recognize specific Avrs from pathogens. Due to the high level of specificity in R-Avr recognitions, single *R* gene knockout mutants usually have no immune defect beyond susceptibility to the specific pathogen strains expressing the corresponding Avrs. As an exception, a number of NLRs have been reported to be required for defense against multiple virulent and avirulent pathogens. These NLRs are often referred to as helper NLRs for the more general role they play in defense. The ACTIVATED DISEASE

RESISTANCE 1 (ADR1) helper NLR family in Arabidopsis consists of three CNL members with overlapping functions (Bonardi et al., 2011). The *adr1* triple knockout mutant loses disease resistance to multiple virulent pathogens, indicating the central role of the ADR1 family helper NLRs as general defense regulators (Bonardi et al., 2011). Interestingly, in tobacco, N REQUIREMENT GENE 1 (NRG1), a CNL, shows high homology to Arabidopsis ADR1 and is required by disease resistance mediated by TNL N (Peart et al., 2005). Structurally, the N-terminal CC domains of the ADR1 family proteins and the NRG1 family proteins resemble that of *Arabidopsis* RESISTANCE TO POWDERY MILDEW 8 (RPW8) protein (Collier et al., 2011). These two families are thus classified as a special type of CNLs termed CC_R-NB-LRR (Collier et al., 2011). Notably, CC_R-NB-LRRs are exceptionally conserved among various monocot and dicot plant species, suggesting their conserved, ancestral function contrary to that of most canonical NLRs (Collier et al., 2011).

Overall, the complex interplay among plant NLRs reflects their high versatility as immune receptors.

1.2 Identifying novel defense components through forward genetic screens

1.2.1 Autoimmune mutant *snc1* harbors a gain-of-function mutation in a TNL

In Arabidopsis, *SNC1* encodes a TNL whose cognate Avr remains unidentified (Zhang et al., 2003). In autoimmune mutant *snc1*, a gain-of-function mutation causes a Glu to Lys single amino acid substitution between the NB domain and the LRR domain (Zhang et al., 2003). As a consequence, the stability of the SNC1 protein is increased in the *snc1* mutant, leading to constitutively activated defense responses in the plant (Cheng et al., 2011; Gou et al., 2012). In addition to an elevated level of SA, increased expression of defense genes and increased disease resistance to various pathogens, *snc1* mutant plants exhibit dwarfed morphology with curled leaves, a feature commonly found in autoimmune mutants (Li et al., 2001). A positive correlation exists between the extent of the *snc1*-like morphological phenotype and the defense output (Xu et al., 2014a). Hence, such

morphological phenotype serves as a reliable proxy of the strength of defense, enabling efficient genetic screens without pathogen infection experiments.

1.2.2 The MOS genetic screen

Because mutant *snc1* has an identifiable autoimmune morphology, it was used as the genetic background for the modifier of *snc1* (MOS) genetic screen to identify positive defense regulators involved in NLR-mediated defense pathways. In total, 13 novel *MOS* genes were identified from the screen (Johnson et al., 2012), characterized and found to play diverse biological roles such as transcriptional regulation (Li et al., 2010a; Zhu et al., 2010; Xia et al., 2013), RNA processing (Zhang et al., 2005; Palma et al., 2007; Xu et al., 2011; Xu et al., 2012), protein modification (Goritschnig et al., 2007; Goritschnig et al., 2008) and nucleo-cytoplasmic trafficking (Palma et al., 2005; Zhang and Li, 2005; Cheng et al., 2009; Germain et al., 2010). The success of the MOS screen provided us with additional insight into the regulation of NLR-mediated defense in plants.

1.2.3 The MUSE genetic screen

In order to identify novel negative regulators of NLR-mediated defense, the Li Lab performed the mutant, *snc1*-enhancing (MUSE) screen (Huang et al., 2013). In the MUSE screen, mutants exhibiting enhanced *snc1*-like autoimmune phenotypes were searched for within the mutagenized populations, as these individuals are likely to harbor loss-of-function mutations in negative regulators of defense. The two genetic backgrounds used for the screen are *snc1 mos4* and *snc1 mos2 npr1*, both WT-like in morphology yet harbor the gain-of-function mutation in *snc1*, which makes them sensitized genetic backgrounds for the detection of *muse* mutants with enhanced immune phenotypes.

Seeds of *snc1 mos4* or *snc1 mos2 npr1* were mutagenized with chemical mutagen ethyl methanesulfonate (EMS) to randomly introduce single nucleotide mutations into the plant genome. The M2 populations were first screened for mutants that exhibit inheritable *snc1*-

enhancing phenotypes, including the dwarfed morphology and curled leaves. Lines that passed the primary screen were subjected to a secondary screen, in which the expression of the defense marker gene *PR2* and resistance to virulent pathogen *H.a.* Noco2 were monitored. Mutants that were confirmed to display authentic autoimmune phenotypes were named *muse* mutants and further characterized.

From the MUSE screen, loss-of-function alleles of known negative regulatory genes of defense were expectedly identified, such as *bonzai1* (*bon1*), *cpr1* and *siz1* (Hua et al., 2001; Lee et al., 2007; Cheng et al., 2011; Gou et al., 2012). In addition, through the study of various *muse* mutants, novel defense regulatory genes or discovered novel roles of previously reported defense components were identified.

1.2.4 Regulation of NLR-mediated immunity by *MUSE* genes

Of the identified defense components encoded by *MUSE* genes, many affect NLR protein stability, emphasizing the major role in defense regulation played by the modulation of NLR protein levels. *MUSE3* encodes an E4 ubiquitin ligase enhancing the polyubiquitination and protein degradation of NLRs SNC1 and RPS2 (Huang et al., 2014b). Similarly, *MUSE13* and *MUSE14* encode a pair of functionally redundant TNF Receptor Associated Factor (TRAF) domain proteins involved in protein turnover of SNC1 and RPS2 (Huang et al., 2016). *MUSE6* encodes a component of the NatA acetyltransferase complex, which destabilizes SNC1 through acetylation at specific residues at the N-terminus of the NLR (Xu et al., 2015b). *MUSE10* and *MUSE12* each encode an isoform of the chaperone HSP90, which possibly assists the formation of SKP1-CULLIN-F-box (SCF) E3 ubiquitin ligase complexes and facilitates the degradation of NLRs including SNC1, RPS2 and RPS4 (Huang et al., 2014a).

In addition to homeostasis regulation by the aforementioned *MUSE* genes through protein stability control, some other *MUSE* genes are involved in transcriptional and post-transcriptional regulation of *NLR* genes. *MUSE4* encodes a subunit of the RNA Polymerase

III subunit, which is thought to play a specific role in the splicing of *NLR* genes, thus affecting their expression (Johnson et al., 2016). *MUSE9* encodes the SWItch/Sucrose Non-Fermentable (SWI/SNF) chromatin remodeler SPLAYED (SYD), which specifically regulates *SNC1* transcription (Johnson et al., 2015).

Functionally distinct from other characterized *MUSE* genes, *MUSE5* encodes mitochondrial protein AtPAM16, which may prevent autoimmunity by negatively regulating the production of reactive oxygen species (ROS) (Huang et al., 2013).

1.3 Ubiquitination in NLR-mediated immunity

1.3.1 The ubiquitination pathway

Ubiquitination is a common type of eukaryotic post-translational protein modification across kingdoms, in which the small peptide ubiquitin is covalently linked to target proteins. Over the past two decades, ubiquitination has been shown to play a major role in various biological processes in plants, with nearly 6% of the *Arabidopsis* proteome predicted to be ubiquitinated and removed by the 26S proteasome pathway (Vierstra, 2009).

Ubiquitination usually occurs through a cascade involving three key enzymes: an E1 ubiquitin-activating enzyme, an E2 ubiquitin-conjugating enzyme and an E3 ubiquitin ligase (Hershko and Ciechanover, 1998). The process begins with the formation of a thiol-ester bond between a ubiquitin molecule and an E1 ubiquitin-activating enzyme. The ubiquitin moiety associated with the E1 enzyme is then passed to an E2 ubiquitin-conjugating enzyme. Subsequently, an E3 ubiquitin ligase mediates the transfer of the ubiquitin moiety from the E2 enzyme onto the specific target protein to be ubiquitinated, also known as the substrate of that E3 ligase. Often, the entire process repeats itself several times, resulting in the formation of a chain of ubiquitin molecules on the substrate. In some cases, the elongation of the ubiquitin chain on substrates is catalyzed by an

additional E4 ubiquitin ligase (Kravtsova-Ivantsiv et al., 2013). On the other hand, deubiquitinating enzymes (DUBs) catalyze the removal of ubiquitins from ubiquitinated substrates (Neutzner and Neutzner, 2012).

The most common function of ubiquitination is marking substrates for protein degradation mediated by the 26S proteasome (Smalle and Vierstra, 2004). Protein degradation not only plays a housekeeping role in removing abnormal proteins, but also has important function in controlling the amount and activity of short-lived regulatory proteins. In addition, recycling of proteins provides a supply of free amino acids, the raw material for synthesizing new proteins. Perturbation in the ubiquitin-proteasome protein degradation pathway may lead to severe consequences, as exemplified by Alzheimer's disease in humans (Riederer et al., 2011).

During ubiquitination, an isopeptide bond is formed between the C terminal carboxyl group of the ubiquitin molecule to be added, and the ε-amino group of a lysine residue from either the substrate or the growing ubiquitin chain. More recent studies have revealed that the consequence of ubiquitination is highly dependent on the length of the ubiquitin chain (Kravtsova-Ivantsiv and Ciechanover, 2012; Kulathu and Komander, 2012). For example, monoubiquitination is often associated with vesicle trafficking and vacuole-dependent proteolysis (Tian and Xie, 2013). Beside chain length, how the ubiquitin elements in a chain are linked to each other also affects the fate of the ubiquitinated substrate (Chen and Sun, 2009; Kravtsova-Ivantsiv and Ciechanover, 2012; Kulathu and Komander, 2012). There are seven lysine residues on the ubiquitin molecule. Linkage through all the seven lysine residues have been detected in ubiquitin chains *in vivo* (Kulathu and Komander, 2012). For example, ubiquitin chains formed through K48 linkage often lead to 26S proteasome-dependent protein degradation (Kravtsova-Ivantsiv et al., 2013), whereas K63-linked ubiquitin chains have been shown to regulate protein trafficking, transcription activation and DNA repair (Haglund and Dikic, 2005). While E3 ubiquitin ligases play a major role in target specificity, the type of ubiquitin chain formed

in a specific ubiquitination cascade is largely determined by the type of E2 ubiquitin-conjugating enzyme involved (Ye and Rape, 2009).

1.3.2 Types of E3 ubiquitin ligases

The *Arabidopsis* genome encodes 2 E1 enzymes, at least 37 E2 enzymes and over 1500 E3 enzymes (Kraft et al., 2005; Hua and Vierstra, 2011). The hierarchical organization of the E1, E2, E3 enzymes is consistent with the fact the specificity of ubiquitination is predominantly determined by the matching between the E3 ubiquitin ligases and their corresponding substrates.

Based on their structural features, E3 ubiquitin ligases can be divided into classes. Simple E3 ligases include HOMOLOGOUS TO THE E6-AP CARBOXYL TERMINUS (HECT), REALLY INTERESTING NEW GENE (RING) and U-box proteins, all of which function as single proteins, together with E1 and E2, mediating the transfer of ubiquitin onto the corresponding substrates (Cheng and Li, 2012). Notably, HECT E3 ligases form covalent bonds with the ubiquitin moiety as an intermediate form before transferring the ubiquitin to their substrates, a unique feature that is absent in all other types of E3 ubiquitin ligases (Rotin and Kumar, 2009). Complex E3 ubiquitin ligases consist of multiple components that are often Cullin-based (Hua and Vierstra, 2011). Common complex E3 ligases are composed of scaffold proteins RING BOX PROTEIN (RBX), CULLIN1 (CUL1) and SUPPRESSOR OF G2 ALLELE OF SKP1 (SKP1) and an adaptor protein with an F-box domain (Somers and Fujiwara, 2009), which determine substrate specificity. Other classes of complex E3 ubiquitin ligases include CULLIN3 - BR-C, TTK AND BAB (CUL3-BTB), CULLIN4 - UV-DAMAGED DNA-BINDING PROTEIN (CUL4-DDB) and Anaphase Promoting Complex (APC) types (Cheng and Li, 2012).

1.3.3 E3 ubiquitin ligases play diverse roles in plants

Regulation of biological processes through ubiquitination-mediated degradation is fast and accurate. Sessile in nature, plants need to rely on fast cellular responses to environmental stimulations in order to compensate for their lack of motility. It is therefore not surprising that numerous studies on the function of various E3 ubiquitin ligases in plants have revealed their essential and diverse roles in a wide range of biological processes such as hormone responses, circadian rhythms, abiotic stress responses and plant immunity.

E3 ubiquitin ligases play central roles in signaling pathways downstream of various plant hormones in Arabidopsis. The F-box protein TRANSPORT INHIBITOR RESPONSE PROTEIN 1 (TIR1) mediates the ubiquitination and subsequent degradation of transcriptional repressor protein family AUX/IAA in response to the plant growth hormone auxin, leading to the de-repression of the transcription of auxin-responsive genes (Gray et al., 1999; Gray et al., 2001). In a similar fashion, in the presence of jasmonic acid (JA), F-box protein CORONATINE INSENSITIVE 1 (COI1) functions as part of an SCF complex to ubiquitinate jasmonate ZIM-domain (JAZ) family proteins, transcriptional repressors of JA responsive genes, leading to their protein degradation (Chini et al., 2007; Thines et al., 2007). Response to gibberellic acid (GA) occurs through the ubiquitination and degradation of DELLA family repressor proteins mediated by F-box protein SLEEPY1 (SLY1) upon the binding of the GA receptor GID1 to the DELLA proteins (Dill et al., 2004). On the contrary, the activation of the ethylene signaling pathway involves the stabilization of downstream transcriptional regulator ETHYLENE-INSENSITIVE3 (EIN3) through the prevention of its constitutive protein degradation by F-box proteins EIN3-BINDING F BOX PROTEIN 1 (EBF1) and EBF2 (Gagne et al., 2004). In addition to the above-mentioned examples of F-box E3 ligases involved in plant hormone signaling, U-box proteins PUB12 and PUB13 ubiquitinate ABA INSENSITIVE 1 (ABI1), a negative regulator of stress hormone abscisic acid (ABA), in the presence of ABA (Kong et al., 2015).

Accumulating evidence suggests that the circadian clock in plants is under regulation by E3 ubiquitin ligases. For example, Arabidopsis RING E3 ubiquitin ligase SINAT5 directly interacts and ubiquitinates circadian oscillator LATE ELONGATED HYPOCOTYL (LHY), as mutant *sinat5* exhibits late flowering phenotype due to increased LHY stability (Park et al., 2010). Interestingly, SINAT5 also plays a role in ubiquitin-related degradation of NAC DOMAIN CONTAINING PROTEIN 1 (NAC1), a transcription activator downstream auxin signaling, thus attenuating auxin signals (Xie et al., 2002). The pleiotropic function of SINAT5 suggests that E3 ubiquitin ligases may function in the cross-talk among various biological processes in plants.

E3 ubiquitin ligases play roles in the sensing of abiotic stresses and the activation of stress responses. For example, tomato RING E3 ubiquitin ligase SpRing functions as a positive regulator of salt tolerance (Qi et al., 2016). Silencing *SpRing* in tomato leads to increased sensitivity to salt stress while overexpression of the tomato gene confers enhanced salt tolerance in Arabidopsis. In another example, an Arabidopsis RING ubiquitin ligase CHY ZINC-FINGER AND RING PROTEIN 1 (CHYR1) promotes ABA-induced stomata closure under drought conditions (Ding et al., 2015).

A number of studies have shown that E3 ubiquitin ligases play important roles in the regulation of defense responses in plants. PUB12 and PUB13, two closely related U-box E3 ubiquitin ligases in Arabidopsis, polyubiquitinate PRR FLS2 and promote PAMP-induced degradation of the receptor, possibly to prevent over-activation of immune signaling (Lu et al., 2011). Notably, a recent study demonstrated the involvement of PUB12 and PUB13 in the ubiquitination and protein degradation of ABI1 (Kong et al., 2015), another example of E3 ubiquitin ligases involved in the cross-talk among different signaling pathways. PUB22, PUB23 and PUB24, three Arabidopsis U-box E3 ubiquitin ligases, act as negative regulators of PTI (Trujillo et al., 2008). PUB22 mediates the degradation of the defense component EXOCYST SUBUNIT EXO70 FAMILY PROTEIN B2 (Exo70B2), a subunit of the exocyst complex, and contributes to the attenuation of the PAMP-induced signaling (Stegmann et al., 2012). In some cases, pathogens suppress host defense by synthesizing E3 ligases

that hijack the host ubiquitination machinery to down-regulate key defense regulators. *Pseudomonas syringae* secrets E3 ubiquitin ligase AvrPtoB, which ubiquitinates and degrades RLK FLS2 and CERK1 in Arabidopsis and hence promotes pathogenesis (Gohre et al., 2008; Gimenez-Ibanez et al., 2009).

1.3.4 E3 ubiquitin ligases are involved in NLR-mediated defense

Emerging evidence indicates that NLR-mediated defense is under regulation by the ubiquitination-proteasome pathway and E3 ubiquitin ligases play important roles in the stability control of key defense regulators involved.

Arabidopsis F-box protein CPR1 physically interacts and promotes the protein degradation of multiple NLRs including SNC1 and RPS2 based on genetic and biochemical analyses. Loss-of-function *cpr1* mutant exhibits autoimmune phenotypes, which can be partially suppressed by knocking out *SNC1*. In addition, overexpression of CPR1 leads to enhanced disease susceptibility to virulent pathogen *P.s.t.* DC3000, suggesting the existence of additional defense regulators as the ubiquitination substrates of CPR1 (Cheng et al., 2011; Gou et al., 2012).

RING1 encodes a RING E3 ubiquitin ligase in Arabidopsis, which is involved in the pathogen-induced programmed cell death. Overexpression of *RING1* in Arabidopsis leads to spontaneous HR (Lin et al., 2008). The pepper *RING1* homolog *CaRING1*, plays a similar role in defense responses, as silencing of *CaRING1* in pepper leads to compromised HR and lowered SA accumulation upon infection with avirulent pathogen *Xanthomonas campestris pv vesicatoria* (Lee et al., 2011). On the other hand, overexpression of *CaRING1* in Arabidopsis results in enhanced disease resistance against *Pseudomonas syringae* pv. *maculicola* (*P.s.m.*) and *H.a*. (Lee et al., 2011).

Tobacco *Avr9/Cf-9 Rapidly Elicited gene 276* (*ACRE276*) encodes a U-Box E3 ubiquitin ligase, whose function is required for the HR triggered by elicitor Avr9 from fungal

pathogen *Cladosporium fulvum*, the causal agent of the tomato leaf mold (Yang et al., 2006). Furthermore, PUB17, the Arabidopsis homolog of ACRE276, also plays a key role in RPM1- and RPS4-mediated ETI against avirulent *P.s.t.* DC3000 strains expressing *AvrB* and *AvrRps4*, respectively (Yang et al., 2006).

1.4 Thesis objectives

The primary goal of my thesis research was the isolation, through map-based cloning, of two *muse* mutants, *muse1* and *muse15*, from the mutant *snc1*-enhancing genetic screen, and the subsequent functional studies of the *MUSE1* and *MUSE15* genes in the context of plant immunity. Through the study of the mechanisms underlying how these two *MUSE* genes regulate plant innate immunity, I aimed to gain additional insights into the complex regulation of ETI in plants.

2. Two E3 ubiquitin ligases with overlapping functions, MUSE1 and MUSE2, negatively regulate SNC1-mediated plant immunity

2.1 Introduction

Plants are under constant threats from diverse microbial pathogens. To effectively defend themselves, plants have evolved complex mechanisms to perceive pathogens and trigger defense responses (Chisholm et al., 2006; Jones and Dangl, 2006; Dangl et al., 2013). However, successful pathogens usually deliver effectors into host cells that help overcome defense in hosts (Kamoun, 2007; Cunnac et al., 2009; Xin and He, 2013). Some effectors are recognized by plant resistance (R) proteins, which trigger rapid and robust defense responses, usually accompanied by the localized programmed cell death event termed hypersensitive response. The majority of R proteins identified so far belong to the nucleotide-binding domain leucine-rich repeat (NLR) class. Typical plant NLR proteins can be further classified based on the presence of either a Toll/Interleukin-1-receptor-like (TIR) or CC domain at their N-terminus (Dangl and Jones, 2001; Maekawa et al., 2011a).

In the autoimmune mutant *suppressor of npr1-1, constitutive 1* (*snc1*), a gain-of-function mutation in the TIR-type NLR (TNL)-encoding gene *SNC1* increases the stability of the TNL, resulting in constitutively activated defense responses (Li et al., 2001; Zhang et al., 2003; Cheng et al., 2011). The *snc1* mutant plants exhibit immune defects including elevated expression of defense marker genes *PR1* and *PR2*, increased defense hormone SA levels, and enhanced resistance to virulent pathogens (Li et al., 2001). Morphologically, *snc1* plants are dwarfed with curly leaves, which is a phenotype commonly observed in Arabidopsis autoimmune mutants (Alcazar and Parker, 2011). The inverse correlation between the size of *snc1* plants and the degree of disease resistance (Xu et al., 2014a) makes *snc1* an enabling tool for mutant screening, as its size can serve as an accurate proxy for immune outputs. Both suppressor screens and enhancer screens have been carried out with *snc1* in order to dissect TNL-mediated immunity (Johnson et al., 2012;

Huang et al., 2013; Li et al., 2015).

Protein ubiquitination plays a major role in the regulation of plant immunity (Trujillo and Shirasu, 2010; Cheng and Li, 2012; Furlan et al., 2012). Ubiquitination occurs through step-wise reactions catalyzed by three enzymes: an E1 ubiquitin-activating enzyme, an E2 ubiquitin-conjugating enzyme, and an E3 ubiquitin ligase, resulting in the transfer of one or more ubiquitin molecules to a substrate protein (Hershko and Ciechanover, 1998; Pickart, 2001). Most often, ubiquitination marks substrate proteins for degradation via the 26S proteasome (Smalle and Vierstra, 2004). However, more recent studies have revealed non-proteolytic functions of ubiquitination such as enzyme activity regulation and protein trafficking (Chen and Sun, 2009). During the ubiquitination process, substrate specificity is largely determined by the E3 ligase (Pickart, 2001). There are more than 1500 predicted E3 ligases encoded in the *Arabidopsis* genome (Hua and Vierstra, 2011), compared to over 600 annotated E3 ubiquitin ligases in the human genome (Li et al., 2008). The larger number of E3-encoding genes in Arabidopsis reflects more diverse and intricate regulations of biological processes through ubiquitination in plants. Based on their structural features and modes of activation, E3 ligases can be classified into several major classes: RING, U-box, HECT, and various complex E3s which are often Cullin-based (Cheng and Li, 2012). A number of these E3 ligases have previously been shown to be involved in regulating plant immunity (Cheng and Li, 2012). For example, the F-box protein CPR1 is part of an E3 ubiquitin ligase complex involved in the turnover of NLR proteins (Cheng et al., 2011).

Negative regulation of plant immunity is crucial to plant survival, as uncontrolled activation of defense responses can lead to autoimmunity, loss of overall fitness, and potentially lethality. Previous studies have shown that NLR-mediated defense in plants is under tight negative regulation (Li et al., 2015), although the mechanisms underlying this regulation remain largely unexplored. In this chapter, I report the identification and functional analysis of *MUSE1* (*Mutant, snc1-enhancing 1*), which encodes a novel E3 ligase that negatively regulates immunity in Arabidopsis. MUSE1 and its paralog, MUSE2, are two

RING E3 ubiquitin ligases which have overlapping functions in controlling SNC1-mediated defense responses.

2.2 Results

2.2.1 Isolation and characterization of *muse1-1* from a modified *snc1* enhancer screen

To identify novel negative regulators of plant immunity, the Li Lab conducted mutant, *snc1*-enhancing (MUSE) genetic screens in the *mos4 snc1* and *mos2 snc1 npr1* genetic backgrounds, both of which are morphologically and immunologically WT-like (Huang et al., 2013). *snc1* provides a sensitized background for the screen, while the presence of the *mos4* or *mos2* and *npr1* mutations reduces the likelihood of lethality caused by severe autoimmunity from the immunity-enhancing mutations in the *snc1* background. A number of mutants with enhanced autoimmune phenotypes were isolated from the mutagenized *mos4 snc1* M2 population, one of which was designated *muse1-1*. Compared with WT-like *mos4 snc1*, the *muse1-1 mos4 snc1* triple mutant plants exhibit *snc1*-like dwarfism with curled leaves (Figure 2.1A). Reverse transcription (RT)-PCR revealed that the expression of the defense marker genes *PR1* and *PR2* is significantly elevated in *muse1-1 mos4 snc1* plants (Figure 2.1B). To examine whether the *snc1*-like phenotypes of the *muse1-1 mos4 snc1* are associated with enhanced disease resistance, infection assay was performed with the virulent oomycete pathogen *Hyaloperonospora arabidopsidis* (*H.a.*) Noco2. While *mos4 snc1* plants are as susceptible as WT (Palma et al., 2007), disease resistance in *muse1-1 mos4 snc1* was restored to a similar level as that in *snc1* (Figure 2.1C). Taken together, these results suggest that the mutation in *muse1-1* enhances the autoimmune phenotypes of *snc1*.

2.2.2 Positional cloning of *muse1-1*

To map the *muse1-1* mutation, homozygous *muse1-1 mos4 snc1* (in the Col-0 ecotype background) was crossed with Landsberg *erecta* (L*er*). F1 individuals were self-fertilized to

produce F2 seeds. 16 F2 plants with *snc1*-enhancing phenotypes were used for crude mapping. Linkage was found between the mutant phenotypes and the molecular marker F15G16 at the bottom of chromosome 3. Further mapping revealed that the mutation was between markers F18O21 and F17J16. A fine mapping population consisting of 1008 F3 individuals was generated from F2 plants that were homozygous for *snc1* and *MOS4*, but heterozygous for *muse1-1*. The region containing *muse1-1* was further narrowed down to a 50kb region.

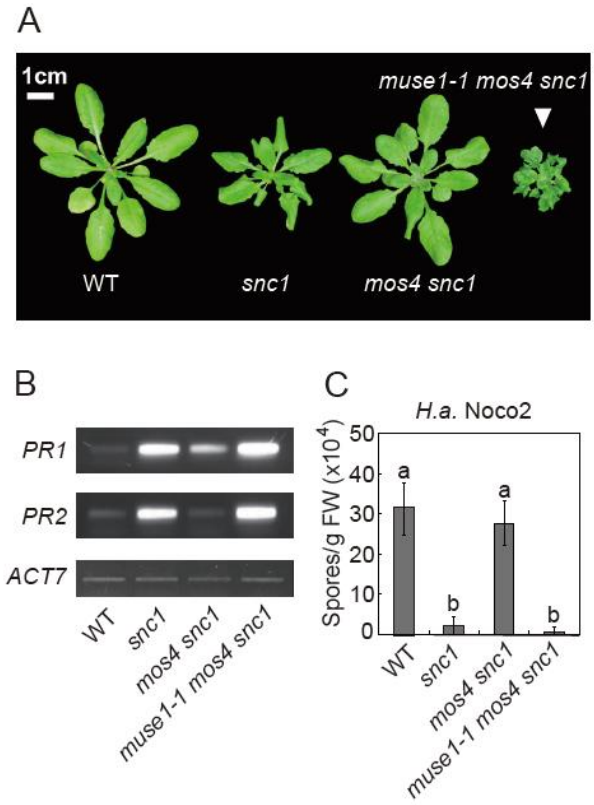

Figure 2.1: *muse1-1* enhances immunity in the *mos4 snc1* background.

(A) Morphology of four-week-old soil-grown Col-0 (WT), *snc1*, *mos4 snc1* and *muse1-1 mos4 snc1* plants.

(B) Expression of *PR1* and *PR2* in WT, *snc1*, *mos4 snc1* and *muse1-1 mos4 snc1* plants. RT-PCR was performed on two-week-old seedlings grown on 1/2 MS plates. *ACT7* was included as a loading control. PCR cycle numbers were: 25 for *PR1*, 25 for *PR2* and 28 for *ACT7*.

(C) Growth of *H.a.* Noco2 was measured seven days after spray-inoculation with 10^5 spores/ml inoculum on WT, *snc1*, *mos4 snc1* and *muse1-1 mos4 snc1* plants. Four replicates were included for each genotype. One-way analysis of variance (ANOVA) was used to calculate the statistical significance among genotypes, as indicated by different letters ($P < 0.005$). Error bar represents mean ± Standard Deviation (SD) (n = 4).

To identify the molecular lesion in *muse1-1*, genomic DNA was extracted from homozygous *muse1-1* plants from the mapping population and sequenced using an Illumina Sequencer. When the sequence of *muse1-1* was compared with that of the Arabidopsis reference sequence, only one G to A mutation was identified in the mapped *muse1-1* region. This mutation is predicted to cause a Pro to Leu amino acid change (Figure 2.2A, B).

Five additional recessive *muse* mutants were later mapped to the *muse1* region (Figure 2.2A, B; 2.3A, B). Direct Sanger sequencing revealed that these mutants all carried non-synonymous mutations in the same gene (Figure 2.2A, B). Furthermore, in an allelism test from pair-wise crosses, these mutants all failed to complement each other in F1 (Figure 2.3C), indicating that they carry mutations in the same gene. I also crossed *snc1* with a T-DNA knockout mutant allele of *muse1* and found that the T-DNA allele enhances the autoimmune phenotypes in *snc1* similarly as all six *muse1* alleles mentioned above (Figure 2.2A, B, C). The T-DNA allele was therefore named *muse1-7*. Taken together, these results indicate that the six *muse* mutants identified are all loss-of-function alleles of the same gene *MUSE1*.

To further confirm the proper cloning of *MUSE1*, a transgenic complementation test was performed. The genomic sequence of the putative *MUSE1* gene with its native promoter was cloned from WT and transformed into *muse1-1 mos4 snc1*. Two out of three independent T1 transformants restored the *mos4 snc1*-like phenotype (Figure 2.2D). In addition, the presence of the transgene co-segregated with the WT-like phenotypes in the T2 generation of both transformants, confirming the cloning of *MUSE1*.

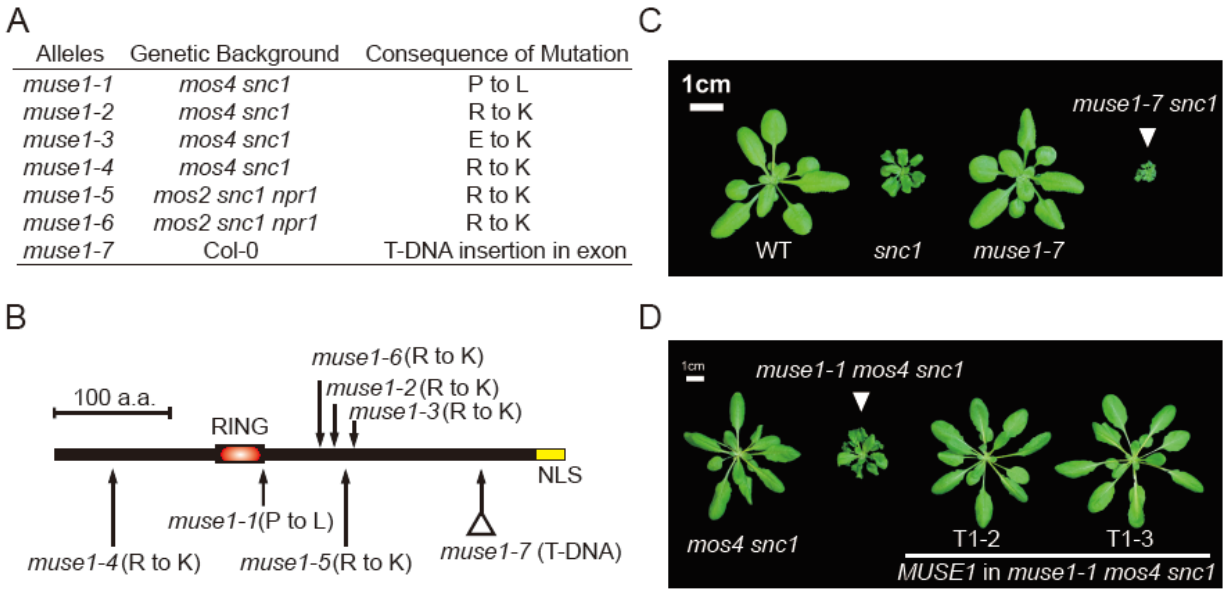

Figure 2.2: Positional cloning of *muse1-1.*

(A) A list of *muse1* mutant alleles and the corresponding consequences of mutations.

(B) A schematic diagram showing the predicted MUSE1 protein structure with arrows indicating the sites of the mutations in different *muse1* alleles. The yellow colored box at the C terminus indicates a predicted nuclear localization signal (NLS).

(C) Morphology of four-week-old soil-grown WT, *snc1*, *muse1-7* and *muse1-7 snc1* plants.

(D) Morphology of four-week-old soil-grown *mos4 snc1*, *muse1-1 mos4 snc1* and two T1 lines of *muse1-1 mos4 snc1* expressing *pMUSE1::MUSE1*.

2.2.3 *MUSE1* encodes a RING domain E3 ubiquitin ligase

MUSE1 encodes a protein with a predicted RING domain (Figure 2.2B). Phylogenetic analysis of the amino acid sequences of MUSE1-like peptides revealed that *MUSE1* is present in all dicots (Figure 2.4). In contrast to its central C3HC4 RING domain which is highly conserved, its N- and C-termini are only moderately conserved among plant species. The 28 amino acid sequence at the C terminus of MUSE1 is predicted to contain a nuclear localization signal according to NLS Mapper (Kosugi et al., 2009) (Figure 2.2B), which is conserved among species, suggesting that MUSE1 is likely a protein that can localize to the nucleus.

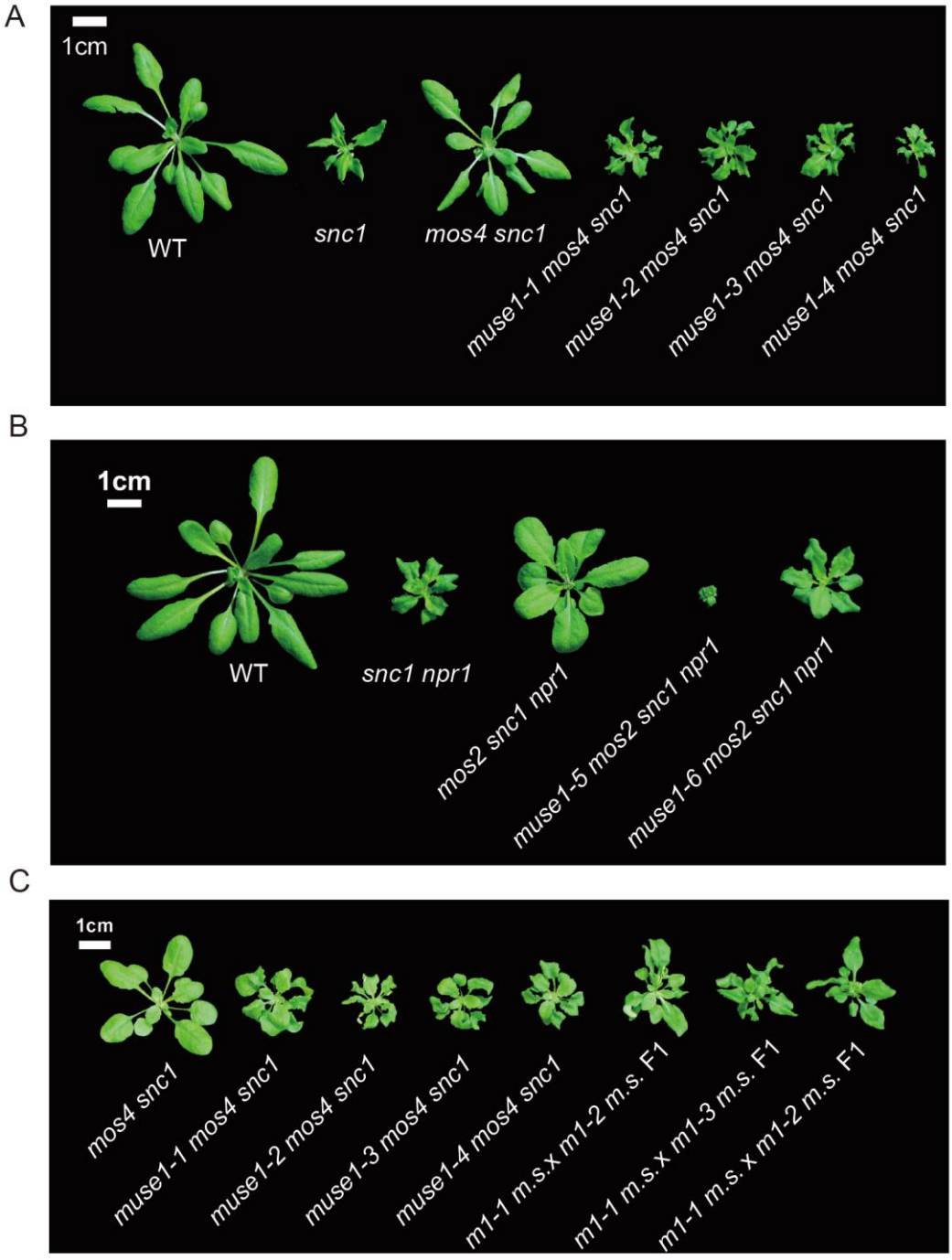

Figure 2.3: Alleles of *muse1* identified from the MUSE screens.

(A) Morphologies of four-week-old *muse1* alleles identified from the *mos4 snc1* background.

(B) Morphologies of four-week-old *muse1* alleles identified from the *mos2 snc1 npr1* background.

(C) Four-week-old F1 plants from pair-wise crosses among the four *muse1* alleles identified in the *mos4 snc1* background. *m1-1* = *muse1-1*; *m.s.* = *mos4 snc1*.

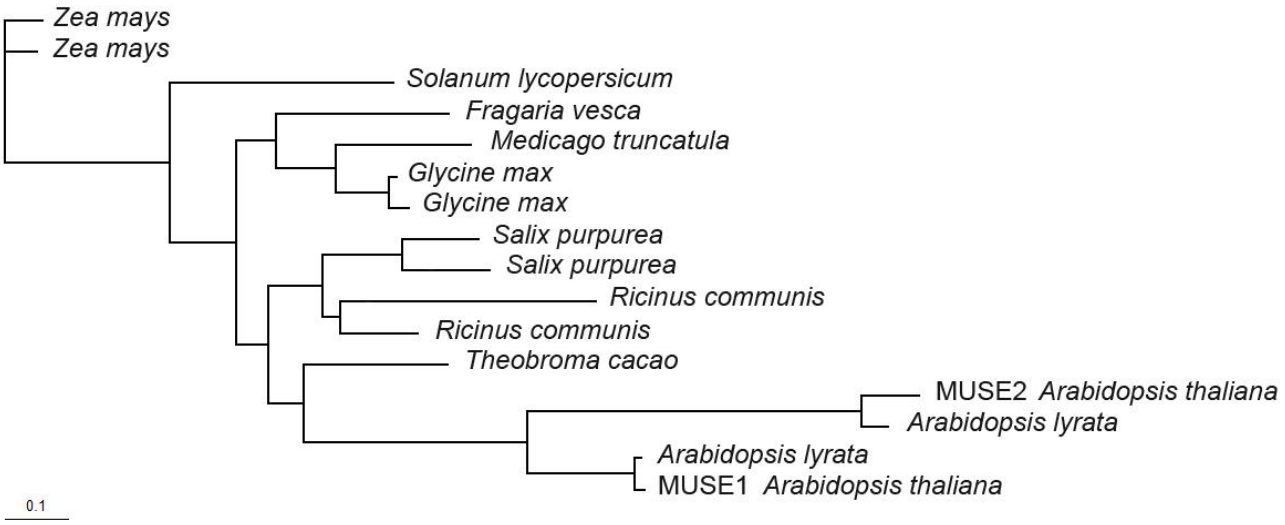

Figure 2.4: Phylogenetic analysis of the MUSE1 and MUSE2 peptides.

Maximum likelihood tree generated using amino acid alignments of MUSE1-like peptides in various selected plant species.

Since the RING domain is a signature of a major class of E3 ligases, MUSE1 was tested for its E3 ubiquitin ligase activity in an *in vitro* ubiquitination assay. *E.coli*-expressed GST-tagged MUSE1 was co-incubated with or without AtUBA2 (E1), ATUBC8 (E2), and Ubiquitin *in vitro*, followed by immunoblotting assays (Figure 2.5A). A tail corresponding to increased molecular weight appeared above MUSE1 on the blot when detected with either anti-Ub or anti-GST antibody, indicating self-ubiquitination of MUSE1. This result suggests that MUSE1 it is a *bona fide* E3 ligase.

Substitution of the Cys or His residues within the RING domain usually disrupts the RING structure (Xie et al., 2002; Dong et al., 2006; Zhang et al., 2007b; Peng et al., 2013), often resulting in a dominant-negative form of the E3 (Xie et al., 2002; Peng et al., 2013). To further test whether MUSE1 functions as a RING-type E3 ubiquitin ligase, I transformed site-mutagenized *MUSE1* constructs encoding either MUSE1^{H156Y} or MUSE1^{C159S} into *snc1* plants with the expectation that these dominant-negative mutations would confer the same phenotype as *muse1-1*. Indeed, 14 out of 60 *MUSE1^{H156Y}* T1 transformants and 20

out of 60 *MUSE1*^{C159S} T1 transformants exhibited *snc1*-enhancing phenotypes (Figure 2.5B) resembling that of *muse1-7 snc1* (Figure 2.2C). These results indicate that the E3 ligase activity of MUSE1 is required for its function.

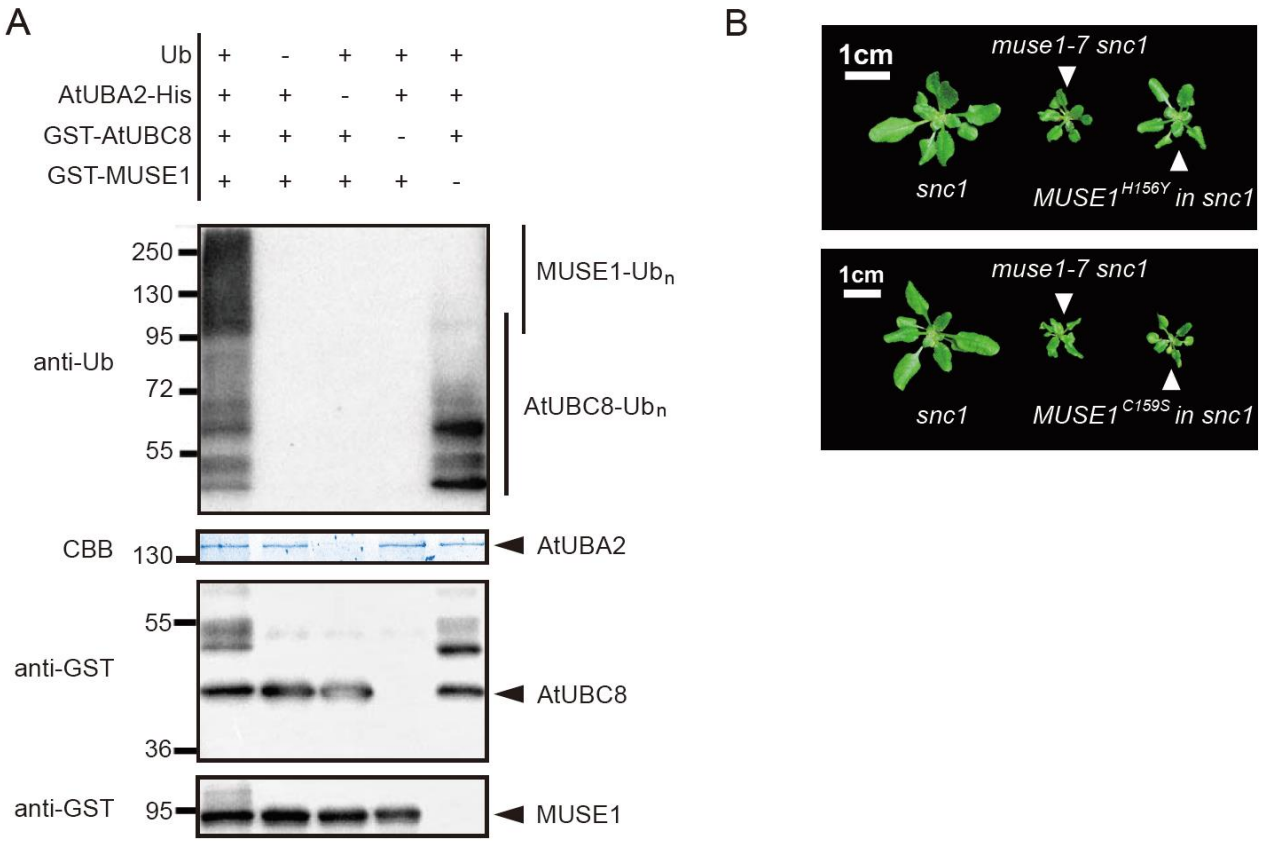

Figure 2.5: MUSE1 exhibits E3 ubiquitin ligase activity.

(A) *In vitro* ubiquitination assays were performed in the presence or absence of *E.coli*-expressed MUSE1 (E3), AtUBC8 (E2), AtUBA2 (E1) or ubiquitin (+ indicates added samples). Ubiquitination was detected by immunoblotting with an anti-ubiquitin antibody. AtUBA2 was detected with Coomassie Brilliant Blue (CBB) staining. AtUBC8 and MUSE1 were detected by immunoblotting with anti-GST antibody. Molecular mass markers are indicated on the left (kDa).

(B) Morphology of three-week-old soil-grown *snc1*, *muse1-7 snc1* and representative *snc1* lines expressing the dominant-negative *MUSE1*^{H156Y} or *MUSE1*^{C159S} transgenes, respectively.

2.2.4 MUSE1 and MUSE2 have overlapping functions

A Basic Local Alignment Search Tool (BLAST) search with *MUSE1* identified a close paralog of *MUSE1*, which encodes another RING domain-containing protein that shares 56% amino acid sequence identity and 68% similarity with MUSE1. A knockout T-DNA mutant of the homolog of *MUSE1* enhances the *snc1* morphological phenotypes to the same level as *muse1* alleles do (Figure 2.6A). Due to its *snc1*-enhancing capability, this *MUSE1* homolog was named *MUSE2* and the T-DNA allele *muse2-1*. To test whether MUSE1 and MUSE2 are functionally redundant, I created the *muse1-7 muse2-1* double mutant by crossing the two T-DNA knockout lines. Although both single mutants appear WT-like, the *muse1-7 muse2-1* double mutant is extremely dwarfed and has curled leaves (Figure 2.6B). Macroscopic lesions can often be observed in the cotyledons of *muse1-7 muse2-1* plants. As with *snc1*, the dwarfism of *muse1-7 muse2-1* can be fully rescued by growing the plants at 28ºC (Figure 2.7), indicative of autoimmunity. Consistent with their morphology, *muse1-7 muse2-1* plants constitutively express defense marker genes *PR1* and *PR2* (Figure 2.6C). In contrast, single mutant *muse1-7* and *muse2-1* plants exhibit slightly increased expression of *PR2* but not *PR1* compared to WT (Figure 2.6C). To test whether the *muse1-7 muse2-1* double mutant exhibits enhanced disease resistance, I challenged the mutant seedlings with the virulent pathogen *H.a.* Noco2. No growth of the oomycete was observed on *muse1-7 muse2-1* seedlings, whereas the *muse1-7* and *muse2-1* single mutants showed the same level of susceptibility as WT (Figure 2.6D). These data demonstrate that MUSE1 and MUSE2 are negative regulators of plant immunity with overlapping functions, as when they are both knocked out the plant mounts a strong autoimmune response.

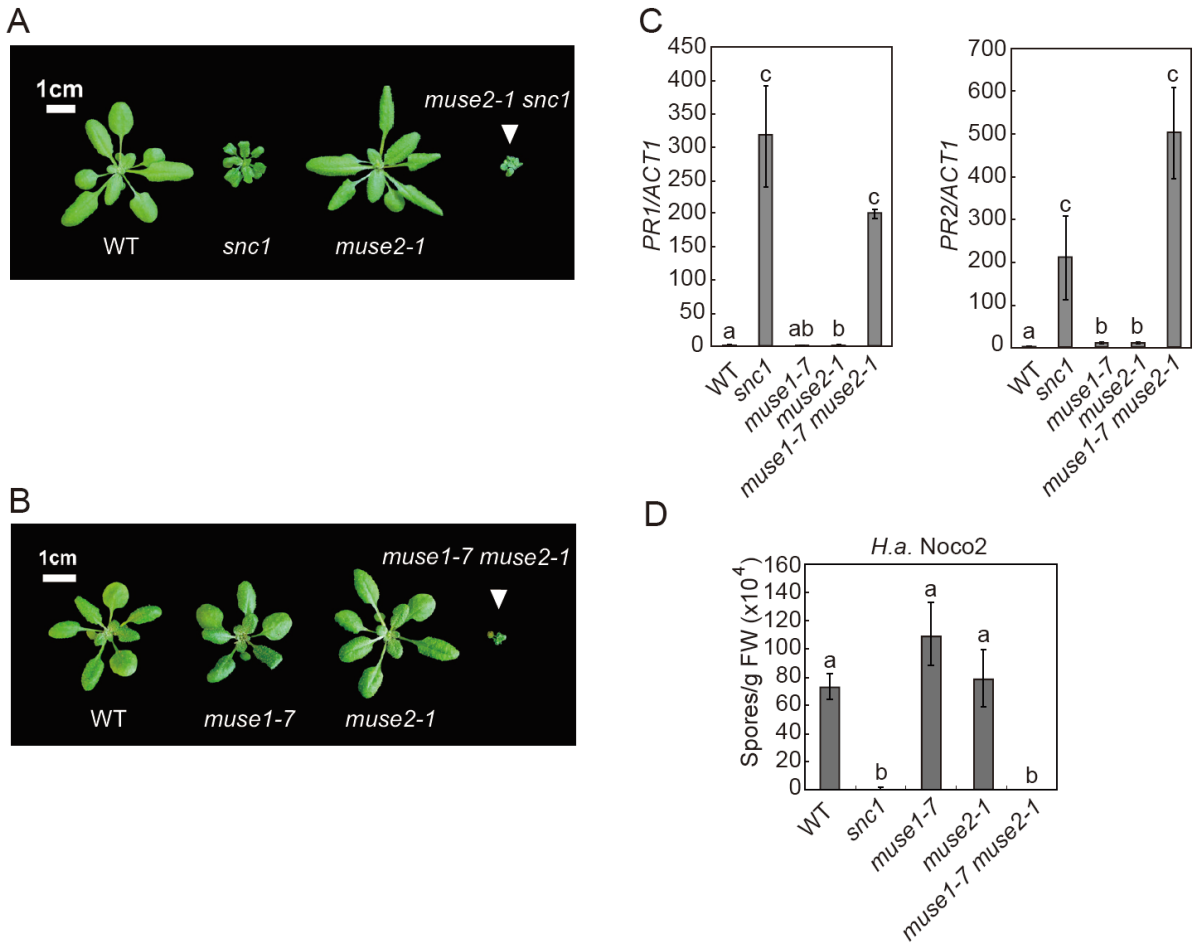

Figure 2.6: MUSE1 and MUSE2 have overlapping functions.

(A) Morphology of four-week-old WT, *snc1*, *muse2-1* and *muse2-1 snc1* plants.

(B) Morphology of three-week-old WT, *muse1-7*, *muse2-1* and *muse1-7 muse2-1* plants.

(C) Expression of *PR1* and *PR2* in WT, *snc1, muse1-7*, *muse2-1* and *muse1-7 muse2-1* plants. qRT-PCR was performed on two-week-old seedlings grown on 1/2 MS plates. *ACT1* was used to normalize the transcript levels. Arbitrary units were used to show the abundance of the transcript levels relative to WT. One-way ANOVA was used to calculate the statistical significance between genotypes, as indicated by different letters ($P < 0.01$). Error bar represents mean ±SD (n = 3).

(D) Growth of *H.a.* Noco2 was measured seven days after spray-inoculation with 10^5 spores/ml inoculum on the indicated genotypes. Four replicates were included for each genotype. One-way ANOVA was used to calculate the statistical significance between genotypes, as indicated by different letters ($P < 0.005$). Error bar represents mean ±SD (n = 4).

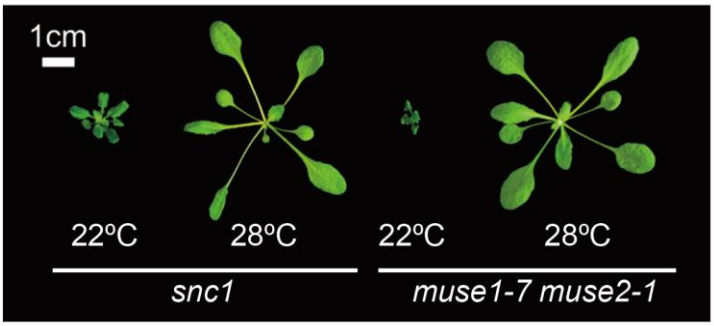

Figure 2.7: The autoimmune dwarfism of *muse1-7 muse2-1* is temperature-sensitive.

Morphology of four-week-old *snc1* and *muse1-7 muse2-1* plants grown at 22ºC and 28ºC, respectively.

2.2.5 Overexpression of *MUSE1* fully suppresses the autoimmune phenotypes of *snc1*

As the loss-of-function *muse1* alleles enhance *snc1* phenotypes, I examined the overexpression phenotype of *MUSE1* in the *snc1* background. Interestingly, when *MUSE1* with its native promoter was transformed into *snc1* plants, 15 out of 21 T1 plants exhibited WT-like morphology. Two of the representative transgenic lines were used for further characterization (Figure 2.8A). Increased *MUSE1* expression was verified in both transgenic lines through qRT-PCR (Figure 2.8B). Decreased expression of *PR1* and *PR2* (Figure 2.8C), and loss of enhanced disease resistance against *H.a.* Noco2 (Figure 2.8D) and *P.s.m.* ES4326 (Figure 2.8E) were observed in these plants. These results show that overexpression of *MUSE1* fully suppresses the autoimmune phenotypes of *snc1*, indicating that MUSE1 negatively regulates a process that is fully required for SNC1-mediated immunity, likely through ubiquitination and protein degradation of its E3 target.

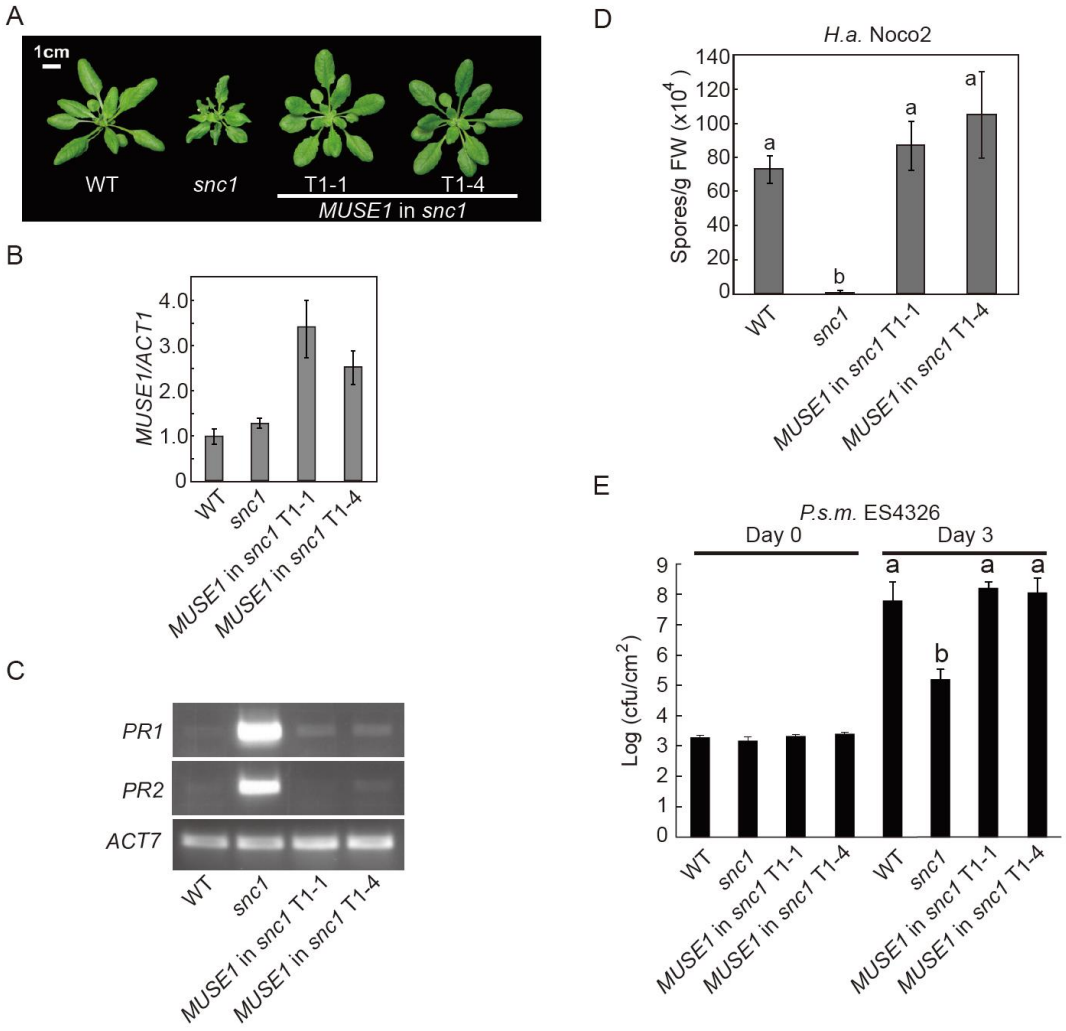

Figure 2.8: Overexpression of *MUSE1* fully suppresses *snc1*-mediated autoimmunity.

(A) Morphology of four-week-old soil-grown WT, *snc1* and two *snc1* transgenic lines expressing *MUSE1* under its native promoter.

(B) *MUSE1* transcript levels in plants described in (A). qRT-PCR was performed on two-week-old seedlings grown on 1/2 MS plates. *ACT1* was used to normalize the transcript levels. Arbitrary units were used to show the abundance of *MUSE1* transcript levels relative to WT. Endogenous and transgenic *MUSE1* transcripts were not distinguished. Error bar represents mean ±SD (n = 3).

(C) Expression of *PR1* and *PR2* in the plants in (A). RT-PCR was performed on two-week-old seedlings grown on 1/2 MS plates. *ACT7* was included as loading control. PCR cycle numbers were: 28 for *PR1*, 30 for *PR2* and 31 for *ACT7*.

(D) Growth of *H.a.* Noco2 was measured seven days after spray-inoculation with 10^5 spores/ml inoculum on ten-day-old seedlings. One-way ANOVA was used to calculate the statistical significance between genotypes, as indicated by different letters ($P < 0.005$). Error bar represents mean ±SD (n = 4).

(E) Growth of *P.s.m.* ES4326 was measured three days after infection of four-week-old plants by leaf-infiltration. Bacterial suspension of OD_{600} = 0.001 was used as inoculum. Leaf discs within the infected area were taken at Day 0 and Day 3 to quantify colony-forming units (cfu). One-way ANOVA was used to calculate the statistical significance between genotypes, as indicated by different letters ($P < 0.005$). Error bar represents mean ±SD (n = 5).

2.2.6 The autoimmunity of *muse1-7 muse2-1* is fully dependent on SNC1

To test whether MUSE1 acts as a general negative regulator of plant immunity, I transformed WT Arabidopsis plants with *MUSE1* with its native promoter. Increased expression of *MUSE1* was verified in four independent T3 homozygous transgenic lines by qRT-PCR (Figure 2.9A). These transgenic lines exhibited WT level of resistance to virulent pathogens *H.a.* Noco2 and *P.s.m.* ES4326, or avirulent pathogens *H.a.* Emwa1 and *P.s.t.* DC3000 *AvrRps4* (Figure 2.9B, C, D). These results suggest that MUSE1 does not seem to negatively regulate basal defense or defense responses mediated by the TNLs RPP4 or RPS4 (Aarts et al., 1998).

To further test the relationship between MUSE1 and SNC1, I crossed *muse1-7 muse2-1* with the loss-of-function deletion alleles *snc1-r1* and *eds1-2*, respectively. EDS1 is known to play a crucial role in defense responses mediated by many TNLs (Aarts et al., 1998). Interestingly, both *snc1-r1* and *eds1-2* fully suppressed the dwarf phenotype (Figure 2.10A), the constitutive expression of *PR* genes (Figure 2.10B) and the enhanced disease resistance to *P.s.m.* ES4326 (Figure 2.10C) of *muse1-7 muse2-1*. These epistasis analyses suggest that the role of MUSE1 is fully dependent on SNC1.

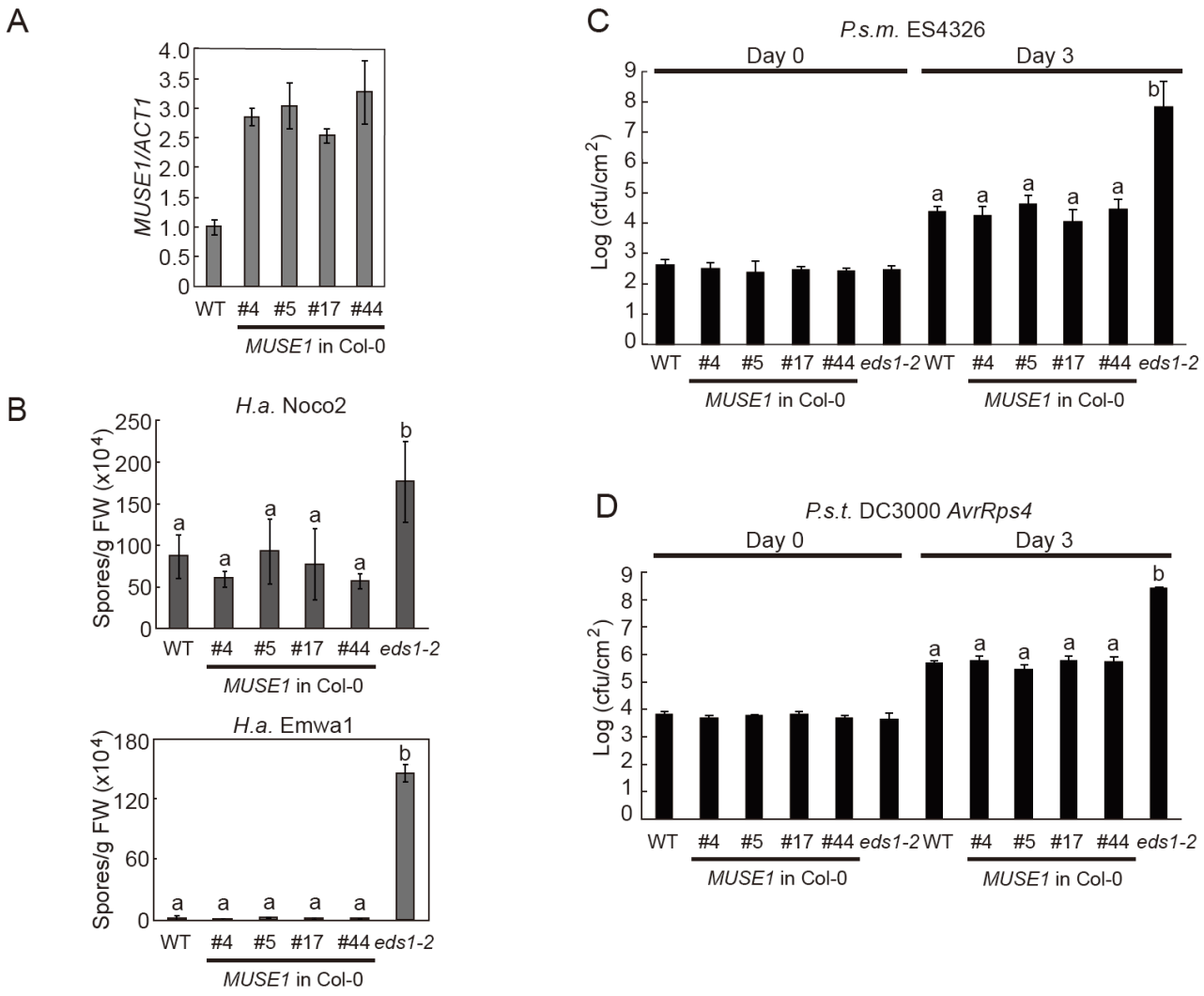

Figure 2.9: Overexpression of *MUSE1* in WT does not lead to enhanced disease susceptibility.

(A) *MUSE1* transcript levels in WT and four independent *MUSE1* transgenic lines. qRT-PCR was performed on two-week-old seedlings grown on 1/2 MS plates. *ACT1* was used to normalize the transcript levels. Arbitrary units were used to show the abundance of *MUSE1* transcript levels relative to WT. Endogenous and transgenic *MUSE1* transcripts were not distinguished. Error bar represents mean ±SD (n = 3).

(B) Growth of *H.a.* Noco2 and *H.a.* Emwa1 was measured seven days after spray-inoculation (10^4 spores/ml for Noco2 and 10^5 spores/ml for Emwa1) on ten-day-old seedlings. *eds1-2* was included as a susceptibility control. One-way ANOVA was used to calculate the statistical significance among genotypes, as indicated by different letters ($P < 0.005$). Error bar represents mean ±SD (n = 4).

(C) Growth of *P.s.m.* ES4326 was measured three days after infection of four-week-old plants by leaf-infiltration. Bacterial suspension of OD_{600} = 0.0001 was used as inoculum. Leaf discs within the infected area were taken at Day 0 and Day 3 to quantify cfu. One-way ANOVA was used to

calculate the statistical significance among genotypes, as indicated by different letters (P < 0.005). Error bar represents mean ±SD (n = 5).

(D) Quantification of the growth of *P.s.t.* DC3000 *AvrRps4* by infection assay as described in (C). Bacterial suspension of OD_{600} = 0.002 was used as inoculum. One-way ANOVA was used to calculate the statistical significance among genotypes, as indicated by different letters (P < 0.005). Error bar represents mean ±SD (n = 5).

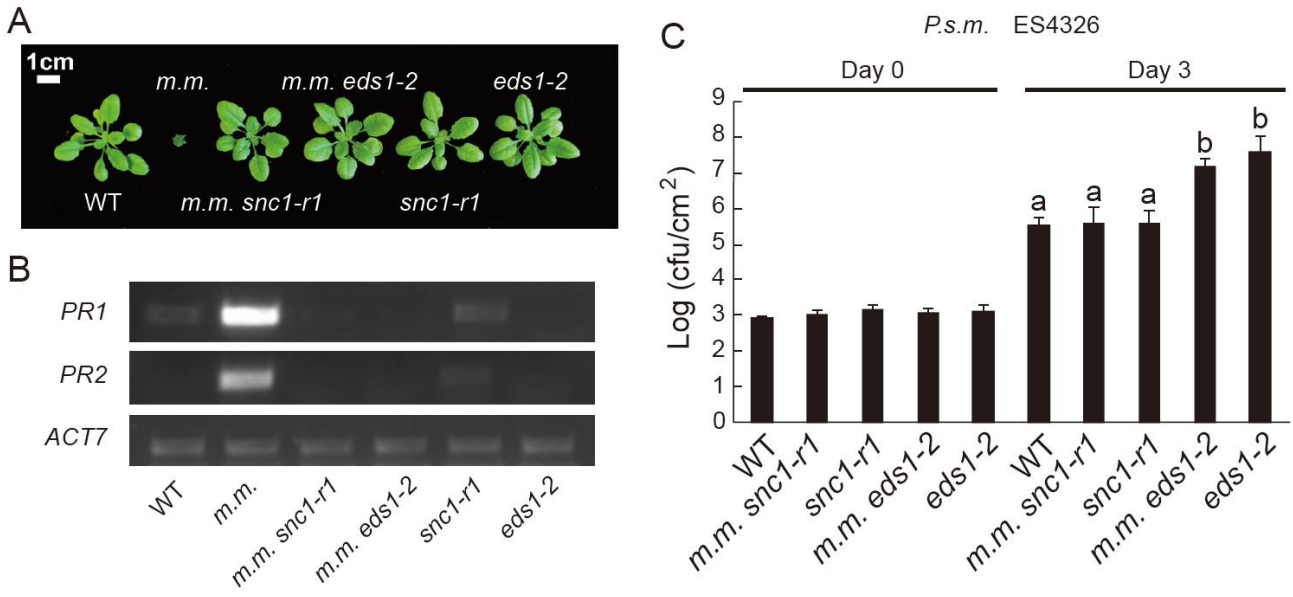

Figure 2.10: The autoimmune phenotypes of *muse1-7 muse2-1* are fully suppressed by loss-of-function *snc1-r1* or *eds1-2*.

(A) Morphology of WT, *muse1-7 muse2-1* (*m. m.*), *muse1-7 muse2-1 snc1-r1* (*m. m. snc1-r1*), *muse1-7 muse2-1 eds1-2* (*m. m. eds1-2*), *snc1-r1* and *eds1-2* plants. Soil-grown plants were photographed four weeks after germination.

(B) Expression of *PR1* and *PR2* in the genotypes as described in (A). RT-PCR was performed on two-week-old seedlings grown on 1/2 MS plates. *ACT7* was included as loading control. PCR cycle numbers were: 24 for *PR1*, 24 for *PR2* and 26 for *ACT7*.

(C) Growth of *P.s.m.* ES4326 three days after infection of four-week-old plants by leaf-infiltration. Bacterial suspension of OD_{600} = 0.001 was used as inoculum. Leaf discs within the infected area were taken at day 0 and day 3 to quantify cfu. One-way ANOVA was used to calculate the statistical significance among genotypes, as indicated by different letters (*P* < 0.005). Error bar represents mean ±SD (n = 5).

NLRs often guard positive regulators of plant immunity, activating defense responses upon detecting modifications made to these positive regulators (Zhang et al., 2012). To test whether MUSE1 and MUSE2 function as positive regulators of basal immunity guarded by

SNC1, bacterial infection assays were performed on the *muse1-7 muse2-1 snc1-r1* triple mutant. As shown in Figure 2.10C, *muse1-7 muse2-1 snc1-r1* is not more susceptible to virulent pathogen *P.s.m.* ES4326 compared to WT. I also performed an infection assay with a type III secretion-deficient strain *P.s.t.* DC3000 *hrcC*- and the avirulent pathogen *P.s.t.* DC3000 *AvrRps4*, respectively. Again, no enhanced disease susceptibility was observed in either assay (Figure 2.11). From these observations, I conclude that MUSE1 and MUSE2 do not seem to play general, positive roles in mediating basal defense, PTI, or RPS4-mediated defense. Their function is rather SNC1-specific.

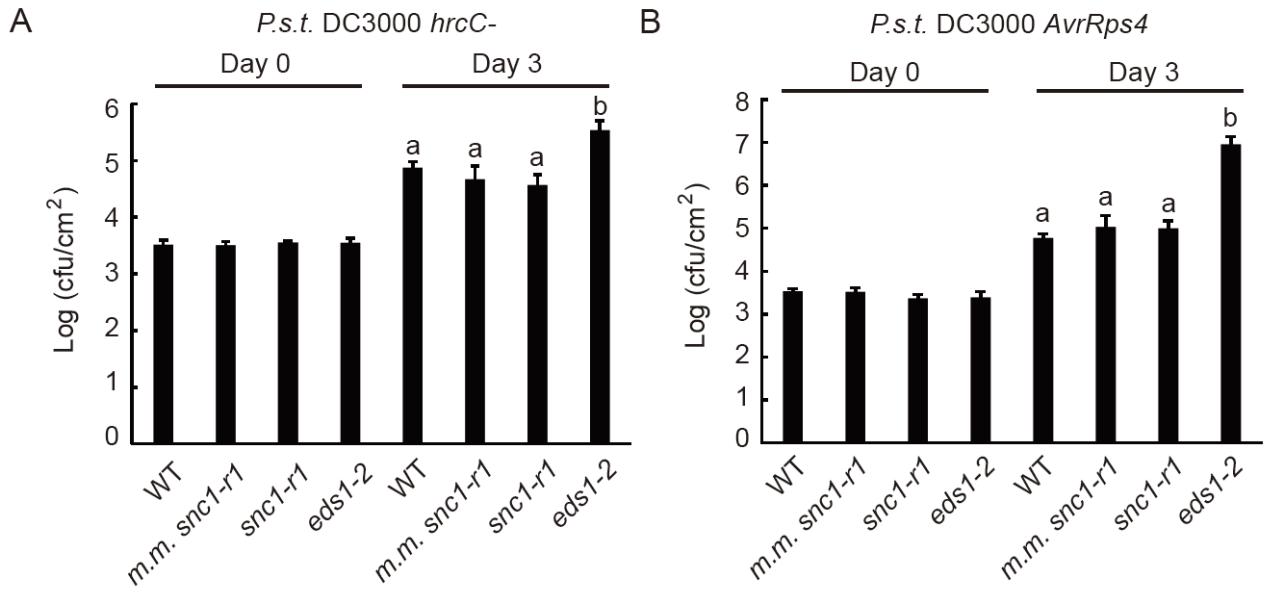

Figure 2.11: MUSE1 and MUSE2 do not function in PTI or RPS4-mediated defense.

(A) Growth of *P.s.t.* DC3000 *hrcC*- after infection of four-week-old plants by leaf-infiltration. Bacterial suspension of OD_{600} = 0.002 was used as inoculum. Leaf discs within the infected area were taken at Day 0 and Day 3 to quantify cfu. One-way ANOVA was used to calculate the statistical significance among genotypes, as indicated by different letters ($P < 0.05$). Error bar represents mean ±SD (n = 5).

(B) Growth of *P.s.t.* DC3000 *AvrRps4* after infection of four-week-old plants by leaf-infiltration. Bacterial suspension of OD_{600} = 0.001 was used as inoculum. Leaf discs within the infected area were taken at Day 0 and Day 3 to quantify cfu. One-way ANOVA was used to calculate the statistical significance among genotypes, as indicated by different letters ($P < 0.005$). Error bar represents mean ±SD (n = 5).

2.2.7 MUSE1 does not influence the protein accumulation of SNC1, MOS10 or bHLH84

Since *MUSE1* encodes an E3 ligase and it is SNC1-specific, I predicted that it is likely involved in the degradation of a positive regulator of SNC1-mediated immunity. I therefore tested three candidate proteins including SNC1, basic Helix-Loop-Helix 84 (bHLH84) (Xu et al., 2014b) and MOS10 (Zhu et al., 2010).

The phenotypes associated with mutations in *MUSE1* somewhat resemble those of the previously characterized E3 ligase mutant *cpr1* (Cheng et al., 2011). Specifically, the loss of MUSE1 and MUSE2 induces autoimmunity similar to that observed in *cpr1*, and overexpression of *MUSE1* fully suppresses *snc1* as does the overexpression of CPR1. As overexpression of CPR1 leads to decreased SNC1 levels, I tested whether MUSE1 and MUSE2 also regulate SNC1 accumulation using a western blot performed with anti-SNC1 antibody. As shown in Figure 2.9A and Figure 2.12A, SNC1 protein levels in all four independent *MUSE1* transgenic lines were comparable to that of WT. These data suggest that MUSE1 does not regulate SNC1 protein accumulation.

bHLH84 functions as a transcription factor that confers autoimmunity in the WT background when overexpressed (Xu et al., 2014b). bHLH84 was found to interact with SNC1 (Xu et al., 2014b). To test if MUSE1 is involved in the degradation of bHLH84, *MUSE1-HA* was transformed into a transgenic line expressing *bHLH84-HA* in the *eds1-2* genetic background (Xu et al., 2014b). As neither N- or C-terminal-tagged *MUSE1* transgenes could suppress the autoimmune phenotypes of *snc1*, I generated a *MUSE1-HA* transgene with a single HA tag inserted between amino acids Ala292 and Ala293, within a weakly conserved region among MUSE1 homologs. This *MUSE1-HA* transgene suppresses the autoimmune phenotypes of *snc1* to a similar degree as the untagged *MUSE1* transgene does (Figure 2.8; 2.13), suggesting that the HA tag does not affect the function of MUSE1. In a western blot analysis, I did not observe a significant alteration in bHLH84 protein level in *eds1-2* upon transgenic expression of *MUSE1-HA* (Figure 2.12B). This suggests that bHLH84 accumulation is unlikely to be regulated by MUSE1.

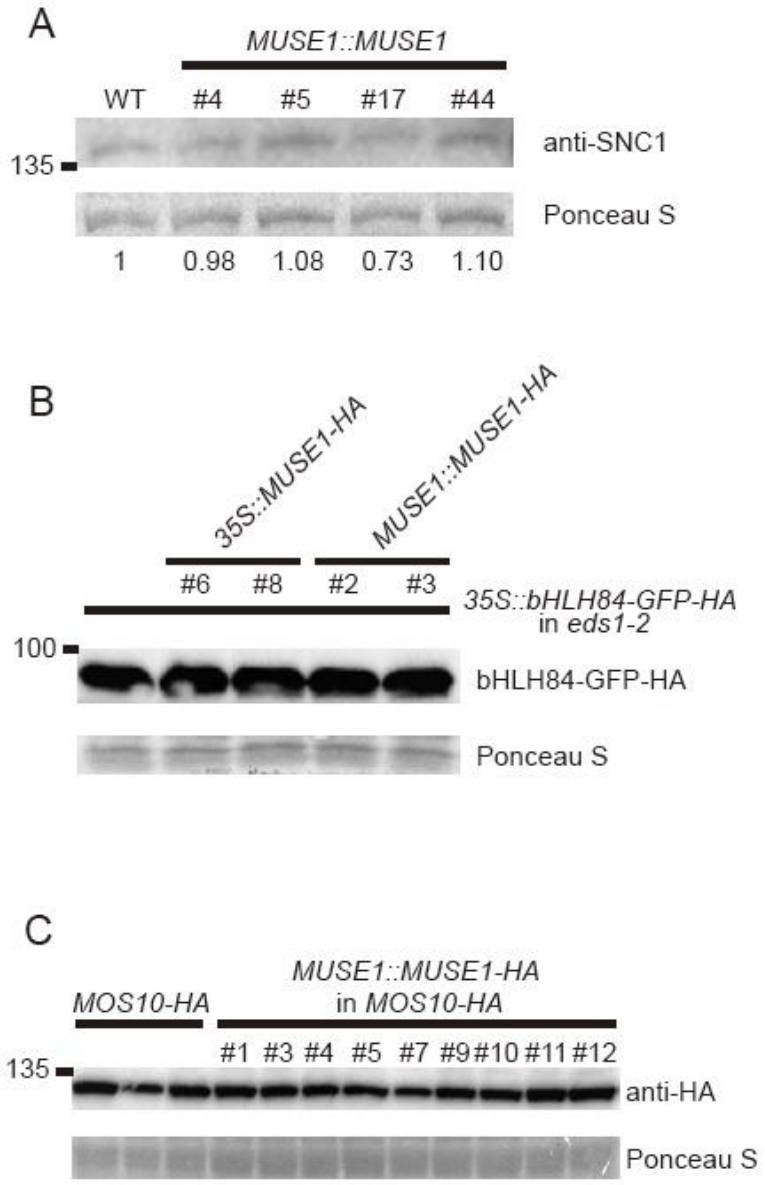

Figure 2.12: SNC1, MOS10 and bHLH84 levels are not altered by overexpression of MUSE1.

(A) Western blot analysis using the anti-SNC1 antibody. Total protein was extracted from two-week-old soil-grown plants. Numbers below the blot represent the relative intensity of the SNC1 band relative to the Ponceau S band, with WT set as 1.

(B) Western blot analysis using the anti-HA antibody to examine the levels of bHLH84-HA. Total protein was extracted from two-week-old plants grown on 1/2 MS plates.

(C) Western blot analysis using the anti-HA antibody to examine the levels of MOS10-HA. Total proteins were extracted from four-week-old plants on soil.

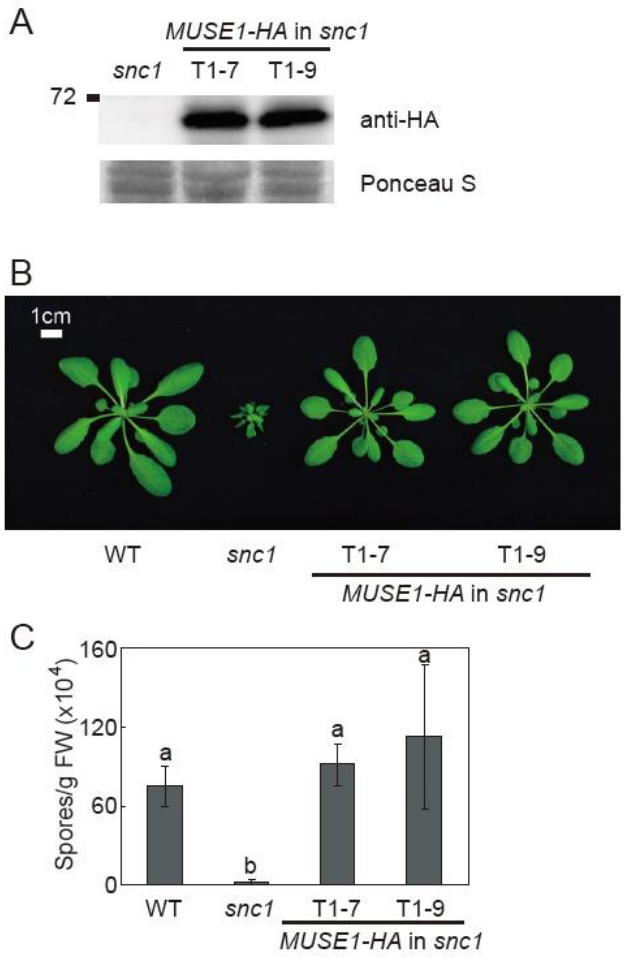

Figure 2.13: The internal HA tag in MUSE1-HA does not affect the function of the protein.

(A) Western blot analysis using the anti-HA antibody. Total proteins were extracted from three-week-old plants grown on 1/2 MS plates.

(B) Morphologies of four-week-old soil-grown plants of the indicated genotypes.

(C) Growth of *H.a.* Noco2 seven days after spray-inoculation with 10^5 spores/ml inoculum on ten-day-old seedlings. One-way ANOVA was used to calculate the statistical significance among genotypes, as indicated by different letters ($P < 0.005$). Error bar represents mean ±SD (n = 4).

MOS10 encodes a transcriptional co-repressor TOPLESS-RELATED 1 (TPR1), which functions with SNC1. Overexpression of *MOS10* leads to autoimmunity, which can be suppressed by the loss-of-function allele *snc1-r1* (Zhu et al., 2010). To test if MUSE1 affects the accumulation of MOS10, *MUSE1-HA* was transformed into a transgenic line expressing *MOS10-HA* (Zhu et al., 2010). In a western blot analysis using the anti-HA

antibody, I did not observe a significant difference in MOS10 protein levels in the 9 independent *MUSE1-HA* T1 transformants compared to that in the *MOS10-HA* background line (Figure 2.12C). This suggests that MUSE1 does not regulate MOS10 protein turnover.

In conclusion, overexpression of MUSE1 did not lead to decreased levels of all tested candidate proteins (Figure 2.12), indicating that these proteins are not likely ubiquitination and degradation substrates of MUSE1.

2.3 Discussion

This chapter reports the identification and characterization of two RING-type E3 ubiquitin ligases with overlapping functions, which specifically regulate defense responses in Arabidopsis mediated by the NLR protein SNC1.

The single knockout mutants *muse1* and *muse2* are WT-like whereas the *muse1-7 muse2-1* double mutant exhibits extreme autoimmune phenotypes (Figure 2.6B, C, D), indicating that MUSE1 and MUSE2 have overlapping functions. Despite this redundancy, multiple mutant alleles of *muse1* were successfully identified as *snc1* enhancers from the MUSE genetic screen (Figure 2.2A). This is reminiscent of the isolation of *muse13* from the MUSE screen, as *MUSE13* also has a functionally redundant paralog *MUSE14* (Huang et al., 2016). One explanation to this phenomenon is that the gain-of-function *snc1* allele serves as a sensitized genetic background for the screen, allowing isolation of mutants with otherwise subtle phenotypes. Another observation of note from the MUSE screen is that although a number of *muse1* alleles were isolated, no *muse2* alleles were found. This could be due to as-of-yet unexamined differences in the genomic architecture surrounding the two loci. For example, the *MUSE1* chromatin region may be less densely packed, thus more vulnerable to EMS mutagenesis.

Analysis of the microarray data from AtGenExpress was performed (Schmid et al., 2005; Winter et al., 2007) to provide insight into the expression pattern of *MUSE1* and *MUSE2*.

The expression profile of *MUSE1* was not available while *MUSE2* displayed no significant change in its expression level upon infection by various pathogens including *Pseudomonas syringae*, *Botrytis cineara*, *Phytophthora infestans* or *Hyaloperonospera arabidopsidis* when compared to the corresponding mock infected groups. It is thus possible that the regulation of the immunity-related activity of MUSE1 and MUSE2 occurs post-transcriptionally.

To determine the nature of the negative regulatory role of MUSE1 and MUSE2, I conducted a series of genetic and phenotypic analyses. Overexpression of *MUSE1* completely supresses the autoimmune phenotypes in *snc1* (Figure 2.8), but does not render these plants more susceptible to virulent pathogens including *P.s.m.* ES4326 or *H.a.* Noco2 (Figure 2.8D, E). Similarly, expression of *MUSE1* in WT does not enhance the susceptibility to *P.s.m.* ES4326 or *H.a.* Noco2 (Figure 2.9B, C). These results suggest that although MUSE1 does not seem to regulate general defense, it has a more SNC1-specific role. Moreover, from the infection assay using avirulent pathogens *H.a.* Emwa1 and *P.s.t.* DC3000 *AvrRps4* (Figure 2.9B, D), no significant difference in disease resistance was observed between *MUSE1* transgenic lines when compared to non-transgenic WT plants. Thus, MUSE1 does not seem to affect immunity mediated by other NLR proteins such as RPP4 or RPS4. In addition, the *muse1-7 muse2-1 snc1-r1* triple mutant is WT-like and exhibits no enhanced disease resistance compared with WT (Figure 2.10), suggesting that the SNC1-mediated defense pathway is fully responsible for the autoimmunity caused by loss of MUSE1 and MUSE2. Based on these exhaustive genetic analyses, I deduced that MUSE1 and MUSE2 likely contribute to the degradation of one or more positive defense regulators specifically involved in SNC1-mediated defense.

The identification of the ubiquitination substrate proteins of MUSE1 and MUSE2 will be the key to understanding the mechanism underlying their regulation of SNC1-specific immunity. The genetic and biochemical assays have ruled out SNC1, bHLH84 or MOS10 for being the ubiquitination and degradation substrate of MUSE1 and MUSE2 (Figure 2.12). To search for potential substrate(s) of MUSE1 and MUSE2, I conducted a yeast two-hybrid (Y2H)

screen using MUSE1 as bait. However, no meaningful interactors of MUSE1 was identified, except for ubiquitin, which is an expected interactor (data not shown). This could be explained by the transient nature of the E3 ligase-substrate interaction. It is also possible that the substrate is a low abundance protein that is under-represented in the cDNA library used and thus was missed in the Y2H screen. In addition, internally tagged MUSE1 could not be overexpressed even with a 35S promoter, suggesting a tight regulation of the protein levels of MUSE1 itself. Such technical difficulties prevent us from using immunoprecipitation-mass spectroscopy (IP-MS) analysis to search for potential MUSE1 interactors *in vivo*. Furthermore, I also attempted to isolate the MUSE1 target by conducting a *muse1 muse2* suppressor screen. However, all I identified from the screen were loss-of-function alleles of *snc1*. Thus MUSE1 and MUSE2 may ubiquitinate multiple substrates with overlapping functions and promote their degradation. Such a situation would have prevented the mutants of these substrates from being isolated from the genetic screen due to functional redundancy.

What could be the ubiquitination and degradation substrate of MUSE1/2? Since MUSE1 carries an NLS at its C-terminus, I propose that it likely ubiquinates an unknown protein that works together with SNC1 in the nucleus. In light of recent reports that NLR proteins often work in pairs (Narusaka et al., 2009; Cesari et al., 2013; Xu et al., 2015a), these substrates may be NLRs with overlapping functions that work together with SNC1 (Figure 2.14). Future identification of the protein substrates of MUSE1 and MUSE2 will reveal their precise roles in regulating SNC1-mediated immunity.

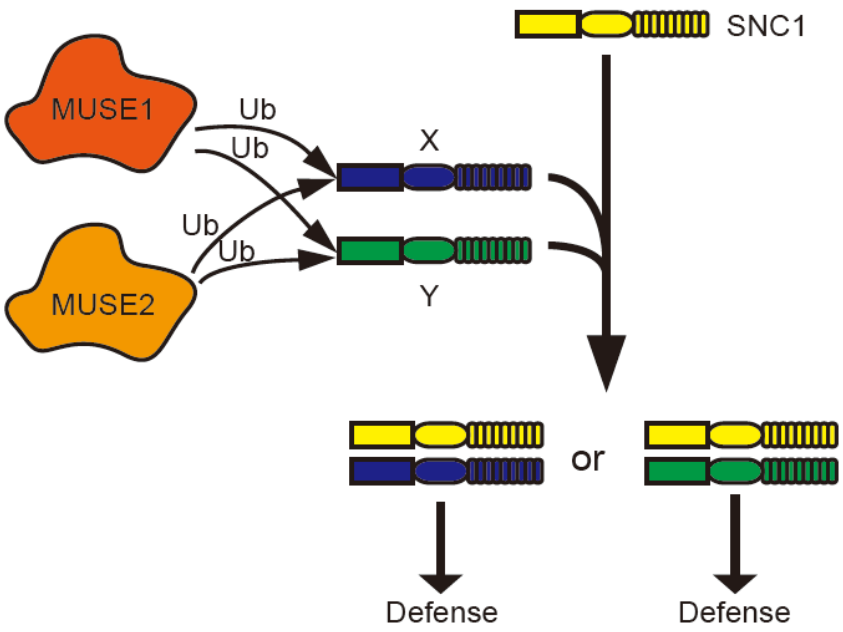

Figure 2.14: A hypothetical model illustrating the role of MUSE1 and MUSE2 in SNC1-mediated defense.

SNC1 likely triggers defense responses together with a pair of NLRs with overlapping functions, designated X and Y. These unknown NLRs are the protein ubiquitination substrates of functionally redundant E3 ubiquitin ligases MUSE1 and MUSE2. In *muse1 muse2* double mutant, X and Y accumulates, leading to autoimmunity.

2.4 Materials and methods

2.4.1 Plant growth, transformation, and genotyping

Arabidopsis plants were grown at 22ºC under 16hr light/8hr dark regime, unless otherwise specified. Binary vectors were constructed and transformed into *Agrobacterium* strain GV3101 by electroporation. Plant transformation was performed by the floral dip approach as previously described (Clough and Bent, 1998). Knockout T-DNA lines *muse1-7* and *muse2-1* were obtained from ABRC. All homozygous mutants or mutant combinations were confirmed by PCR genotyping. Homozygous *muse1-7* was crossed with *muse2-1,* and the *muse1-7 muse2-1* double mutant was isolated from the F2 generation. The *muse1-7 muse2-1* double mutant was crossed with homozygous *snc1-r1* and *eds1-2* to obtain

homozygous *muse1-7 muse2-1 snc1-r1* and *muse1-7 muse2-1 eds1-2* mutants, respectively. To genotype *snc1-r1*, primers F: 5'-CCT GGT GCC TGA ATG AAT TG-3' and R: 5'-ATC ATC CGA TGG TGT CAT AG-3' were used. To genotype *eds1-2*, primers F: 5'-ACA AGC CAA AGT GTC AAG CC-3' and R: 5'-CAA GCA TCC CTT CTA ATG TC-3' were used.

2.4.2 Construction of plasmids

The genomic sequence of *MUSE1* with 1596 bp upstream of the start codon was amplified. The amplified fragment was digested with *Bam* HI and *Sal* I and cloned into the binary vector *pCambia1305* to create the *pMUSE1::MUSE1* construct. To generate the HA-tagged MUSE1 recombinant protein, a DNA sequence encoding an HA tag was inserted at a predicted loop site through site-directed mutagenesis. The amplified *MUSE1-HA* coding sequence with 1596 bp upstream the start codon was digested with *Kpn* I and *Sal* I and cloned into binary vector *pGreen229*. Alternatively, the amplified *MUSE1-HA* coding sequence was digested with *Sal* I and *Bam* HI and cloned into binary vector *pGreen229-Han* which contains a 35S promoter. The coding sequence of *MUSE1* was amplified and digested with *Eco* RI and *Sal* I and cloned into expression vector *pGEX-4T-1* to create the *pGEX-GST-MUSE1* construct. To generate the dominant negative MUSE1^{H156Y} and MUSE1^{C159S} constructs, mutations were introduced by site-directed mutagenesis. The genomic sequences of *MUSE1^{H156Y}* and *MUSE1^{C159S}* with 1596 bp upstream of the start codon were amplified. The amplified fragment was digested with *Bam* HI and *Sal* I and cloned into binary vector *pCambia1305.*

2.4.3 Positional cloning of *muse1-1*

Primers used in mapping were designed based on Monsanto Arabidopsis polymorphism and Landsberg sequence collections (Jander et al., 2002). Map-based cloning was performed as previously described (Zhang et al., 2007a).

2.4.4 RNA extraction and quantitative RT-PCR

Total RNA was extracted from two-week-old seedlings grown on ½ MS medium using the Totally RNA kit (Ambion). Reverse transcription was performed using Superscript III (Invitrogen). RT-PCR was performed as described before (Zhang et al., 2003). Real-time PCR was performed using the Perfect Realtime Kit (TAKARA). The primers used for amplification of *PR1*, *PR2*, *ACT1* and *ACT7* were described previously (Cheng et al., 2009).

2.4.5 Pathogen infection assays

Infection assays by *Hyaloperonospora arabidopsidis* (*H.a.*) were performed as previously described (Clarke et al., 2000). Ten-day-old soil grown seedlings were spray-infected with freshly harvested *H.a.* spores re-suspended in water. Infected plants were kept at 18ºC with 80% humidity for 7 days before data collection. Growth of the pathogen was measured by counting the number of conidia spores per gram fresh weight. *Pseudomonas syringae* infection assays were performed as previously described (Bowling et al., 1997). Four-week-old soil grown plants were infected with various *Pseudomonas syringae* strains by leaf infiltration. Leaves were either harvested immediately after infection as Day 0 or harvested 72 hours after infection as Day 3 samples. Leaf discs from infected leaves were collected using a hole puncher and were ground in 10mM $MgCl_2$ solution and plated on LB medium with 50 μg/ml Streptomycin (for ES4326), Rifamycin (for DC3000 *hrcC*-) or Kanamycin (for DC3000 *AvrRps4*). The growth of the bacteria was quantified by the numbers of cfu per square centimeter.

2.4.6 *In vitro* ubiquitination assay

In vitro ubiquitination assay was performed according to previously described (Zhao et al., 2013), with modifications. Recombinant AtUBA2-His, GST-AtUBC8 and GST-MUSE1 were expressed in *E. coli* and purified by Ni-NTA chromatograph (QIAGEN) or GST affinity chromatograph (GSTrap FF, GE Healthcare), respectively. Ubiquitination reactions were

performed in a total volume of 30 µl, consisting of 50 mM Tris-HCl (pH 7.5), 10 mM $MgCl_2$, 10 mM ATP (Sigma), 100 ng AtUBA2-His, 200 ng GST-AtUBC8, 375 ng of GST-MUSE1 and 2 µg ubiquitin (Boston Biochem). Reactions were incubated at 30°C for 2 hours and terminated by adding sodium dodecyl sulfate (SDS) loading buffer (50 mM Tris-HCl (pH 6.8), 1% β-mercaptoethanol, 0.1% SDS, 0.1% bromophenol blue, 10% glycerol).

2.4.7 Plant protein quantification

Plant total protein was extracted from 100 mg of twelve-day-old 1/2 MS plate-grown plants by homogenization followed by addition of extraction buffer (100 mM Tris-HCl pH 8.0, 0.1% SDS and 2% β-mercaptoethanol). SDS loading buffer was added to each protein sample and boiled for 5 min. The resulting protein samples were subjected to western blot analyses. Bands were quantified using Image J.

2.4.8 Antibodies used

Anti-ubiquitin (Sigma U0508) or anti-GST (Sigma U7781) antibodies were used for the ubiquitination assay. The anti-SNC1 antibody was generated against a SNC1-specific peptide in rabbit (Li et al., 2010b). Anti-HA (Roche 11867423001) antibody was used to detect MUSE1-HA, MOS10-HA or bHLH84-HA.

2.4.9 Phylogenetic analysis

MUSE1-like peptides from *Zea mays*, *Solanum lycopersicum*, *Fragaria vesca*, *Medicago truncatula*, *Glycine max*, *Ricinus communis*, *Theobroma cacao*, *Arabidopsis thaliana* and *Arabidopsis lyrata* were identified by a BLASTp search using the amino acid sequence of *Arabidopsis thaliana* MUSE1 using database Plaza Dicot 3.0 (Proost et al., 2015) at http://bioinformatics.psb.ugent.be/plaza/versions/plaza_v3_dicots. Amino acid sequences of the MUSE1-like peptides in the above-mentioned species were obtained from Plaza Dicot 3.0. Amino acid sequences of the two MUSE1-like peptides from *Salix pupurea* were

download from Phytozome v11 at https://phytozome.jgi.doe.gov/pz/portal.html (Goodstein et al., 2012). The alignment was generated by MUSCLE with default settings (Edgar, 2004b, a). Maximum likelihood tree was generated by RAxML v7 (Stamatakis, 2014). Substitution model JTT+G+I+F based on prottest was adopted (Abascal et al., 2005).

3. TNL-mediated immunity in *Arabidopsis* requires complex regulation of the redundant *ADR1* gene family[1]

3.1 Introduction

Defense responses against pathogens in plants are mainly initiated by two types of immune receptors (Chisholm et al., 2006; Jones and Dangl, 2006). Plasma membrane-localized receptors perceive common pathogen associated molecular patterns (PAMPs) and initiate downstream signal transduction events, leading to host responses including the production of ROS, the deposition of callose and the increased expression of defense genes (Macho and Zipfel, 2014). Defense initiated through PAMP recognition is also known as PAMP-triggered immunity (PTI). In contrast, pathogen-encoded virulence factors (termed effector proteins) that have been delivered into host cells can be perceived by specific plant receptors typically belonging to the nucleotide-binding leucine-rich repeat protein (NLR; also as Nod-like receptor) family. Activation of NLRs usually triggers more rapid and robust defense responses, and is often characterized by the occurrence of cell death at the site of infection termed the hypersensitive response (HR). Immunity triggered by NLR activation is also known as effector-triggered immunity (ETI). NLR proteins have important functions in plant immunity, yet the molecular mechanisms by which they are activated remain largely unclear.

Based on their N-termini, typical plant NLRs can be further classified into Toll-like/Interleukin 1 receptor (TIR)-type NLRs (TNLs) and coiled-coil NLRs (CNLs) (Dangl and Jones, 2001; Li et al., 2015). In the mutant *snc1*, a gain-of-function mutation caused by a single amino acid substitution in TNL SNC1 leads to constitutive defense responses (Li et al., 2001; Zhang et al., 2003). Mutant *snc1* plants exhibit a characteristic autoimmune

---

[1] This chapter is based on part of a published article. Oliver Xiaoou Dong, Meixuezi Tong, Vera Bonardi, Farid El Kasmi, Virginia Woloshen, Lisa K. Wünsch, Jeffery L. Dangl and Xin Li. (2016). TNL-mediated immunity in Arabidopsis requires complex regulation of the redundant ADR1 gene family. *New Phytologist*. 10.1111/nph.13821

morphology including stunted growth and curled leaves (Li et al., 2001). The severity of the *snc1* phenotypes correlates with the level of defense output, making *snc1* a useful tool for genetic screening. Indeed, from the previous *modifier of snc1* (*mos*) screen, 13 MOS proteins were identified that contribute to *SNC1*-mediated immunity (Johnson et al., 2012).

In *Arabidopsis*, *ACTIVATED DISEASE RESISTANCE 1* (*ADR1, At1g33560*), *ADR1-LIKE 1* (*ADR1-L1, At4g33300*) and *ADR1-LIKE 2* (*ADR1-L2*, *At5g04720*) all encode CNLs (Bonardi et al., 2011). ADR1 family members function redundantly as positive regulators of basal defense and ETI mediated by the CNL protein RPS2 and TNLs RECOGNITION OF *PERONOSPERA PARASITICA* 2 (RPP2) and RPP4 (Bonardi et al., 2011). A common feature of all three ADR1 family members is their N terminal coiled-coil domain, which resembles *Arabidopsis* RPW8 and is referred to as CC_R (Collier et al., 2011). Another CC_R-NB-LRR protein is NRG1 in *Nicotiana benthamiana*, which is required for the function of tobacco TNL N (Peart et al., 2005; Collier et al., 2011). These studies defined CC_R-NB-LRRs as helper NLRs in the signaling of other NLR proteins. It is important to note that their designation as helper NLRs does not discount a possible additional function as sensor NLRs in the context of as yet undiscovered effectors that could be recognized by this fascinating NLR class (Bonardi et al., 2011).

This chapter reports that loss-of-function *adr1-L1* mutants enhance *snc1*. Quantitative RT-PCR analysis indicates that the enhanced autoimmunity may be due to transcriptional over-compensation by *ADR1* and *ADR1-L2* in the *adr1-L1* background. These results suggest that homeostasis of the ADR1 family is a key feature of their combined function as helper NLRs.

3.2 Results

3.2.1 Isolation and characterization of two allelic *muse* mutants from a modified *snc1* enhancer screen

Novel negative regulators of plant immunity were screened for in either *snc1 mos4* or *snc1 mos2 npr1* genetic backgrounds using EMS as mutagen (Huang et al., 2013). Two *muse* mutants, *muse15-1* and *muse15-2,* were isolated independently from the *snc1 mos4* and *snc1 mos2 npr1* genetic backgrounds, respectively (Figure 3.1A, B). Both mutants altered the *snc1 mos* morphology back to *snc1*-like. Segregation from backcrossed F2 populations suggested the presence of a single recessive mutation in each mutant. *snc1 mos4 muse15-1* and *snc1 mos2 npr1 muse15-2* failed to complement each other in an F1 allelism test (Figure 3.1C), suggesting that they carry mutations in the same gene. Besides their dwarf stature and curled leaves (Figure 3.1A, B), both mutants exhibited increased expression of defense marker genes *PR1* and *PR2* (Figure 3.1D), and enhanced disease resistance to the virulent oomycete pathogen *H.a.* Noco2 (Figure 3.1E). As both *muse15* alleles are recessive, they likely carry loss-of-function mutations that enhance the *snc1* autoimmune phenotypes.

3.2.2 *MUSE15* encodes ADR1-L1, a CC_R-NB-LRR protein

To map the *muse15-1* and *muse15-2* mutations, the original enhancer mutants (in Col-0 ecotype) were crossed with Landsberg *erecta* (L*er*). The F1 individuals were selfed to generate a mapping population. Among F2s, individuals displaying enhanced *snc1* phenotypes were selected for linkage analysis. Consistent with the allelism test result (Figure 3.1C), crude mapping revealed that *muse15-1* and *muse15-2* are both located at the bottom of chromosome 4. Subsequently, *muse15-1* was further mapped between markers F26P21 and F17I5 (Figure 3.2A). To identify the molecular lesion in *muse15-2*, nuclear DNA from plants homozygous for *muse15-2* was used for whole-genome re-sequencing by an Illumina sequencer. When the *muse15-2* sequence was compared with

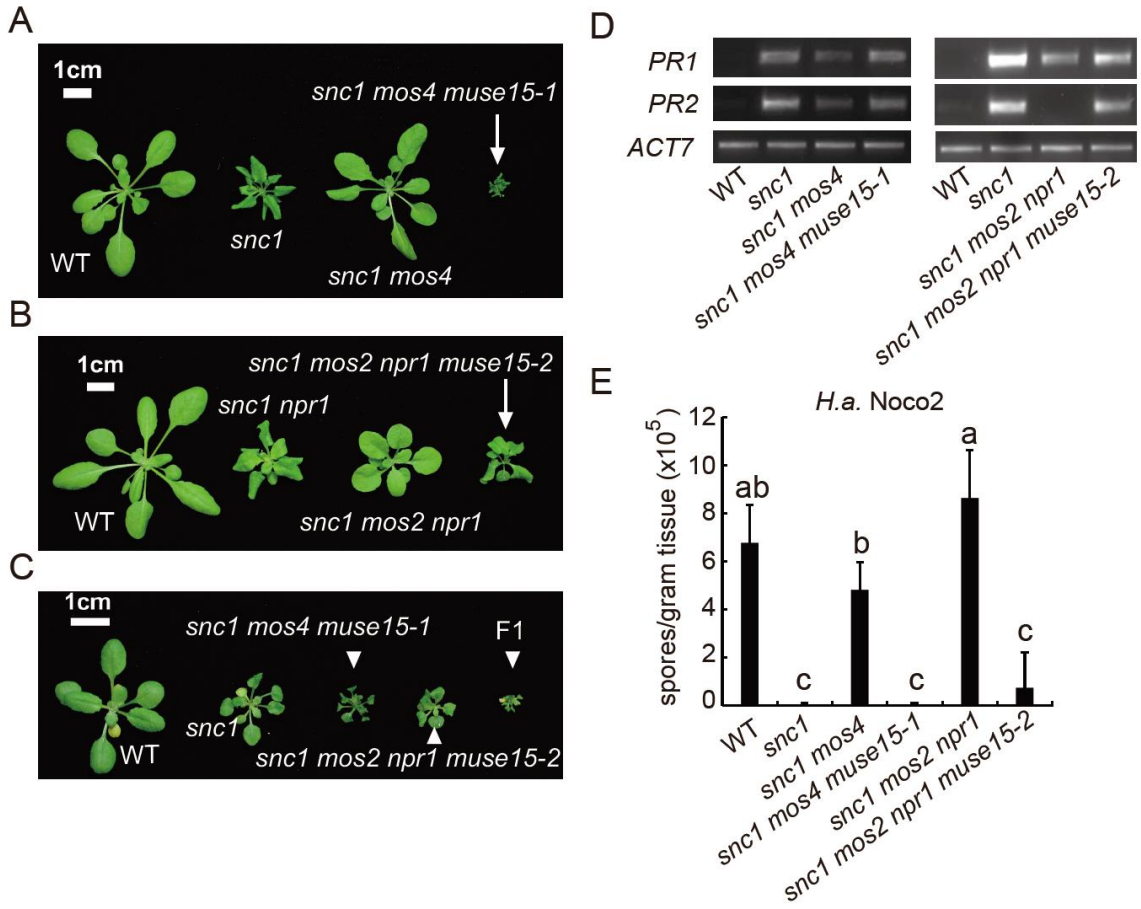

Figure 3.1: Two allelic *muse15* mutants enhance immunity in the *snc1 mos4* or *snc1 mos2 npr1* background.

(A) Morphological phenotypes of four-week-old Col-0 (WT), *snc1*, *snc1 mos4* and *snc1 mos4 muse15-1* plants grown at 22°C under long day conditions (16hr light/8hr dark).

(B) Morphological phenotypes of four-week-old WT, *snc1*, *snc1 mos2 npr1* and *snc1 mos2 npr1 muse15-2* plants grown at 22°C under long day conditions.

(C) Morphological phenotypes of three-week-old WT, *snc1*, *snc1 mos4 muse15-1*, *snc1 mos2 npr1 muse15-2* and an F1 plant from the cross between *snc1 mos4 muse15-1* and *snc1 mos2 npr1 muse15-2* grown at 22°C under long day conditions.

(D) Expression of defense marker genes *PR1* and *PR2* in WT, *snc1*, *snc1 mos4*, *snc1 mos4 muse15-1*, *snc1 mos2 npr1* and *snc1 mos2 npr1 muse15-2* plants. Reverse Transcription (RT)-PCR was performed on two-week-old seedlings grown on 1/2 MS plates. *ACT7* was included as loading control.

(E) Growth of *H.a.* Noco2 seven days after spray-infection with 10^5 spores/mL inoculum on WT, *snc1*, *snc1 mos4*, *snc1 mos4 muse15-1*, *snc1 mos2 npr1* and *snc1 mos2 npr1 muse15-2* plants. One-way ANOVA was used to calculate the statistical significance between genotypes, as indicated by different letters ($P < 0.01$). Bars represent mean ±SD (n = 4).

WT Col-0 reference sequence in the region between F26P21 and F17I5, a single G to A mutation was identified, which is consistent with EMS mutagenesis. This mutation is predicted to cause a single amino acid Pro513 to Leu change in the polypeptide encoded by *ADR1-L1* (*At4g33300*) (Figure 3.2B). I then sequenced *ADR1-L1* in homozygous *muse15-1* plants by Sanger method and identified a separate G to A mutation located at an exon-intron junction (Figure 3.2C). This mutation presumably alters the splicing pattern of the gene, leading to early truncation of the encoded protein.

To further confirm that the two mutations identified in *muse15* alleles are responsible for the *snc1*-enhancing phenotypes, *snc1* was crossed with a known loss-of-function T-DNA *adr1-L1* allele, SAIL_302_C06 (Bonardi et al., 2011). Compared with *snc1* plants, the *snc1 adr1-L1* double mutant exhibits more severe stunted growth and curled leaves, which is consistent with the *snc1*-enhancing phenotypes of *muse15-1* and *muse15-2* mutants (Figure 3.2D, E). Taken together, *MUSE15* is *ADR1-L1* and that the new, herein identified *adr1-L1* alleles are also loss-of-function mutants.

ADR1-L1 encodes a RPW8 CC_R-type CNL protein (Figure 3.2B). Together with ADR1 and ADR1-L2, these three NLRs function redundantly to regulate the accumulation of the defense hormone SA (Bonardi et al., 2011). *adr1 triple* mutants exhibit enhanced susceptibility to virulent and avirulent pathogens, suggesting ADR1 proteins function redundantly in immune signaling (Bonardi et al., 2011). However, the *snc1*-enhancing phenotypes of *adr1-L1* observed here are seemingly opposite to the *adr1 triple* mutant phenotypes, suggesting that ADR1-L1 has a unique negative regulatory role in defense besides its redundant positive functions with ADR1 and ADR1-L2.

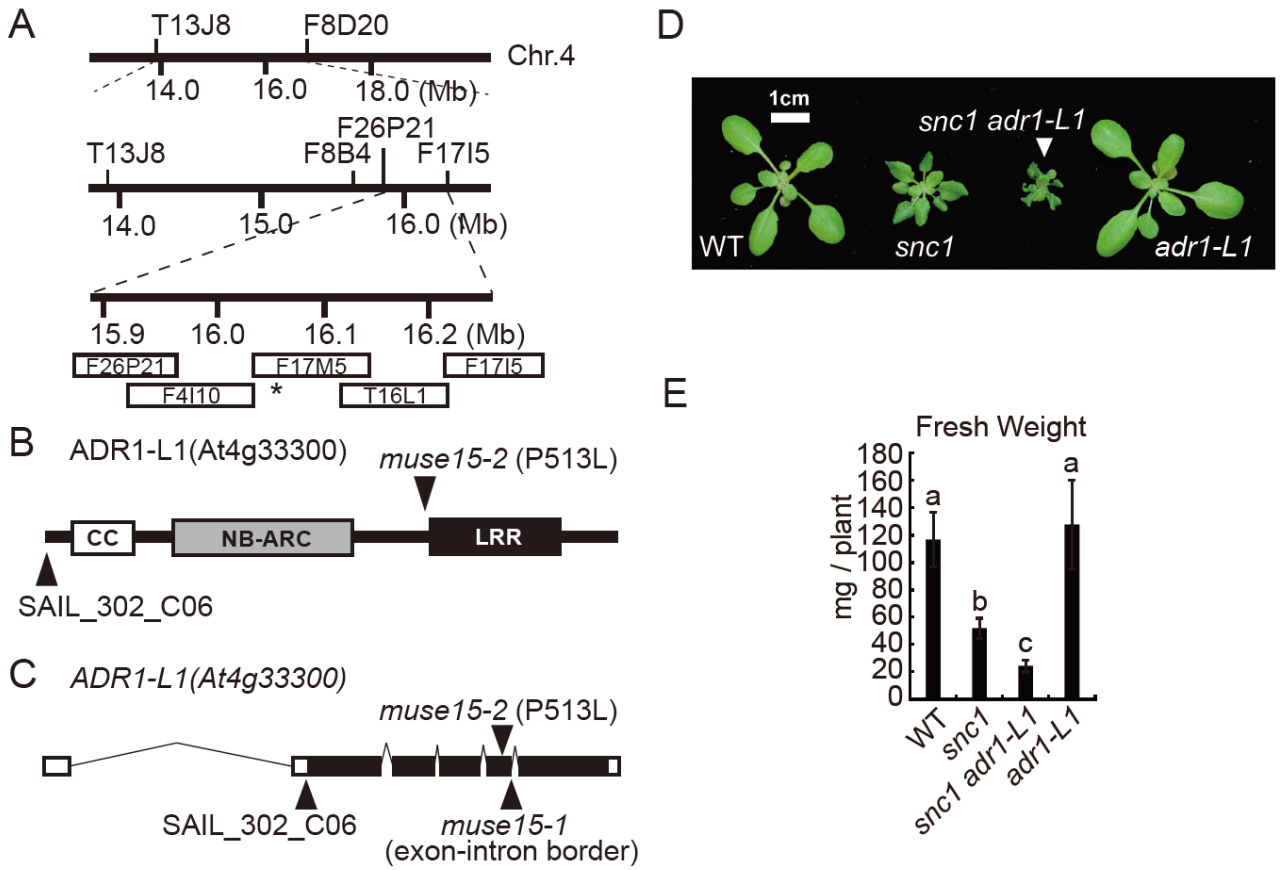

Figure 3.2: Positional cloning of *muse15.*

(A) Map position of *muse15*. The asterisk indicates the site of *muse15-2* mutation.

(B) Schematic diagram showing the predicted ADR1-L1 protein structure with arrows indicating the sites of mutations in *muse15-2* and *adr1-L1* (SAIL_302_C06).

(C) Schematic diagram showing the predicted *ADR1-L1* gene structure with arrows indicating the sites of mutations in *muse15-1*, *muse15-2* and SAIL_302_C06.

(D) Morphological phenotypes of four-week-old WT, *snc1*, *snc1 adr1-L1* and *adr1-L1* plants grown at 22°C under long day conditions.

(E) Fresh weights of four-week-old WT, *snc1*, *snc1 adr1-L1* and *adr1-L1* plants grown at 22°C under long day conditions. One-way ANOVA was used to calculate the statistical significance between genotypes, as indicated by different letters ($P < 0.01$). Bars represent mean ±SD (n = 20).

3.2.3 ADR1-L1 does not affect SNC1 protein turnover

Several previously described *muse* mutants exhibit increased SNC1 protein accumulation (Huang et al., 2014a; Huang et al., 2014b; Xu et al., 2015b), therefore these MUSE proteins contribute to SNC1 turnover. To address why *adr1-L1* enhances *snc1*, I first tested whether ADR1-L1 regulates the autoimmune phenotypes in *snc1* through affecting SNC1 protein accumulation. SNC1 protein level is increased significantly in *snc1 adr1-L1* compared to that in *snc1* (Figure 3.3A). However, this accumulation correlates with the enhanced *SNC1* transcription observed in the double mutant (Figure 3.3B). To avoid the feedback up-regulation of *SNC1* transcription as in *snc1 adr1-L1*, I examined SNC1 protein accumulation in *adr1-L1*. No difference in steady-state SNC1 levels was observed between WT and *adr1-L1* (Figure 3.3C). Similarly, in the WT like *snc1 pad4 adr1-L1* triple mutant, where the SA-dependent positive feedback transcriptional up-regulation of *SNC1* is blocked, no significant difference in SNC1 protein level was observed when compared to *snc1 pad4* (Figure 3.3D, E). These results suggest that ADR1-L1 does not enhance the autoimmune phenotypes in *snc1* through affecting SNC1 protein turnover.

3.2.4 The autoimmune-enhancing phenotype of *snc1 adr1-L1* is not fully dependent on SA accumulation

SA plays a major role in defense amplification. Since the autoimmune phenotypes of *snc1* are partly dependent on SA levels (Zhang et al., 2003), and the ADR1 family regulates SA accumulation (Bonardi et al., 2011), I tested whether the *snc1*-enhancing phenotypes in *snc1 adr1-L1* depend on SA accumulation. The SA deficient mutant *enhanced disease susceptibility 5* (*eds5*) was crossed with *snc1 adr1-L1* to generate the *snc1 eds5-3 adr1-L1* triple mutant. Although the triple mutant partially rescued the *snc1 adr1-L1* phenotype, it was significantly smaller than *snc1 eds5-3* (Figure 3.4), suggesting that the *snc1*-enhancing effects observed from *adr1-L1* are not fully dependent on SA accumulation.

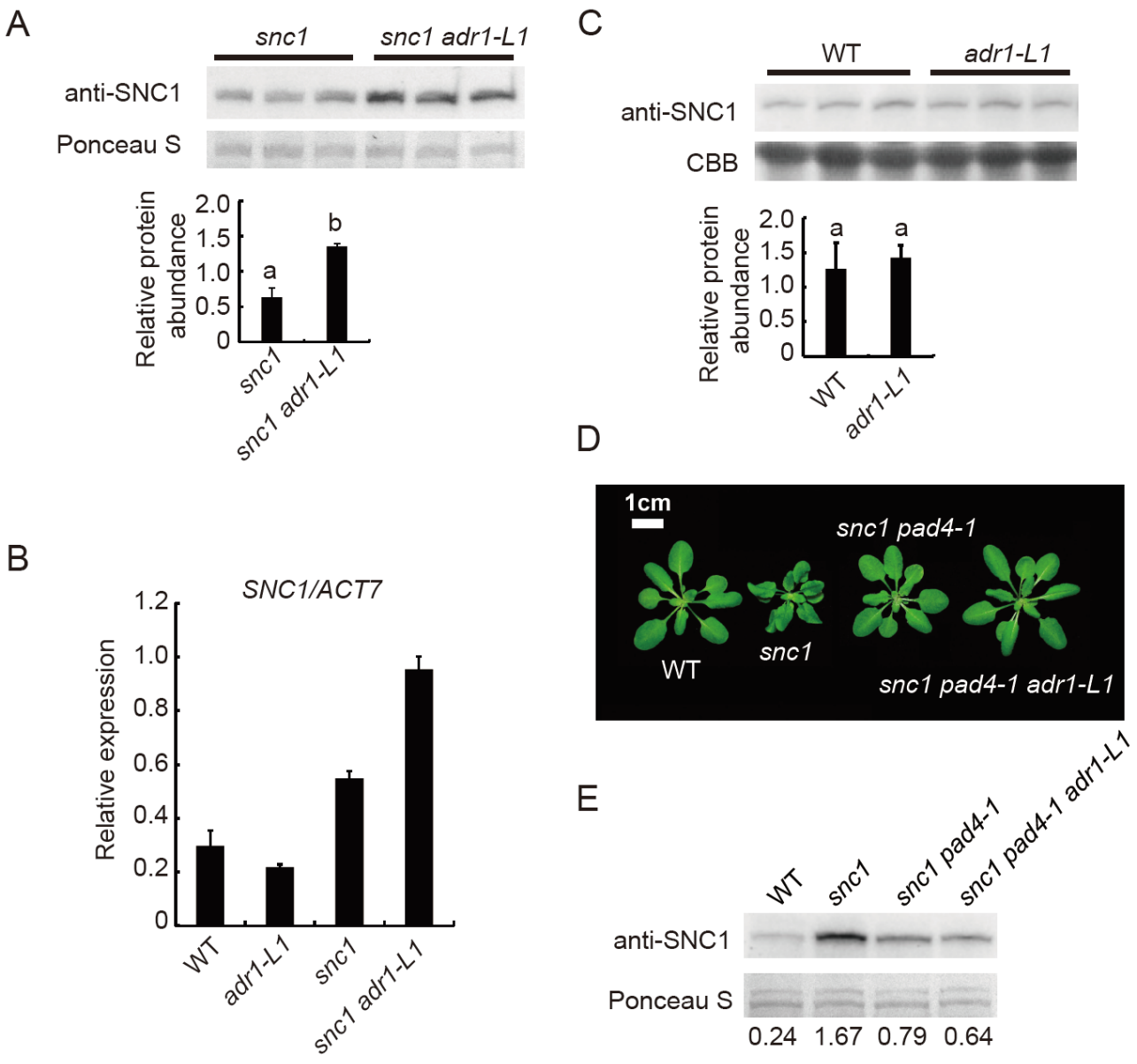

Figure 3.3: ADR1-L1 does not affect SNC1 turnover.

(A) Upper: western blot analysis using an anti-SNC1 antibody. Leaf total protein was extracted from four-week-old plants grown at 22°C under long day conditions. Lower: Quantification of the relative intensity of the SNC1 bands to a nonspecific band in Ponceau S staining in the upper panel. Pairwise t-test was used to calculate the statistical significance between genotypes, as indicated by different letters ($P < 0.05$). Bars represent mean ±SD (n = 3).

(B) *SNC1* transcript levels in WT, *adr1-L1*, *snc1* and *snc1 adr1-L1* plants. qRT-PCR was performed on four-week-old plants grown at 22°C under long day conditions. *ACT7* was used to normalize the transcript levels. Arbitrary unit was used to show the relative abundance of *SNC1* transcript levels as compared to that in WT. Bars represent mean ±SD (n = 3).

(C) Upper: western blot analysis using an anti-SNC1 antibody. Leaf total protein was extracted from four-week-old plants grown at 22°C under long day conditions. Lower: Quantification of the relative intensity of the SNC1 bands to a nonspecific band from CBB staining in the upper panel. Pairwise t-test was used to calculate the statistical significance between genotypes, as indicated by different letters ($P < 0.01$). Bars represent mean ±SD (n = 3).

(D) Morphological phenotypes of four-week-old WT, *snc1*, *snc1 pad4-1* and *snc1 pad4-1 adr1-L1* plants grown at 22°C under long day conditions.

(E) Western blot analysis using an anti-SNC1 antibody on the indicated genotypes. Leaf total protein was extracted from four-week-old plants grown at 22°C under long day conditions. Numbers underneath indicate the relative intensity of the SNC1 band to a nonspecific band in Ponceau S staining.

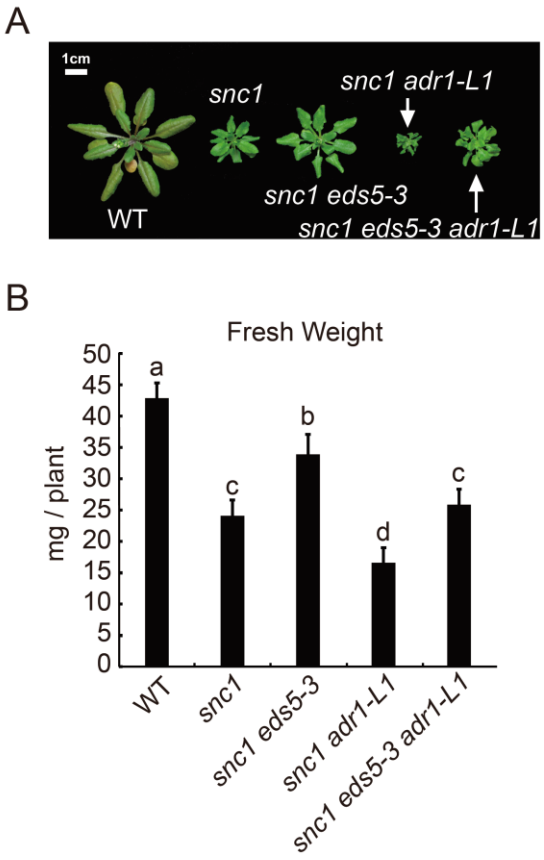

Figure 3.4: The defense-enhancing phenotypes in *snc1 adr1-L1* are not fully dependent on SA accumulation.

(A) Morphological phenotypes of four-week-old WT, *snc1*, *snc1 eds5-3*, *snc1 adr1-L1* and *snc1 eds5-3 adr1-L1* plants grown at 22°C under long day conditions.

(B) Fresh weights of three-week-old WT, *snc1*, *snc1 eds5-3*, *snc1 adr1-L1* and *snc1 eds5-3 adr1-L1* plants grown at 22°C under long day conditions. One-way ANOVA was used to calculate the statistical significance between genotypes, as indicated by different letters ($P < 0.001$). Bars represent mean ±SD (n = 10).

3.2.5 Loss of ADR1-L1 leads to transcriptional up-regulation of *ADR1* and *ADR1-L2*

Constitutive increase in steady state NLR protein levels often results in autoimmune phenotypes (Tang et al., 1999; Tao et al., 2000; Frost et al., 2004; Cheng et al., 2011; Gou et al., 2012). Not surprisingly, over-expression of *ADR1* also leads to autoimmunity (Grant et al., 2003). I therefore tested if the loss of *ADR1-L1* could be over-compensated by increased expression of its paralogs, *ADR1* and *ADR1-L2*. When the transcript levels of *ADR1* and *ADR1-L2* in WT, *adr1-L1*, *snc1* and *snc1 adr1-L1* were compared, I noted a consistent two-fold increase in *ADR1* transcript levels, and a 50% increase in *ADR1-L2* expression in *snc1 adr1-L1* compared to *snc1* (Figure 3.5A, B). I also consistently observed a slight, yet not always significant, increase of both *ADR1* and *ADR1-L2* transcripts in *adr1-L1* compared to WT (Figure 3.5A, B; 3.6). *ADR1* seems to compensate more than *ADR1-L2*.

3.2.6 *adr1-L1* enhances the autoimmune phenotypes in some, but not all autoimmune mutants

To test the specificity of the immunity-enhancing effects of *adr1-L1*, I crossed the T-DNA knockout allele of *adr1-L1* with a collection of autoimmune mutants. Increased SNC1 protein level leads to a similar autoimmune phenotype as that observed in mutant *snc1* (Xu et al., 2014a). Therefore, I crossed *adr1-L1* with a set of genetic backgrounds that exhibit increased SNC1 protein levels. These included *cpr1*, *bal* and *SNC1* transgenic over-expression lines. *CPR1* encodes an F-box protein that facilitates the degradation of SNC1 and RPS2 (Cheng et al., 2011). In knockout mutant *cpr1-3*, over-accumulation of SNC1 contributes partly to its autoimmune phenotypes (Cheng et al., 2011). In the *cpr1-3 adr1-L1* double mutant, the autoimmune phenotypes of *cpr1-3* were significantly enhanced by *adr1-L1*, as illustrated by plant size (Figure 3.5C), fresh weight (Figure 3.5D) and total SA measurements of the mutant plants (Figure 3.5E). A duplication within the *RPP4* cluster also results in heightened expression of *SNC1* in the *bal* mutant, resulting in *snc1*-like autoimmunity (Stokes et al., 2002; Yi and Richards, 2009). Similarly, transgenic

overexpression of WT *SNC1* or mutant *snc1* in Col-0 results in severe autoimmune phenotypes (Xu et al., 2014a). The autoimmune phenotypes of *bal* and transgenic *SNC1-* or *snc1*-overexpression lines were all enhanced by *adr1-L1* (Figure 3.5F, G), suggesting that SNC1-mediated defense can be enhanced by knocking out *ADR1-L1,* independent of the gain-of-function mutation in *snc1.* Such enhancement does not rely on the chromosomal location of the *SNC1* gene, as manifested by the phenotypic enhancement of transgenic *SNC1-* or *snc1*-overexpression lines by *adr1-L1*.

Lesion Simulating Disease 1 (*LSD1*) encodes a zinc finger protein involved in the negative regulation of pathogen-induced cell death (Dietrich et al., 1997). Loss-of-function mutant *lsd1-2* plants exhibit abnormal superoxide accumulation and excessive cell death upon induction (Jabs et al., 1996). Under the growth conditions in the Li Lab, the *lsd1-2 adr1-L1* double mutant exhibited a *snc1*-like autoimmune phenotype (Figure 3.5H), which was absent in the *lsd1-2* single mutant. The *lsd1-2* mutant exhibited spontaneous cell death (Figure 3.5H), which differs from the previously reported inducible cell death phenotype of *lsd1-2* (Jabs et al., 1996). This could be due to the difference in the light regime used for plant growth. Interestingly, the cell death phenotype of *lsd1-2* is suppressed by *adr1-L1* (Figure 3.7A). Overall, the *lsd1 adr1-L1* phenotypes suggest that the immunity-enhancing effect of *adr1-L1* is also active in the *lsd1-2* background, and is not specific to *snc1*.

In the autoimmune mutant *suppressor of npr1-1, constitutive 2* (*snc2-1D*), a gain-of-function mutation in a receptor-like protein (RLP) confers constitutively activated defense responses (Zhang et al., 2010). SNC2 likely functions with other membrane-bound proteins in the perception of unidentified PAMPs (Yang et al., 2012). As shown in Figure 3.8A, the autoimmune phenotype of *snc2-1D* was not enhanced by *adr1-L1*. Similarly, the autoimmune phenotypes of *snc4-1D*, a gain-of-function mutation in the RLK SUPPRESSOR OF NPR1-1, CONSTITUTIVE 4 (SNC4) that leads to constitutive defense responses (Bi et al., 2010), were not enhanced by *adr1-L1* either (Figure 3.8B). These results suggest that *adr1-L1* does not enhance autoimmunity triggered by gain-of-function mutants of these specific RLP and RLK.

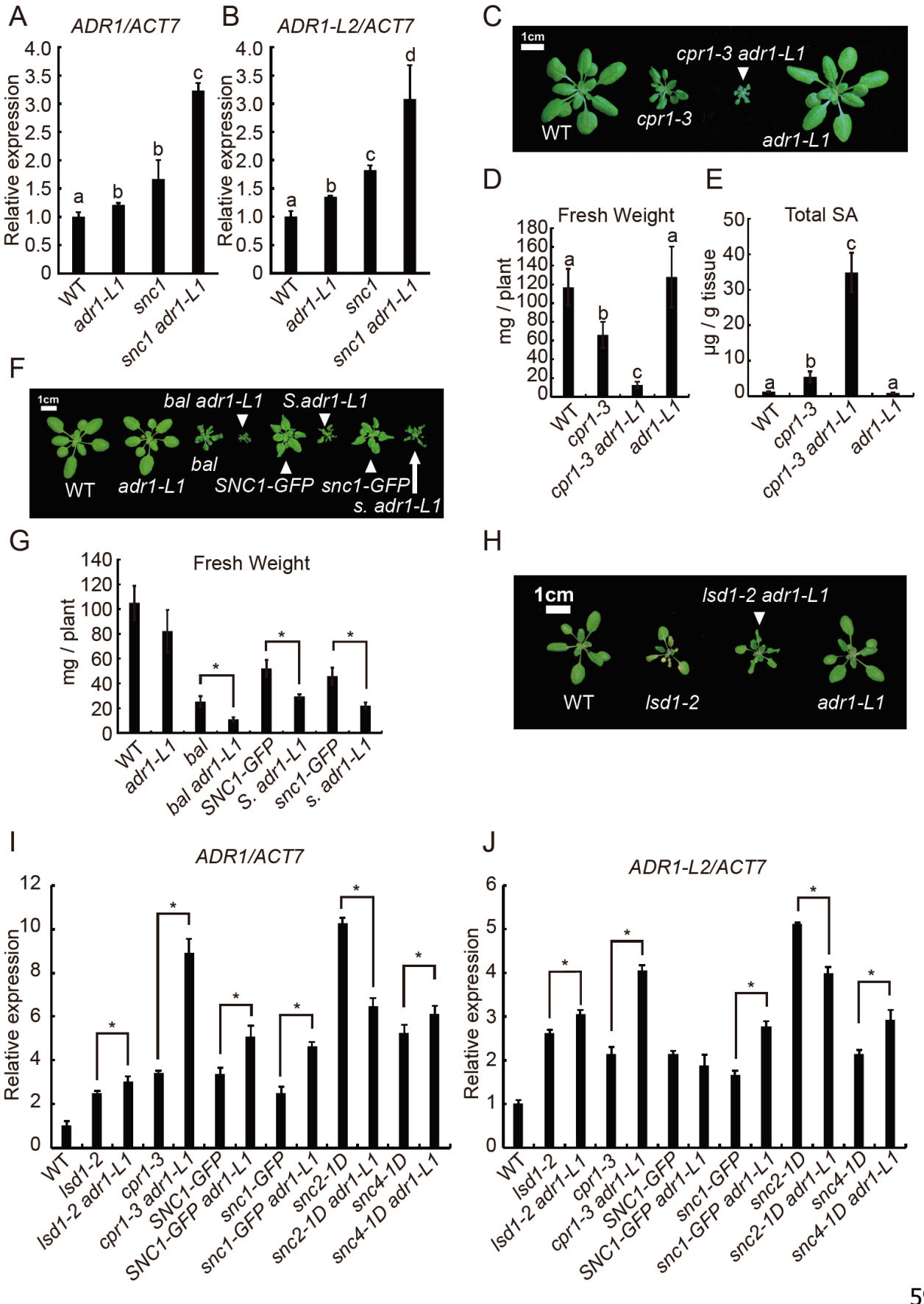
A
ADR1/ACT7
Relative expression
WT
adr1-L1
snc1
snc1 adr1-L1
B
ADR1-L2/ACT7
C
1cm
cpr1-3 adr1-L1
cpr1-3
WT
adr1-L1
D
Fresh Weight
mg / plant
cpr1-3 adr1-L1
E
Total SA
µg / g tissue
F
bal adr1-L1
S.adr1-L1
bal
SNC1-GFP
snc1-GFP
s. adr1-L1
G
Fresh Weight
bal
bal adr1-L1
SNC1-GFP
S. adr1-L1
snc1-GFP
s. adr1-L1
H
lsd1-2 adr1-L1
lsd1-2
I
ADR1/ACT7
lsd1-2
lsd1-2 adr1-L1
cpr1-3
cpr1-3 adr1-L1
SNC1-GFP
SNC1-GFP adr1-L1
snc1-GFP
snc1-GFP adr1-L1
snc2-1D
snc2-1D adr1-L1
snc4-1D
snc4-1D adr1-L1
J
ADR1-L2/ACT7

Figure 3.5: *adr1-L1* enhances the autoimmune phenotypes of some, but not all, autoimmune mutants tested, leading to increased *ADR1* and *ADR1-L2* transcript levels.

(A, B) *ADR1* and *ADR1-L2* transcript levels in the indicated genotypes. qRT-PCR was performed on two-week-old seedlings grown on 1/2 MS plates. *ACT7* was used to normalize the transcript levels. Values for WT were set as 1.0. Pairwise t-tests were used to calculate the statistical significance between genotypes, as indicated by different letters ($P < 0.05$). Bars represent mean ±SD (n = 3). The whole experiment involving all four genotypes was biologically repeated twice. Experiment with WT and *adr1-L1* was biologically repeated for two additional times (four times in total). Please refer to Figure 3.6 for data from the other three biological repeats on WT and *adr1-L1.*

(C) Morphological phenotypes of four-week-old WT, *cpr1-3*, *cpr1-3 adr1-L1* and *adr1-L1* plants grown at 22°C under long day conditions.

(D) Fresh weights of four-week-old WT, *cpr1-3*, *cpr1-3 adr1-L1* and *adr1-L1* plants grown at 22°C under long day conditions. One-way ANOVA was used to calculate the statistical significance between genotypes, as indicated by different letters ($P < 0.01$). Bars represent mean ±SD (n = 20).

(E) Total SA levels of four-week-old WT, *cpr1-3*, *cpr1-3 adr1-L1* and *adr1-L1* plants grown at 22°C under long day conditions. Multiple t-tests were used to calculate the statistical significance between genotypes, as indicated by different letters ($P < 0.01$). Bars represent mean ±SD (n = 4).

(F) Morphological phenotypes of four-week-old WT, *adr1-L1*, *bal*, *bal adr1-L1*, *SNC1-GFP*, *SNC1-GFP adr1-L1* (*S. adr1-L1*), *snc1-GFP* and *snc1-GFP adr1-L1* (*s. adr1-L1*) plants grown at 22°C under long day conditions.

(G) Fresh weights of four-week-old WT, *adr1-L1*, *bal*, *bal adr1-L1*, *SNC1-GFP*, *SNC1-GFP* in *adr1-L1*, *snc1-GFP* and *snc1-GFP* in *adr1-L1* plants grown at 22°C under long day conditions. Pairwise t-tests were used to calculate the statistical significance between genotypes, as indicated by asterisks ($P < 0.001$). Bars represent mean ±SD (n = 5).

(H) Morphological phenotypes of three-week-old WT, *lsd1-2*, *lsd1-2 adr1-L1* and *adr1-L1* plants grown at 22°C under long day conditions.

(I, J) *ADR1* and *ADR1-L2* transcript levels in the indicated genotypes. qRT-PCR was performed on three-week-old soil-grown plants grown at 22°C under long day conditions. *ACT7* was used to normalize the transcript levels. Values for WT were set as 1.0. Pairwise t-tests were used to calculate the statistical significance between genotypes, as indicated by asterisks ($P < 0.05$). Bars represent mean ±SD (n = 3). The whole experiment was biologically repeated twice with similar trends.

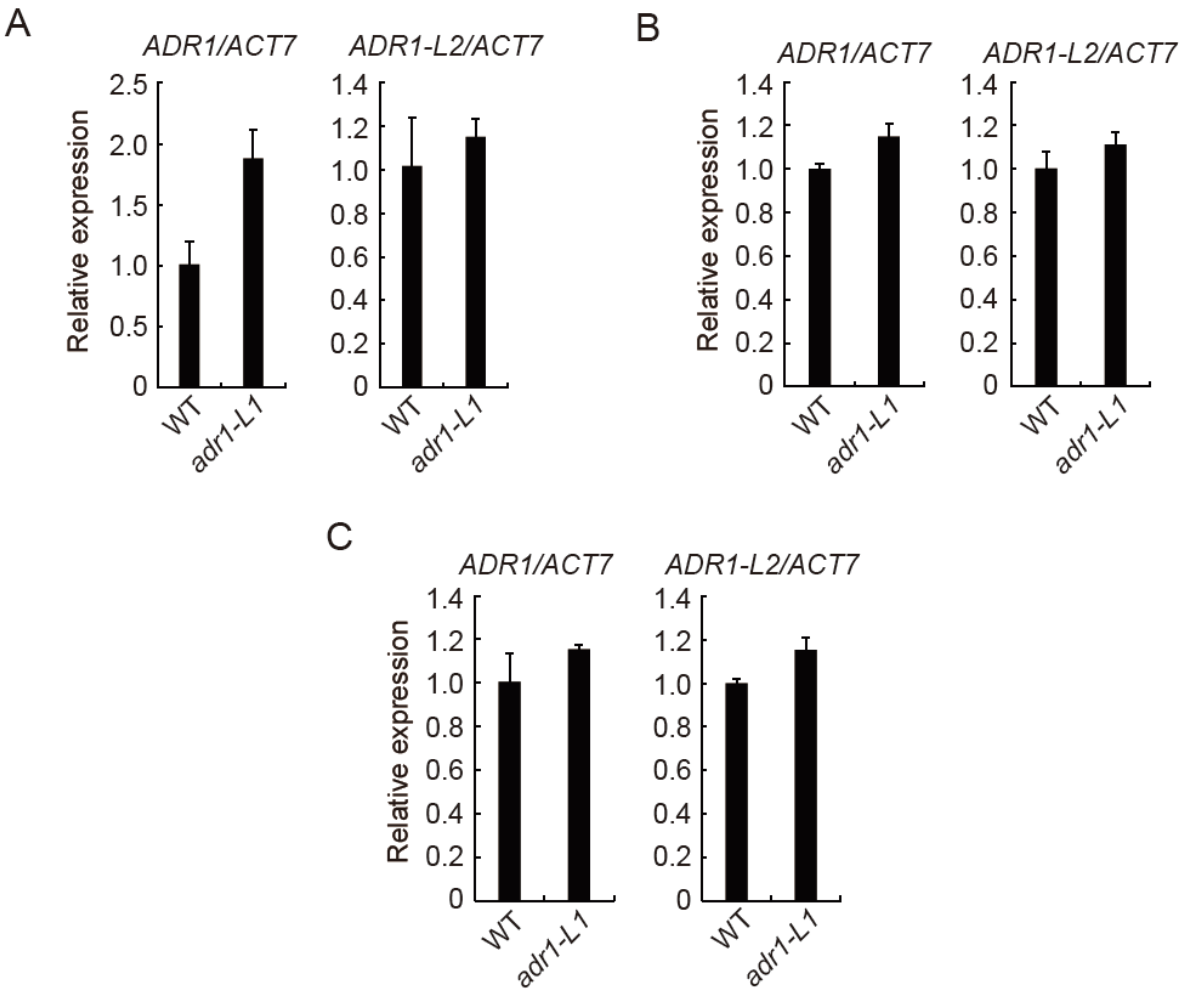

Figure 3.6: Three additional biological repeats showing that transcript levels of *ADR1* and *ADR1-L2* are consistently up-regulated in *adr1-L1*.

(A-C) *ADR1* and *ADR1-L2* transcript levels in WT and *adr1-L1* plants in three independent biological repeats. qRT-PCR was performed on two-week-old seedlings grown on 1/2 MS plates. *ACT7* was used to normalize the transcript levels. Values for WT were set as 1.0. Bars represent mean ±SD (n = 3).

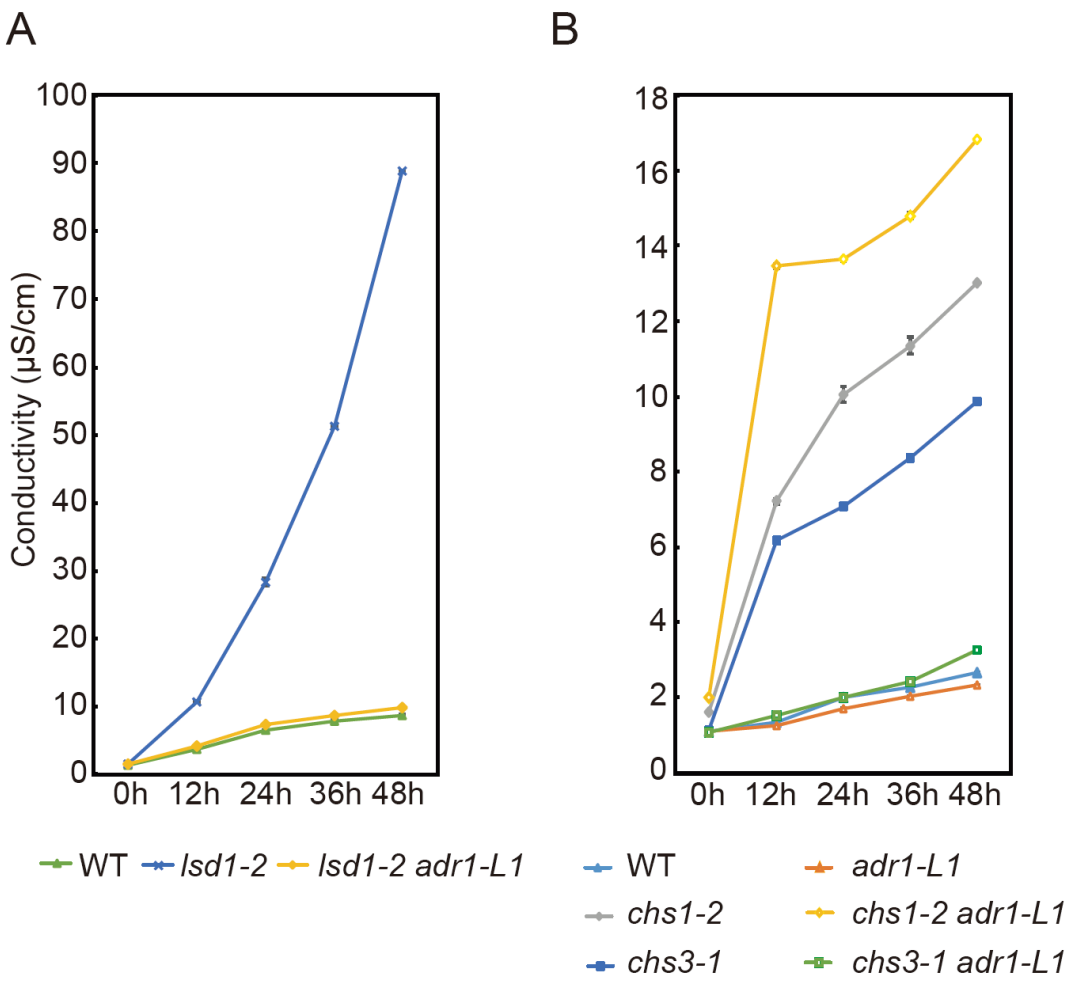

Figure 3.7: *adr1-L1* fully suppresses the cell death phenotype of *lsd1-2* and *chs3-1*, but not that of *chs1-2*.

(A) Ion leakage measurements for WT, *lsd1-2* and *lsd1-2 adr1-L1* plants. Six leaf discs from four-week-old plants grown at 22°C under long day conditions were used for each genotype. Three consecutive measurements were performed. Values are means ±SD (n = 3). The whole experiment was repeated with independent samples twice, with similar results.

(B) Ion leakage measurements for WT, *adr1-L1*, chs1-2, *chs1-2 adr1-L1*, *chs3-1* and *chs3-1 adr1-L1* plants. Seeds were germinated at 22°C under long day conditions and one-week-old seedlings were transferred to 18°C for the cell death phenotypes to be observed. Two two-week-old seedlings were used for each genotype. Three consecutive measurements were performed. Values are means ±SD (n = 3). The whole experiment was repeated with independent samples twice, with similar results.

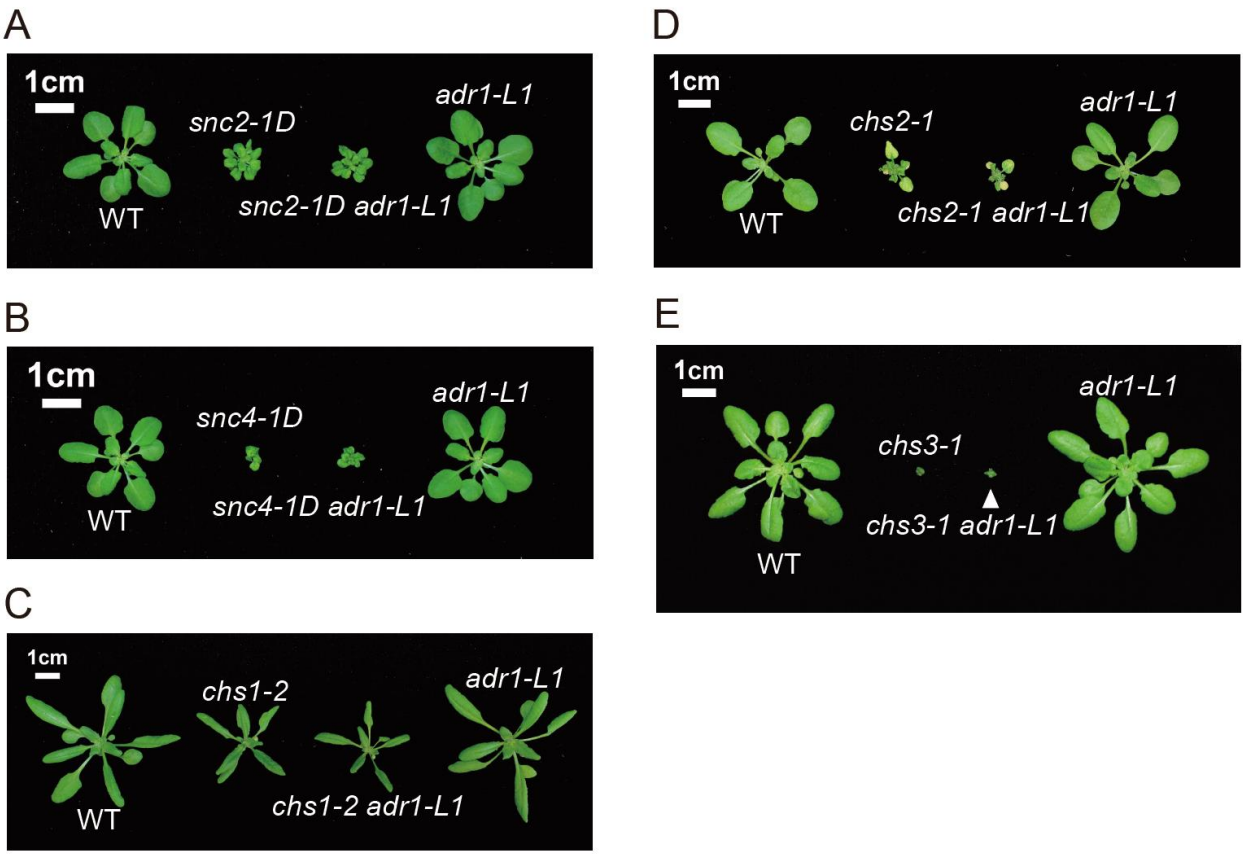

Figure 3.8: *adr1-L1* does not enhance the autoimmune phenotypes of *snc2-1D*, *snc4-1D*, *chs1-2*, *chs2-1* or *chs3-1*.

(A) Morphological phenotypes of four-week-old WT, *snc2-1D*, *snc2-1D adr1-L1* and *adr1-L1* plants grown at 22°C under short day conditions (9hr light/15hr dark).

(B) Morphological phenotypes of four-week-old WT, *snc4-1D*, *snc4-1D adr1-L1* and *adr1-L1* plants grown at 22°C under short day conditions.

(C) Morphological phenotypes of four-week-old WT, *chs1-2*, *chs1-2 adr1-L1* and *adr1-L1* plants grown at 22°C under long day conditions.

(D) Morphological phenotypes of four-week-old WT, *chs2-1*, *chs2-1 adr1-L1* and *adr1-L1* plants. Seeds were germinated at 22°C. One-week-old seedlings were transferred to 18°C for autoimmune phenotypes to be observed.

(E) Morphological phenotypes of four-week-old WT, *chs3-1*, *chs3-1 adr1-L1* and *adr1-L1* plants grown at 22°C under long day conditions.

In the mutant *chilling sensitive 1* (*chs1-2*), a missense mutation in a TIR-NB protein causes autoimmune phenotypes under chilling conditions (Wang et al., 2013). Under the growth condition in the Li Lab, *chs1-2* exhibited dwarfed stature and curled leaves, yet these phenotypes were not enhanced in *chs1-2 adr1-L1* (Figure 3.8C). The difference between the *chs1-2* phenotypes observed under 22°C and those as previously reported (Wang et al., 2013) are likely due to differences in growth condition. Another chilling sensitive mutant *chilling sensitive 2* (*chs2-1*) harbors a gain-of-function mutation in *RPP4*, which encodes a typical TNL (Huang et al., 2010). The autoimmune phenotypes of *chs2-1* were not enhanced by *adr1-L1* either (Figure 3.8D). In the mutant *chilling sensitive 3* (*chs3-1*), a mutation in the C-terminal LIM domain of the atypical TNL protein CHS3 leads to chilling sensitivity and constitutive activated defense responses, which can be alleviated at higher temperatures (Yang et al., 2010). I did not detect enhancement of *chs3-1* by *adr1-L1* (Figure 3.8E). Additionally, the cell death phenotype under chilling condition in *chs3-1*, but not in *chs1-2*, was suppressed by *adr1-L1* (Figure 3.7B). These results suggest that loss of ADR1-L1 function does not affect defense responses mediated through CHS1, CHS2 or CHS3. Taken together, the autoimmunity-enhancing ability of *adr1-L1* seems to be specific to only certain autoimmune mutant backgrounds.

To further test whether the up-regulation of *ADR1* and *ADR1-L2* transcription over compensates the loss of ADR1-L1, I compared the transcript levels of *ADR1* and *ADR1-L2* in additional autoimmune mutants with or without *adr1-L1* mutation (Figure 3.5I, J). Significantly increased *ADR1* transcription with *adr1-L1* was observed under all mutant backgrounds tested except for *snc2-1D*, and significantly increased *ADR1-L2* transcription in *adr1-L1* under all mutant backgrounds tested except for the *SNC1*-overexpressing line (difference insignificant) and *snc2-1D* (Figure 3.5I, J). Therefore, the up-regulation of *ADR1* and *ADR1-L2* transcription is not specific to the *snc1* mutant background.

Taken together, these results suggest that the transcription levels of *ADR1* and *ADR1-L2* are both up-regulated in mutant *adr1-L1*, which may compensate for the loss of *ADR1-L1*. This over-compensation becomes more obvious in autoimmune backgrounds.

3.2.7 Genetic interplay among the three redundant *ADR1* gene family members

To further address whether the immunity-enhancing effects of *adr1-L1* are dependent on ADR1 and ADR1-L2, knockout mutations in *adr1* and *adr1-L2* were introduced into the *snc1 adr1-L1* background by my colleague. The *snc1*-enhancing phenotypes in *snc1 adr1-L1* are largely suppressed by *adr1* and fully suppressed by *adr1 adr1-L2* as observed in morphology, fresh weight and the expression of *PR1* and *PR2* (Figure 3.9A-C), suggesting that ADR1 and ADR1-L2 are indeed responsible for the enhanced immunity in *adr1-L1*.

ADR1 and *ADR1-L2* transcript levels were also quantified in various *snc1 adr* mutant combinations by qPCR (Figure 3.9D). *ADR1* transcript level is elevated in *snc1 adr1-L1* but not in *snc1 adr1-L2* when compared to *snc1* (Figure 3.9D). Similarly, *ADR1-L2* transcript level is elevated in *snc1 adr1-L1* but not in *snc1 adr1* when compared to *snc1* (Figure 3.9D). These results suggest that the over-compensation effect seems to be specific to *adr1-L1*, but not with *adr1* or *adr1-L2*.

3.3 Discussion

This chapter reports immunity-enhancing phenotypes of the loss-of-function helper NLR mutant *adr1-L1* in combination with *snc1*. Interestingly, the ADR1-L1 paralogs ADR1 and ADR1-L2 are required for this phenotype. Transcripts of *ADR1* and *ADR1-L2* are up-regulated in *adr1-L1* mutant. Thus, it is plausible that transcriptional up-regulation of *ADR1* and *ADR1-L2* may over-compensate for the loss of *ADR1-L1*, leading to the defense-enhancing phenotypes observed in *snc1*. This study extends our knowledge on the functional interplay among helper NLRs.

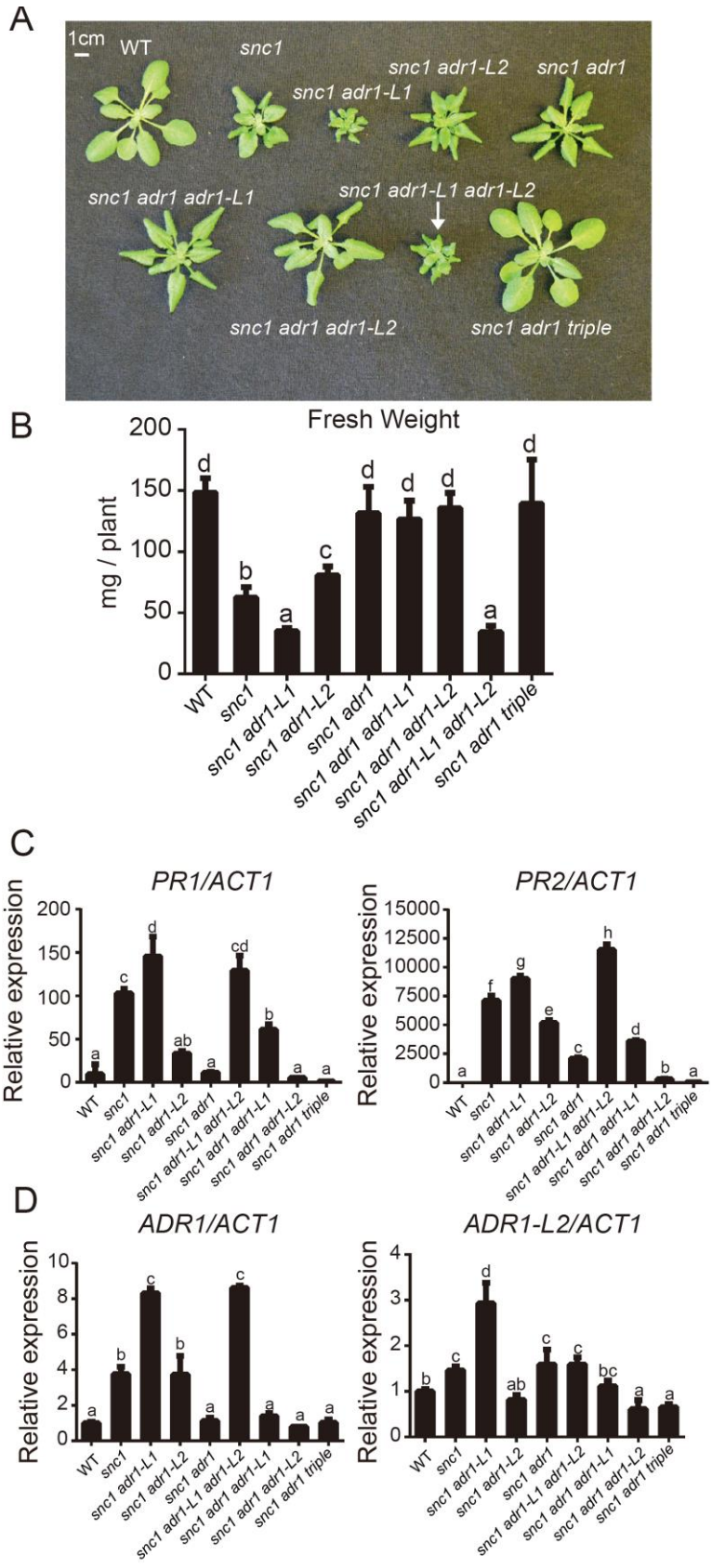

(Contributed by Meixuezi Tong)

Figure 3.9: Characterization of combinatory mutants between *snc1* and *adr*s.

(A) Morphological phenotypes of four-week-old WT, *snc1*, *snc1 adr1-L1*, *snc1 adr1-L2*, *snc1 adr1*, *snc1 adr1-L1 adr1-L2*, *snc1 adr1 adr1-L1*, *snc1 adr1 adr1-L2* and *snc1 adr1 triple* plants grown at 22°C under long day conditions.

(B) Fresh weights of four-week-old plants of the indicated genotypes grown at 22°C under long day conditions. One-way ANOVA was used to calculate the statistical significance between genotypes, as indicated by different letters ($P < 0.05$). Bars represent mean ±SD (n = 6).

(C, D) Relative transcript levels of *PR1* and *PR2* (C); *ADR1* and *ADR1-L2* (D) in the indicated genotypes as determined by qRT-PCR. Total RNA was extracted from four-week-old plants grown at 22°C under long day conditions. *ACT1* was used to normalize the transcript levels. One-way ANOVA was used to calculate the statistical significance between genotypes, as indicated by different letters ($P < 0.05$). Bars represent mean ±SD (n = 3).

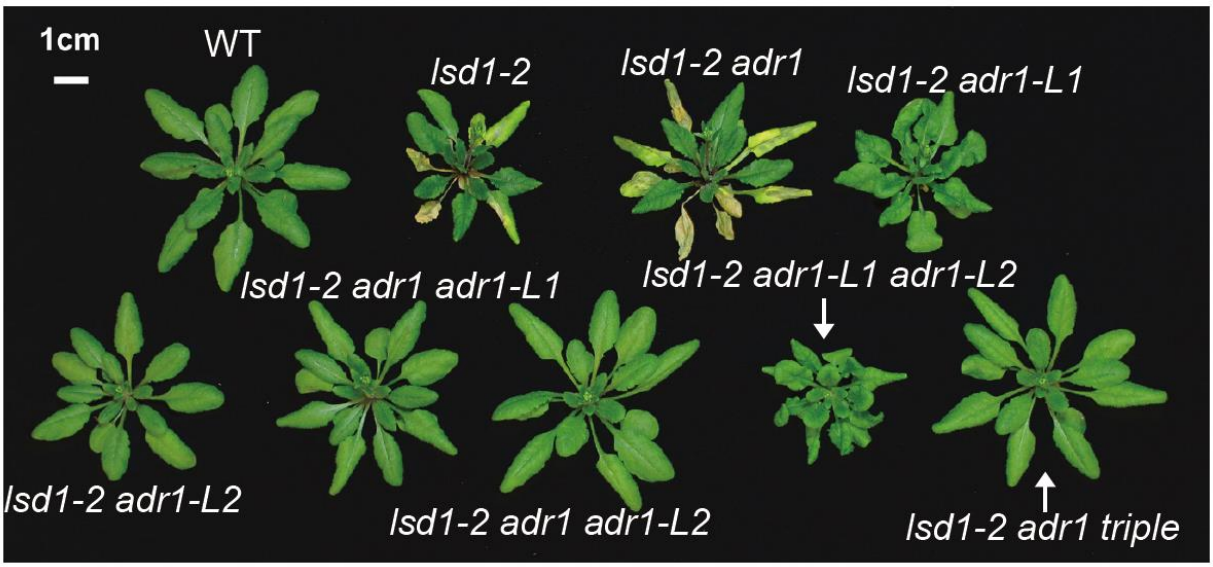

Figure 3.10: *adr1*, *adr1-L1* or *adr1-L2* affects *lsd1-2* phenotypes differently.

Morphological phenotypes of four-week-old WT, *lsd1-2*, *lsd1-2 adr1*, *lsd1-2 adr1-L1*, *lsd1-2 adr1-L2*, *lsd1-2 adr1 adr1-L1*, *lsd1-2 adr1 adr1-L2*, *lsd1-2 adr1-L1 adr1-L2* and *lsd1 adr1 triple* plants grown at 22°C under long day conditions.

ADR1-L1 serves as a positive regulator of immunity redundantly with ADR1 and ADR1-L2 (Bonardi et al., 2011). Using *snc1*-suppressing phenotype as a criterion, these three *ADR* genes seem to exhibit unequal redundancy, where *ADR1* seems to be the leading while *ADR1-L1* is the least contributor (Figure 3.9). The unexpected *snc1*-enhancing phenotypes

of *adr1-L1* loss-of-function alleles reveal an apparent negative role in plant defense. I sought to define the mechanism for this unexpected autoimmunity-enhancing effect. I first examined the possibility that ADR1-L1 regulates SNC1 turnover, as do several *muse* mutants identified in the same screen that exhibit enhanced autoimmune phenotypes due to increased SNC1 protein levels (Huang et al., 2014a; Huang et al., 2014b; Xu et al., 2015b; Huang et al., 2016). Although heightened SNC1 level was observed in *snc1 adr1-L1* double mutant plants compared to *snc1* (Figure 3.3A), steady state SNC1 protein accumulation was unaffected in *adr1-L1* or when the feedback transcriptional up-regulation of *SNC1* was blocked by *pad4-1* (Figure 3.3C, E). Therefore ADR1-L1 does not seem to be involved in the stability control of steady state SNC1 protein.

Secondly, I tested the specificity of the autoimmunity-enhancing effect of *adr1-L1*. Although *adr1-L1* did not enhance the autoimmunity of *snc2-1D*, *snc4-1D*, *chs1-2*, *chs2-1*, or *chs3-1* (Figure 3.8), it did exhibit enhanced autoimmunity in *bal* and other *SNC1/snc1*-overexpression contexts, and in *lsd1-2* (Figure 3.5; 3.10). These observations suggest that the enhancement of the autoimmune phenotypes in *snc1* by *adr1-L1* is unlikely through a direct regulation of SNC1-mediated immunity.

How does the specificity of ADR1-L1 come about? One possibility is that the autoimmune-enhancing effects from *adr1-L1* rely on a certain threshold level of immune signaling (Figure 3.11) defined by immune outputs such as the expression of defense-related genes. When the autoimmune phenotypes are weak, the level of enhancement from *adr1-L1* is not enough to be transformed into a significant plant size difference. On the other hand, when the background autoimmunity is too strong, it is more difficult to detect a marginal decrease in plant size due to increased immunity caused by the loss of ADR1-L1.

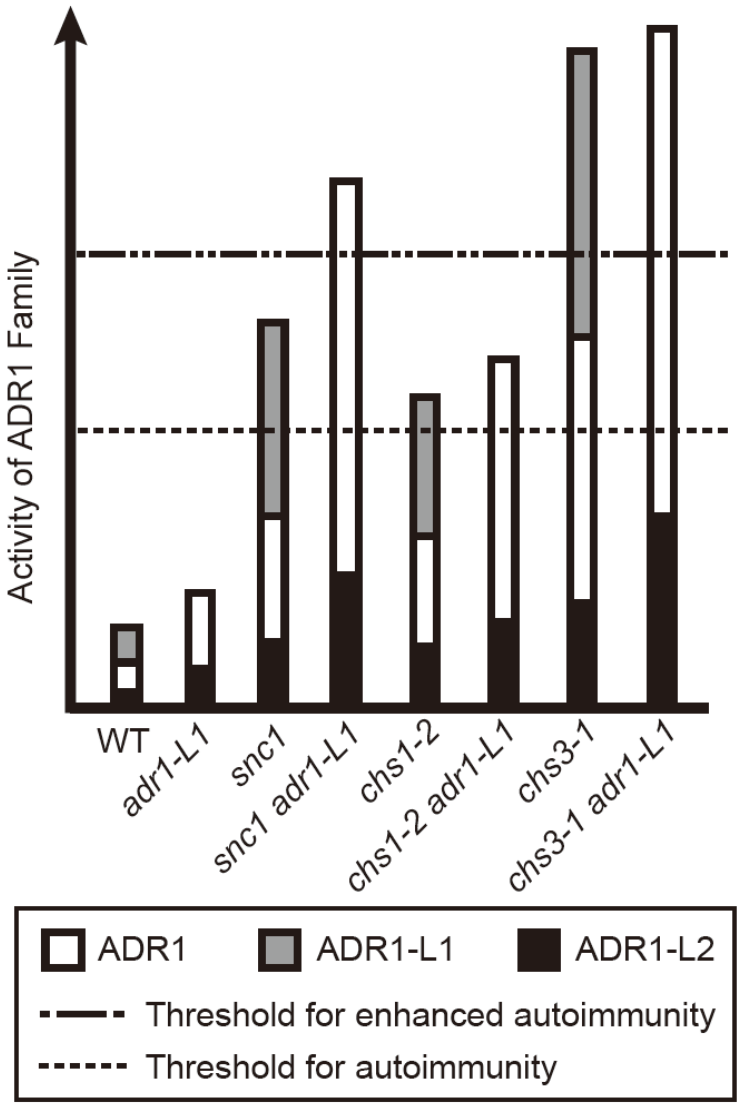

Figure 3.11: Working model: ADR1 and ADR1-L2 over-compensate the loss of ADR1-L1 in defense regulation.

Among the three *ADR* genes, *ADR1-L1* and *ADR1-L2* are expressed at higher levels, while *ADR1* is expressed at a lower level (Figure 3.12)(Roberts et al., 2013). Therefore, there are potentially different amounts of the paralogous ADR proteins in WT plants required for their normal function. Loss of ADR1-L1 leads to heightened expression of *ADR1* and *ADR1-L2*, resulting in overcompensation of defense outputs. In WT, this overcompensation is not sufficient to lead to autoimmune response and enhanced disease resistance. However, in *snc1*, enhancement of the autoimmune phenotype becomes apparent. On the other hand, as in *chs1-2* where the autoimmunity is weak, the over-compensated ADR1 levels are insufficient to cross the autoimmune-enhancing threshold. By contrast, the autoimmunity as in *chs3-1* has reached a maximal limit and enhancement by *adr1-L1* is not observable at the level of plant size.

Gene expression may be up-regulated to compensate for the loss of their functionally redundant paralogs (Diss et al., 2014). The *Arabidopsis* R-SNARE (soluble N-ethylmaleimide sensitive factor attachment protein receptor) genes *VESICLE-ASSOCIATED MEMBRANE PROTEIN 721* (*VAMP721*) and *VAMP722* are transcriptionally upregulated in the respective mutant to compensate for the loss of the other (Kwon et al., 2008). In tomato, silencing of one ethylene receptor gene, *NR*, results in increased mRNA level of its redundant paralog *LeETR4* (Tieman et al., 2000). In a more recent example, Bethke et al. reported that *Arabidopsis* pectin methylesterases (PMEs) contribute to disease resistance against *Pseudomonas syringae*. Two PME loss-of-function mutants, *pme3* and *pme12,* exhibited enhanced disease resistance to *Pseudomonas syringae*, possibly by a similar over-compensation effect (Bethke et al., 2014). Another example involves two human retinoblastoma family members, p107 and p130. Loss-of-function p130 in T lymphocytes leads to higher levels of p107, and the predominant p130-E2F protein complex is replaced by a p107-E2F complex (Mulligan et al., 1998). Similar examples were also reported for redundant mammalian gene families, including retinoic acid receptor and connexin gene families (Berard et al., 1997; Minkoff et al., 1999).

Consistent with the paralogous gene over-compensation hypothesis, I repeatedly observed increased expression of *ADR1* and *ADR1-L2* in the *adr1-L1* mutant compared to WT (Figure 3.5A, B; 3.6). This increase is magnified in the *snc1* autoimmune mutant background (Figure 3.5A, B). Similar to a previous report (Roberts et al., 2013), it was observed that individual *adr1*, *adr1-L1* and *adr1-L2* knockout mutants affect *lsd1-2* phenotypes differently under the growth conditions in the Li Lab(Figure 3.10), suggesting an unequal redundancy among the ADR1 family members. Further analyses of the microarray data from AtGenExpress (Schmid et al., 2005; Winter et al., 2007) revealed that the three *ADR1* gene family members are not expressed at the same level, nor do their expression levels respond to abiotic stresses to the same magnitude (Figure 3.12). It is therefore possible that transcriptional up-regulation of *ADR1* and *ADR1-L2* in the *adr1-L1* mutant would yield more ADR1 and ADR1-L2 proteins to replace ADR1-L1, thus over-

compensating for the loss of ADR1-L1 due to higher gross activity of the other two ADR1 family proteins.

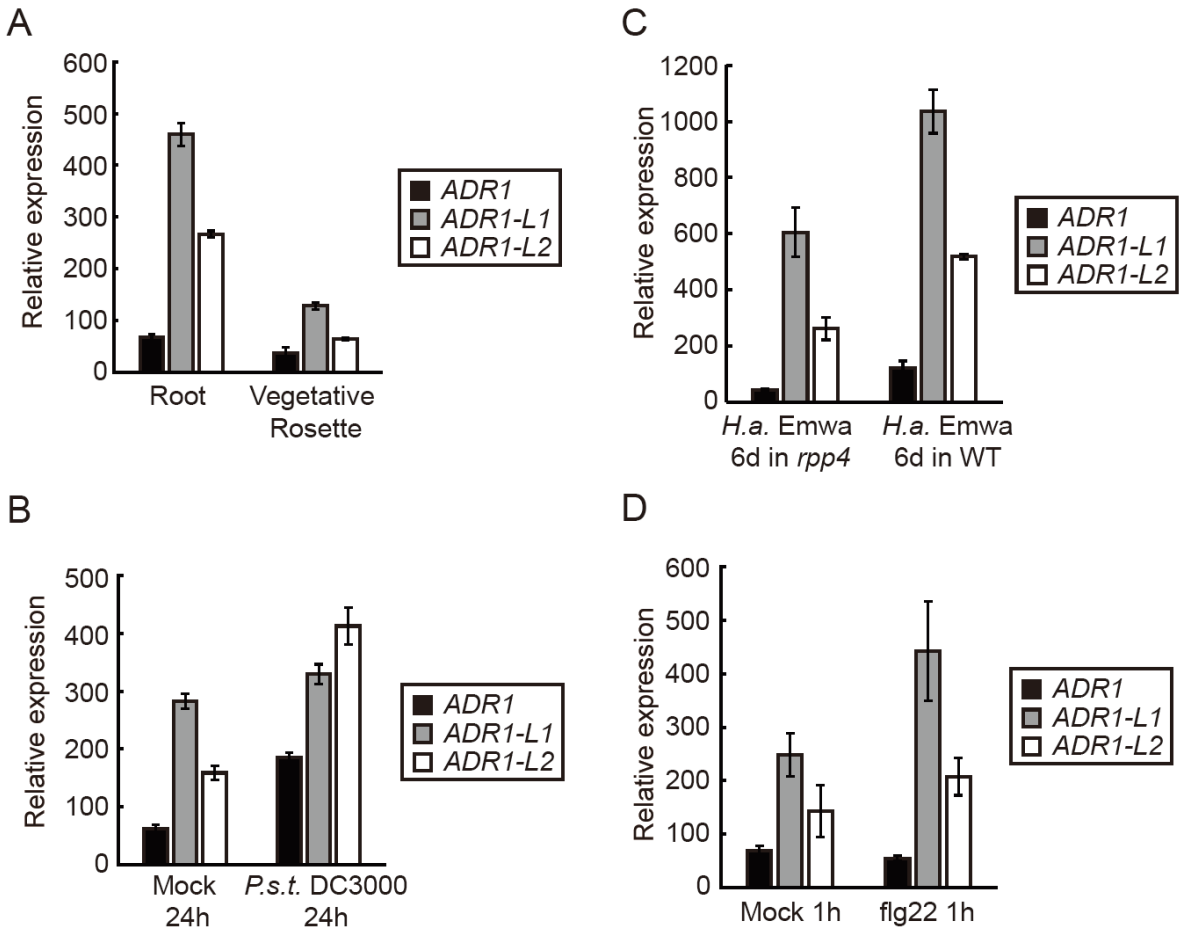

Figure 3.12: *ADR1*, *ADR1-L1* and *ADR1-L2* have different expression levels.

Expression of *ADR1*, *ADR1-L1* and *ADR1-L2* extracted from microarray data from AtGenExpress. All bars represent means ±SD (n = 3). Samples are as follows: (A) Root or vegetative rosette from 15-day-old *Arabidopsis* seedlings grown on MS medium. (B) Five-week-old *Arabidopsis* leaves 24 hours after infiltration with either 10mM $MgCl_2$ (Mock) or virulent pathogen *Pseudomonas syringae* pv. *tomato* DC3000. (C) Two-week-old *Arabidopsis* mutant *rpp4* or WT seedlings six days after spray inoculation of avirulent pathogen *Hyaloperonospora arabidopsidis* Emwa1 spores. (D) Five-week-old *Arabidopsis* leaves one hour after infiltration with either water (Mock) or 1µM bacterial-derived elicitor flg22.

To search for potential transcription factors involved in the proposed transcriptional over-compensation, sequence analysis of the predicted promoter plus 5'-UTR regions of the

three *ADR1* gene family members was performed. Within 1500 bp upstream the start codon of *ADR1*, a W-box motif (C/TTGACC/T) (Pandey and Somssich, 2009) was identified, whereas five W-box motifs were identified within 1500 bp upstream the start codon of *ADR1-L1*. W-box motifs are recognized by WRKY transcription factors, which are notably involved in the regulation of biotic and abiotic stress responses in plants (Pandey and Somssich, 2009). In addition, three predicted SARD1 binding sequence (GAAATTT) (Sun et al., 2015) was identified in the *ADR1-L1* promoter plus 5'-UTR region. SARD1 function as master transcriptional regulator of plant immune responses (Sun et al., 2015). In fact, a chromatin immunoprecipitation-sequencing (ChIP-Seq) assay using SARD1 as bait has identified all three *ADR1* gene family members as binding targets of SARD1 (Sun et al., 2015). These evidences suggest that the proposed transcriptional over compensation within the *ADR1* gene family may involve interplay among multiple transcriptional regulators such as SARD1 and WRKY. No conspicuous sequence similarity was observed among the predicted promoter plus 5'-UTR regions of the three *ADR1* gene family members, indicating a unique regulatory mechanism may exist for each of the three individual members of the *ADR1* gene family.

In addition, we cannot exclude the possibility that the functional over-compensation proposed involves unequal protein stability or activity among the ADR1 family members. ADR1 and ADR1-L2 protein function or stability might be enhanced, for example, by the elimination of the potentially less-effective family member ADR1-L1 as a competitor.

How exactly loss of ADR1-L1 leads to up-regulation of ADR1 and ADR1-L2 will be an interesting question to pursue in the future. It could be possible that the expression of the three *ADR* genes is coordinated by a common transcription factor that is able to sense the loss of ADR1-L1 and to enhance the expression of the other two paralogs. It is plausible that ADR1-L1 may be directly involved in transcriptional repression of its two paralogs. In both scenarios, loss of *ADR1-L1* would lead to an up-regulation in the expression of *ADR1* and *ADR1-L2*, leading to enhanced immunity.

3.4 Materials and methods

3.4.1 Plant materials used

Arabidopsis thaliana (L.) Heynh. mutants used in this chapter include *snc1* (Li et al., 2001), *adr1-1* (Bonardi et al., 2011), *adr1-L1-2* (Bonardi et al., 2011), *adr1-L2-4* (Bonardi et al., 2011), *bal* (Yi and Richards, 2009), *SNC1-GFP* and *snc1-GFP* (Xu et al., 2014a), *cpr1-3* (Cheng et al., 2011), *lsd1-2* (Jabs et al., 1996), *chs1-2* (Wang et al., 2013), *chs2-1* (Huang et al., 2010), *chs3-1* (Yang et al., 2010), *pad4-1* (Glazebrook et al., 1996), and *eds5-3* (Nawrath and Metraux, 1999; Igari et al., 2008).

3.4.2 Growth conditions

For soil grown plants, seeds were vernalized at 4°C for two days, sown onto sterile soil and transferred to plant growth rooms for either long day (22°C/18°C, 16h light/8h dark; ~50% relative humidity) or short day (21°C/18°C, 9h light/15h dark; ~50% relative humidity) or continuous light (22°C) conditions as specified in figure legends. Phenotypes were scored at indicated time points. For all agar plate-grown seedlings, seeds were surface sterilized and sown on 1/2 MS agar plates, vernalized for two days and grown under long day at 22°C.

3.4.3 Plant genotyping

Mutant genotyping primers used are as follows: *adr1* (SAIL_842_B05) ADR1-1_s-Gen: CAA AGG ACG ATG ATG TTC GAG, ADR1-1_as: CGG ATT GTT CAC TAT AGT AAG G, LB_SAIL: TTT CAT AAC CAA TCT CGA TAC AC; *adr1-L1-1* (SAIL_302_C06) L1_1-s: ATG GCC ATC ACC GAT TTT TTC, adr1-L1_as: GTC AGG AAC AGG ATT TCC AG, LB_SAIL; *adr1-L2-4* (Salk_126422) PHX21_1_s: ATG GCA GAT ATA ATC GGC GG, PHX_ReT4_as: TGG GAG ATT GTG ACA CAG TC, LB1.3: ATT TTG CCG ATT TCG GAA C;; *chs2* (*RPP4*) VB12: GAT TGA CCT TGT ATA TGA GGT GG, VB13: CAC TCA TCT TTG TCC CTT CCT TTT GAA, cut

amplicon with *Mbo*II at 37°C o/n, Col-0 138 bp and 35 bp, *chs2* 138 bp and 60 bp; *chs3* VB10: TCC TCC TTA CTC CTT GTG AGA C, VB11: TCT CTC TCT CAC TCT CTT CGT AGT TCC CA, cut amplicon with *Bci*130I at 37°C or 8hr, Col-0 170 bp and 25 bp, *chs3* 194 bp; *cpr1* (SALK_045148) LP: TTT CGT AAA TTT TTA CAC AAA ATC G, RP: TGT GAG TAG CCT TGT CTT GGG. To genotype homozygous *eds5-3*, SNP primers F: ACT TCA GAG CGG TGA TCA GA and R: CAT CAA CGG TCC ACA AGT C were used. All mutant combinations were confirmed by genotyping.

3.4.4 Map-based cloning of *muse15*

Rough and fine mapping of *muse15* was performed as previously described (Huang et al., 2013). Primers involved in mapping were designed based on Monsanto *Arabidopsis* polymorphism and Landsberg sequence collections (Jander et al., 2002). Marker primers used include: FCA8 F: CTC CAA GCT TAG TGC AAC TC, R: TGA ACT GCA TTA ACA TGG AAC; T13J8 F: ATG TTC CCA GGC TCC TTC CA, R: GAG ATG TGG GAC AAG TGA CC; F8D20 F: TTG ATC TGA ATA GGT CCC CC, R: ACT GTT GCG ATA ATG CAG TG; F26P21 F: TCT TCA ATG ATA CCC ATC CC, R: ATA TTT GCG ATT TCT ATT TTG GAG; F17I5 F: ATG GGC TAG ATA ATT TCT AAG G, R: AAT GAA TTG TTA CAT GAG GTC G.

3.4.5 Infection assay

Infection assays by *Hyaloperonospora arabidopsidis* (*H.a.*) were performed as previously described (Clarke et al., 2000). Ten-day-old soil-grown *Arabidopsis* seedlings were spray-inoculated with freshly harvested *H.a.* Noco2 spores re-suspended in water. Infected plants were kept at 18ºC with 80% humidity for seven days before data collection. Growth of the pathogen was measured by totaling the number of spores per gram of fresh weight of host tissue.

3.4.6 Total SA measurement

Leaf tissue was harvested from four-week-old *Arabidopsis* plants and homogenized and mixed with 0.2 mL 90% methanol. Samples were sonicated using a water bath sonicator for 20 minutes and centrifuged at 15000 g for 20 minutes. 0.3 mL 100% methanol was added to the debris for a second extraction. Samples were thoroughly vortexed, spun down again and the supernatants from the two extractions were combined and left to dry overnight at room temperature. The next day, 0.1 mL β-glucosidase solution (80 unit/mL β-glucosidase (Sigma G0395), in 0.1M NaAc, pH 5.2) was added to each sample. Samples were vortexed and sonicated for 5 minutes and incubated at 37°C for 90 minutes. 0.5 mL 0.5% trichloroacetic acid (Sigma T6399) was added to the samples. Samples were spun down at 15000 g for 15 minutes and the supernatant was transferred to a new set of tubes and was extracted 3 times using extraction medium (ethylacetate : cyclopentane : isopropanol = 100 : 99 : 1). The combined extraction product was left to dry overnight at room temperature. SA samples were dissolved in mobile phase (0.2 M KAc, 0.5 mM EDTA, pH 5.0) and the quantity of SA was measured using HPLC as previously described (Li et al., 1999).

3.4.7 RNA extraction and gene expression analyses

Total RNA was extracted from two-week-old seedlings grown on 1/2 MS medium or four-week-old soil grown plants using Totally RNA Kit (Ambion). Reverse transcription was performed using Easyscript Reverse Transcription Kit (ABM). Semi-quantitative PCR was performed as described before (Zhang et al., 2003). Real-time PCR was performed using Perfect Realtime Kit (TAKARA). Sequences of the primers used are *ACT1* F: CGA TGA AGC TCA ATC CAA ACG A, R: CAG AGT CGA GCA CAA TAC CG; *ACT7* F: GGT GTC ATG GTT GGT ATG GGT C, R: CCT CTG TGA GTA GAA CTG GGT GC; *PR1* F: GTA GGT GCT CTT GTT CTT CCC, R: CAC ATA ATT CCC ACG AGG ATC; *PR2* F: GCT TCC TTC TTC AAC CAC ACA GC, R: CGT TGA TGT ACC GGA ATC TGA C; *SNC1* F: CTG GGA TAA GTT GTA TCG TGT TG, R: AGA TGT CCC CGA TGT CAT CCG; *ADR1* F: ATA GTG AAC AAT CCG AGG TT, R: TTT

CAT CCA TTT CCC CTG T; *ADR1-L2* F: CTT GTG AAA GAT CCA AGG TT, R: TGA GTC ATT TCT CCT GTG T.

3.4.8 Ion leakage measurement

Rosette leaves were harvested from four-week-old plants and 6 leaf discs (6 mm diameter) were collected and then floated in 20 mL water for 30 min. These leaf discs were transferred to tubes containing 6 mL distilled water. Conductivity of the solution (μSiemens/cm) was determined with a conductivity meter (Model 2052, Amber Science) at the indicated time points. For mutants that exhibit cell death (those with *chs1-2* or *chs3-1*) at earlier developmental stages, the experiment was performed with two whole two-week-old seedlings.

3.4.9 Protein extraction and western blot analysis

Total protein was extracted from two-week-old *Arabidopsis* seedlings grown on 1/2 MS medium. The whole extraction was performed either on ice or in a 4°C cold room. Tissues were homogenized and mixed with extraction buffer (100 mM Tris-HCl pH 8.0, 0.1% SDS and 2% β-mercaptoethanol). Samples were vortexed and centrifuged at 15000 g for 10 minutes. SDS loading buffer was added to supernatants and samples were boiled for 5 minutes before loading onto a SDS polyacrylamide gel electrophoresis (SDS-PAGE) gel. After electrophoresis, separated protein samples were transferred to a membrane and subjected to western blot analyses. The anti-SNC1 antibody was generated against a SNC1-specific peptide from rabbit (Li et al., 2010b). Protein bands were quantified using ImageJ.

4. Final summary and future perspectives

Current plant disease control in the agriculture industry relies heavily on the application of chemical agents to directly inhibit the growth of the pathogens (Handford et al., 2015). Crop protection by using such strategies poses high risk to the environment and the health of the consumers (Lu et al., 2015). In depth understanding of how ETI is regulated in plants lays the foundation for the development of novel crop protection strategies that exploits the robust host defense mechanism. The application of these strategies in the agricultural industry would not only reduce the damage to the ecosystem caused by excessive use of pesticides, but also provide us with heathier food on tomorrow's tables.

My thesis research describes the identification and functional characterization of two ETI-enhancing mutants in Arabidopsis, *muse1* and *muse15*, from a forward genetic screen. Multiple loss-of-function alleles were independently isolated for both mutants, all of which exhibited enhanced autoimmune phenotypes (Figure 2.3; 3.1). Through map-based cloning, it was determined that *MUSE1* encodes an E3 ubiquitin ligase (Figure 2.2) whereas *MUSE15* encodes the helper NLR ADR1-L1 (Figure 3.2). MUSE1 and its paralog MUSE2 are specifically involved in the negative regulation of SNC1-mediated immunity, possibly by promoting the degradation of multiple NLRs required by SNC1 (Figure 2.14). On the contrary, MUSE15 plays a more general role in fine-tuning defense, as the *adr1-L1* mutant enhanced the defense phenotypes of multiple autoimmune mutants, likely through over-compensation by the other two members of the ADR helper NLR family, ADR1 and ADR1-L2 (Figure 3.11).

The discovery of the functions of MUSE1/2 and MUSE15 in the regulation of SNC1-mediated defense in this thesis research provides new insight into the complex mechanism underlying ETI regulation. The discovery that the E3 ubiquitin ligases MUSE1 and MUSE2 are involved in the SNC1-meidated defense as is CPR1 (Cheng et al., 2011; Gou et al., 2012) provides evidence that defense mediated by a single NLR may be controlled by multiple ubiquitination pathways. The exclusion of SNC1 itself as the substrate of MUSE1

and MUSE2 suggests that regulation through ubiquitination may occur at multiple steps in signalling pathway mediated by a single NLR.

The results on the enhancement of the autoimmune phenotypes in *snc1* by knocking out *ADR1* helper NLR gene family member *ADR1-L1* revealed the complex regulation among plant NLRs. This unexpected enhancement may be due to over-compensation by ADR1 and ADR1-L2, the other two family members of the ADR helper NLR family (Figure 3.11). The elevated *ADR1* and *ADR1-L2* transcript levels observed in the *adr1-L1* mutant backgrounds suggest that the proposed over-compensation might occur through transcriptional regulation.

4.1 Using *snc1* in the MUSE genetic screen to dissect ETI

NLRs play central roles in ETI, as they account for the majority of the canonical R proteins, which mediate isolate-specific effector recognition (Li et al., 2015). In Arabidopsis, *RPP4* NLR gene cluster member *SNC1* encodes a TNL showing high similarity to canonical R proteins *RPP4* and *RECOGNITION OF PERONOSPORA PARASITICA* 5 (*RPP5*) in amino acid sequence (Zhang et al., 2003). The functional *SNC1* locus is specific to the Columbia ecotype, indicating that *SNC1* is highly polymorphic. These features suggest that SNC1 is likely a canonical R protein. Thus, the SNC1-mediated defense pathway is representative of ETI pathways.

The gain-of-function mutation in mutant *snc1* causes autoimmune phenotypes due to the constitutive activation of the SNC1-mediated defense pathway (Zhang et al., 2003). This feature makes *snc1* a useful tool in genetic screens to study NLR regulation (Johnson et al., 2012; Huang et al., 2013), as subtle changes in defense regulation are often amplified under *snc1* background, resulting in an observable change in morphology. Despite the fact that *muse1* and *muse15* loss-of-function single mutants are both WT-like (Figure 2.2C; 3.2D), they were successfully isolated from the MUSE screen. In addition, mutants corresponding to gene pairs with overlapping functions such as MUSE1/MUSE2 and

MUSE13/MUSE14 (Huang et al., 2016) were isolated from the muse screen. These cases emphasize the power of using *snc1* as a sensitized genetic background to identify of otherwise indistinguishable mutants. Furthermore, six loss-of-function *muse1* alleles (Figure 2.2A, B) and two loss-of-function *muse15* alleles (Figure 3.2A, B, C) were isolated independently from the MUSE screen, indicating that the Arabidopsis genome is well covered in the mutagenesis process.

4.2 Ubiquitination catalyzed by MUSE1 and MUSE2

In an *in vitro* ubiquitination assay, *E. coli* -expressed recombinant MUSE1 exhibited ubiquitin ligase activity by poly-ubiquitinating itself (Figure 2.5). However, I was not able to determine whether MUSE1 catalyzes mono-ubiquitination or poly-ubiquitination *in vivo*. Also, it remains unclear how the ubiquitins added by MUSE1 are linked to each other and to the substrate. Knowledge of the type of ubiquitination catalyzed by MUSE1 an MUSE2 is crucial to understanding their function in the regulation of plant immunity, as different types of ubiquitination perform diverse functions (Hicke, 2001; Chen and Sun, 2009; Kravtsova-Ivantsiv and Ciechanover, 2012; Kulathu and Komander, 2012; Sadanandom et al., 2012; Tian and Xie, 2013).

The most frequently reported type of ubiquitination, the K48-linked poly-ubiquitination, usually directs substrate for 26S proteasome-mediated protein degradation (Kravtsova-Ivantsiv et al., 2013). On the contrary, atypical ubiquitin chains may form through linkage via the other 6 lysine residues on an ubiquitin molecule: K6, K11, K27, K29, K33 and K63 (Walsh and Sadanandom, 2014). The functions of these atypical ubiquitin chains in plants have been less well-understood. In one case, K29-linked ubiquitin chains have been reported to target Arabidopsis DELLA proteins for 26S proteasome-mediated protein degradation (Wang et al., 2009). In another example, Arabidopsis auxin transporter PIN2 is marked by K63-liked ubiquitin chains for endocytosis followed by a vacuolar proteolysis pathway (Leitner et al., 2012). In animals, atypical ubiquitin chains have also been reported to play roles non-proteolytic pathways such as DNA repair and kinase activation,

although these functions have not yet been reported in plants. In addition, mono-ubiquitination has been shown to play a crucial role in histone modification and transcriptional control in animals (Pham and Sauer, 2000; Robzyk et al., 2000).

Most of the previously characterized Arabidopsis E3 ubiquitin ligases involved in defense promote protein degradation (Cheng et al., 2011; Lu et al., 2011; Gou et al., 2012; Stegmann et al., 2012). It is therefore highly plausible that MUSE1 and MUSE2 negatively regulate defense by promoting the turnover of positive defense components. However, it is also possible that MUSE1 and MUSE2 activate negative defense regulators repressing the SNC1-mediated defense pathway, through non-canonical ubiquitination.

Since the type of ubiquitination is largely determined by the E2 enzyme involved (Ye and Rape, 2009), it would be informative to identify the MUSE1-interacting E2 enzyme in future experiments. This may be achieved by *in vivo* immunoprecipitation (IP) of MUSE1 followed by mass spectrum (MS) analysis. A major challenge is to overcome the low expression level of transgene *MUSE1-HA* to yield sufficient protein for IP-MS assay.

4.3 Possible substrates of MUSE1 and MUSE2

Identification of the ubiquitination substrates of E3 ubiquitin ligases is crucial to studying the underlying mechanism by which the E3s regulate biological processes. Epistatic analyses indicated that MUSE1 and MUSE2 are specifically involved in the negative regulation of the SNC1-mediated defense pathway (Figure 2.9, 2.10, 2.11). Therefore, the substrates of MUSE1 and MUSE2 are likely specific regulators involved in defense mediated by SNC1.

MUSE1 was used as bait in a yeast two-hybrid screen against an Arabidopsis cDNA library generated under the pathogen-induced condition. I did not isolate meaningful candidate interactors of MUSE1 besides ubiquitin, possibly due to the transient nature of the interaction between E3 ligases and substrates proteins. Specific mutations in the RING

domain often abolish E3 ligase activity by disrupting the RING domain (Xie et al., 2002; Dong et al., 2006; Zhang et al., 2007b; Peng et al., 2013) (Figure 2.5B). Such mutations often result in dominant-negative forms of E3 ligases through unclear mechanisms (Xie et al., 2002; Peng et al., 2013). Usually, the RING domain is where an E2 ubiquitin conjugating enzyme binds (Deshaies and Joazeiro, 2009). Hence, a plausible explanation for the dominant-negative effect observed in the RING domain mutant E3s is that these E3s compete with the endogenous RING E3s for the substrate proteins and protect them from being ubiquitinated and degraded by the 26S proteasome pathway. In addition, dominant-negative MUSE1-H156Y-HA tends to accumulate to a higher level when transiently expressed in tobacco compared to native MUSE1-HA (data not shown), possibly due to stabilized protein through the prevention of auto-ubiquitination (Galan and Peter, 1999; Stegmann et al., 2012). Taken together, the potentially transient interaction between MUSE1 and its substrates in yeast may be enhanced by using the dominant-negative form MUSE1-H156Y as bait.

If the consequence of the ubiquitination catalyzed by MUSE1 and MUSE2 is proteolytic, the autoimmune phenotypes observed in the *muse1 muse2* double mutant are likely the result of the over-accumulation of the substrates of MUSE1 and MUSE2. Under this situation, MUSE1 and MUSE2 ubiquitinate positive regulators specific to the SNC1-mediated defense pathway (Figure 2.14). Three candidate proteins that satisfy this criterion, SNC1, MOS10 and bHLH84, were tested for being the potential substrates of MUSE1 in biochemical assays, but none of them exhibited reduced protein level upon increased expression of *MUSE1* (Figure 2.12). Besides, over-accumulation of SNC1, MOS10 or bHLH84 each results in *snc1*-like autoimmune phenotypes (Zhu et al., 2010; Cheng et al., 2011; Xu et al., 2014b), different from the WT-like phenotypes of the *muse1* or *muse2* knockout mutant (Figure 2.6). These results suggest that it is unlikely that SNC1, MOS10 or bHLH84 is the substrate of MUSE1 and MUSE2. In search of the substrates whose turnover is promoted by MUSE1 and MUSE2, a suppressor screen by using EMS mutagenesis under the *muse1 muse2* double mutant background was performed. I was not able to identify suppressors of the autoimmune phenotype of *muse1 muse2* other than loss-of-function *snc1* alleles.

This indicates that more than one MUSE1/MUSE2 substrate with overlapping functions may exist (Figure 2.14), as mutants corresponding to genes with redundant function tend to be missed in forward genetic screens in which EMS is used as the mutagen (Zhang et al., 2007a).

If, on the other hand, MUSE1 and MUSE2 promote the activities of substrate proteins through uncanonical ubiquitination, the substrates of MUSE1 and MUSE2 would be negative defense regulators specifically involved in the repression of the SNC1 pathway. The autoimmune mutant phenotypes of *muse1 muse2* are thus due to the failure in activation of the substrate proteins of the substrate proteins of MUSE1 and MUSE2. Furthermore, under this scenario, a *muse1 muse2* suppressor screen would not yield loss-of-function mutants of substrates of MUSE1 and MUSE2. Instead, a suppressor screen may be conducted using the "*snc1* with transgene *MUSE1* (WT-like)" background (Figure 2.8). In such screen, mutants that restores *snc1*-like phenotypes may harbor mutations in the substrates of MUSE1 and MUSE2.

4.4 SNC1 may form heterodimers with additional TNLs

Multiple studies have reported the co-operation between plant NLR pairs through physical interaction (Cesari et al., 2014; Williams et al., 2014). In addition, functional NLR interaction without identified physical association have been reported in plants (Aarts et al., 1998; Peart et al., 2005; Eitas et al., 2008; Bonardi et al., 2011; Xu et al., 2015a). It is thus entirely plausible that the function of SNC1 relies on one or more additional NLRs. Furthermore, in both reported cases where plant NLRs form heterodimers, the two corresponding loci are in proximity to each other in the genome and the two NLRs have the same type of N terminal domain (Cesari et al., 2014; Williams et al., 2014).

Future experiments will focus on testing whether *TNL* knockout mutants would suppress the *snc1* autoimmune phenotypes. This can be performed by a reverse genetic screen in

which *TNL* genes with similar expression pattern as *SNC1* are knocked out under the *snc1* background.

4.5 Complex interplay among helper NLRs

The three functional members of the ADR1 NLR family have been previously shown to have overlapping functions in the regulation of defense mediated by multiple NLRs, and were thus designated as helper NLRs (Bonardi et al., 2011). However, additional interplay among these ADR1 family members beyond their functional redundancy was not reported. My thesis research concludes that loss of ADR1-L1 may lead to the increased expression of *ADR1* and *ADR1-L2*, possibly through transcriptional regulation.

A major challenge in the future is to determine the specific transcription factors involved in such over-compensatory regulation. This may be accomplished by a yeast one-hybrid assay using promoters of *ADR1* and *ADR1-L2*. Besides, IP-MS assay using *ADR1-L1* as bait may shed light on the underlying mechanisms by which the ADR helper NLR family members are co-ordinated. It would be interesting to determine whether the over-compensatory phenomenon exists among other NLR family members in plants. NRG1, a helper NLR first identified in tobacco, is required for the activation of TNL N (Peart et al., 2005). Three orthologues of *NRG1* exist In Arabidopsis as a gene cluster. The NRG1 family and the ADR1 family NLRs both belong to the RPW8 CNL subtype of NLRs and share high similarity in amino acid sequences (Collier et al., 2011). It is worth testing whether the NRG1 family members function as helper NLRs in Arabidopsis, whether the ADR1 and NRG1 family members function synergistically in regulating ETI and whether the over-compensation effect is also observed among members of the *NRG1* gene family.

References

Aarts, N., Metz, M., Holub, E., Staskawicz, B.J., Daniels, M.J., and Parker, J.E. (1998). Different requirements for EDS1 and NDR1 by disease resistance genes define at least two R gene-mediated signaling pathways in Arabidopsis. *Proc Natl Acad Sci U S A* **95,** 10306-10311.

Abascal, F., Zardoya, R., and Posada, D. (2005). ProtTest: selection of best-fit models of protein evolution. *Bioinformatics* **21,** 2104-2105.

Alcazar, R., and Parker, J.E. (2011). The impact of temperature on balancing immune responsiveness and growth in Arabidopsis. *Trends Plant Sci* **16,** 666-675.

Bednarek, P. (2012). Chemical warfare or modulators of defence responses - the function of secondary metabolites in plant immunity. *Curr Opin Plant Biol* **15,** 407-414.

Berard, J., Luo, H., Chen, H., Mukuna, M., Bradley, W.E., and Wu, J. (1997). Abnormal regulation of retinoic acid receptor beta2 expression and compromised allograft rejection in transgenic mice expressing antisense sequences to retinoic acid receptor beta1 and beta3. *J Immunol* **159,** 2586-2598.

Bernoux, M., Ellis, J.G., and Dodds, P.N. (2011a). New insights in plant immunity signaling activation. *Curr Opin Plant Biol* **14,** 512-518.

Bernoux, M., Ve, T., Williams, S., Warren, C., Hatters, D., Valkov, E., Zhang, X., Ellis, J.G., Kobe, B., and Dodds, P.N. (2011b). Structural and functional analysis of a plant resistance protein TIR domain reveals interfaces for self-association, signaling, and autoregulation. *Cell Host Microbe* **9,** 200-211.

Bethke, G., Grundman, R.E., Sreekanta, S., Truman, W., Katagiri, F., and Glazebrook, J. (2014). Arabidopsis PECTIN METHYLESTERASEs contribute to immunity against Pseudomonas syringae. *Plant Physiol* **164,** 1093-1107.

Bi, D., Cheng, Y.T., Li, X., and Zhang, Y. (2010). Activation of plant immune responses by a gain-of-function mutation in an atypical receptor-like kinase. *Plant Physiol* **153,** 1771-1779.

Bonardi, V., Tang, S., Stallmann, A., Roberts, M., Cherkis, K., and Dangl, J.L. (2011). Expanded functions for a family of plant intracellular immune receptors beyond specific recognition of pathogen effectors. *Proc Natl Acad Sci U S A* **108,** 16463-16468.

Bowling, S.A., Clarke, J.D., Liu, Y., Klessig, D.F., and Dong, X. (1997). The cpr5 mutant of Arabidopsis expresses both NPR1-dependent and NPR1-independent resistance. *Plant Cell* **9,** 1573-1584.

Caillaud, M.C., Asai, S., Rallapalli, G., Piquerez, S., Fabro, G., and Jones, J.D. (2013). A downy mildew effector attenuates salicylic acid-triggered immunity in Arabidopsis by interacting with the host mediator complex. *PLoS Biol* **11,** e1001732.

Cesari, S., Kanzaki, H., Fujiwara, T., Bernoux, M., Chalvon, V., Kawano, Y., Shimamoto, K., Dodds, P., Terauchi, R., and Kroj, T. (2014). The NB-LRR proteins RGA4 and RGA5 interact functionally and physically to confer disease resistance. *EMBO J* **33,** 1941-1959.

Cesari, S., Thilliez, G., Ribot, C., Chalvon, V., Michel, C., Jauneau, A., Rivas, S., Alaux, L., Kanzaki, H., Okuyama, Y., Morel, J.B., Fournier, E., Tharreau, D., Terauchi, R., and Kroj, T. (2013). The rice resistance protein pair RGA4/RGA5 recognizes the Magnaporthe oryzae effectors AVR-Pia and AVR1-CO39 by direct binding. *Plant Cell* **25,** 1463-1481.

Chen, Z.J., and Sun, L.J. (2009). Nonproteolytic functions of ubiquitin in cell signaling. *Mol Cell* **33,** 275-286.

Cheng, Y.T., and Li, X. (2012). Ubiquitination in NB-LRR-mediated immunity. *Curr Opin Plant Biol* **15,** 392-399.

Cheng, Y.T., Li, Y., Huang, S., Huang, Y., Dong, X., Zhang, Y., and Li, X. (2011). Stability of plant immune-receptor resistance proteins is controlled by SKP1-CULLIN1-F-box (SCF)-mediated protein degradation. *Proc Natl Acad Sci U S A* **108,** 14694-14699.

Cheng, Y.T., Germain, H., Wiermer, M., Bi, D., Xu, F., Garcia, A.V., Wirthmueller, L., Despres, C., Parker, J.E., Zhang, Y., and Li, X. (2009). Nuclear pore complex component MOS7/Nup88 is required for

innate immunity and nuclear accumulation of defense regulators in Arabidopsis. *Plant Cell* **21,** 2503-2516.

Chinchilla, D., Zipfel, C., Robatzek, S., Kemmerling, B., Nurnberger, T., Jones, J.D., Felix, G., and Boller, T. (2007). A flagellin-induced complex of the receptor FLS2 and BAK1 initiates plant defence. *Nature* **448,** 497-500.

Chini, A., Fonseca, S., Fernandez, G., Adie, B., Chico, J.M., Lorenzo, O., Garcia-Casado, G., Lopez-Vidriero, I., Lozano, F.M., Ponce, M.R., Micol, J.L., and Solano, R. (2007). The JAZ family of repressors is the missing link in jasmonate signalling. *Nature* **448,** 666-671.

Chisholm, S.T., Coaker, G., Day, B., and Staskawicz, B.J. (2006). Host-microbe interactions: shaping the evolution of the plant immune response. *Cell* **124,** 803-814.

Chung, E.H., da Cunha, L., Wu, A.J., Gao, Z., Cherkis, K., Afzal, A.J., Mackey, D., and Dangl, J.L. (2011). Specific threonine phosphorylation of a host target by two unrelated type III effectors activates a host innate immune receptor in plants. *Cell Host Microbe* **9,** 125-136.

Clarke, J.D., Volko, S.M., Ledford, H., Ausubel, F.M., and Dong, X. (2000). Roles of salicylic acid, jasmonic acid, and ethylene in cpr-induced resistance in arabidopsis. *Plant Cell* **12,** 2175-2190.

Clough, S.J., and Bent, A.F. (1998). Floral dip: a simplified method for Agrobacterium-mediated transformation of Arabidopsis thaliana. *Plant J* **16,** 735-743.

Collier, S.M., Hamel, L.P., and Moffett, P. (2011). Cell death mediated by the N-terminal domains of a unique and highly conserved class of NB-LRR protein. *Mol Plant Microbe Interact* **24,** 918-931.

Cui, H., Tsuda, K., and Parker, J.E. (2015). Effector-triggered immunity: from pathogen perception to robust defense. *Annu Rev Plant Biol* **66,** 487-511.

Cunnac, S., Lindeberg, M., and Collmer, A. (2009). Pseudomonas syringae type III secretion system effectors: repertoires in search of functions. *Curr Opin Microbiol* **12,** 53-60.

Dangl, J.L., and Jones, J.D. (2001). Plant pathogens and integrated defence responses to infection. *Nature* **411,** 826-833.

Dangl, J.L., Horvath, D.M., and Staskawicz, B.J. (2013). Pivoting the plant immune system from dissection to deployment. *Science* **341,** 746-751.

Deshaies, R.J., and Joazeiro, C.A. (2009). RING domain E3 ubiquitin ligases. *Annu Rev Biochem* **78,** 399-434.

Dietrich, R.A., Richberg, M.H., Schmidt, R., Dean, C., and Dangl, J.L. (1997). A novel zinc finger protein is encoded by the Arabidopsis LSD1 gene and functions as a negative regulator of plant cell death. *Cell* **88,** 685-694.

Dill, A., Thomas, S.G., Hu, J., Steber, C.M., and Sun, T.P. (2004). The Arabidopsis F-box protein SLEEPY1 targets gibberellin signaling repressors for gibberellin-induced degradation. *Plant Cell* **16,** 1392-1405.

Ding, S., Zhang, B., and Qin, F. (2015). Arabidopsis RZFP34/CHYR1, a Ubiquitin E3 Ligase, Regulates Stomatal Movement and Drought Tolerance via SnRK2.6-Mediated Phosphorylation. *Plant Cell* **27,** 3228-3244.

Diss, G., Ascencio, D., DeLuna, A., and Landry, C.R. (2014). Molecular mechanisms of paralogous compensation and the robustness of cellular networks. *J Exp Zool B Mol Dev Evol* **322,** 488-499.

Dodds, P.N., and Rathjen, J.P. (2010). Plant immunity: towards an integrated view of plant-pathogen interactions. *Nat Rev Genet* **11,** 539-548.

Dong, C.H., Agarwal, M., Zhang, Y., Xie, Q., and Zhu, J.K. (2006). The negative regulator of plant cold responses, HOS1, is a RING E3 ligase that mediates the ubiquitination and degradation of ICE1. *Proc Natl Acad Sci U S A* **103,** 8281-8286.

Edgar, R.C. (2004a). MUSCLE: multiple sequence alignment with high accuracy and high throughput. *Nucleic Acids Res* **32,** 1792-1797.

Edgar, R.C. (2004b). MUSCLE: a multiple sequence alignment method with reduced time and space complexity. *BMC Bioinformatics* **5,** 113.

Eitas, T.K., Nimchuk, Z.L., and Dangl, J.L. (2008). Arabidopsis TAO1 is a TIR-NB-LRR protein that contributes to disease resistance induced by the Pseudomonas syringae effector AvrB. *Proc Natl Acad Sci U S A* **105,** 6475-6480.

Flor, H. (1971). Current Status of the Gene-For-Gene Concept. *Annu Rev Phytopathol* **9,** 275-296.

Frost, D., Way, H., Howles, P., Luck, J., Manners, J., Hardham, A., Finnegan, J., and Ellis, J. (2004). Tobacco transgenic for the flax rust resistance gene L expresses allele-specific activation of defense responses. *Mol Plant Microbe Interact* **17,** 224-232.

Furlan, G., Klinkenberg, J., and Trujillo, M. (2012). Regulation of plant immune receptors by ubiquitination. *Front Plant Sci* **3,** 238.

Gagne, J.M., Smalle, J., Gingerich, D.J., Walker, J.M., Yoo, S.D., Yanagisawa, S., and Vierstra, R.D. (2004). Arabidopsis EIN3-binding F-box 1 and 2 form ubiquitin-protein ligases that repress ethylene action and promote growth by directing EIN3 degradation. *Proc Natl Acad Sci U S A* **101,** 6803-6808.

Galan, J.M., and Peter, M. (1999). Ubiquitin-dependent degradation of multiple F-box proteins by an autocatalytic mechanism. *Proc Natl Acad Sci U S A* **96,** 9124-9129.

Germain, H., Qu, N., Cheng, Y.T., Lee, E., Huang, Y., Dong, O.X., Gannon, P., Huang, S., Ding, P., Li, Y., Sack, F., Zhang, Y., and Li, X. (2010). MOS11: a new component in the mRNA export pathway. *PLoS Genet* **6,** e1001250.

Gimenez-Ibanez, S., Hann, D.R., Ntoukakis, V., Petutschnig, E., Lipka, V., and Rathjen, J.P. (2009). AvrPtoB targets the LysM receptor kinase CERK1 to promote bacterial virulence on plants. *Curr Biol* **19,** 423-429.

Glazebrook, J., and Ausubel, F.M. (1994). Isolation of phytoalexin-deficient mutants of Arabidopsis thaliana and characterization of their interactions with bacterial pathogens. *Proc Natl Acad Sci U S A* **91,** 8955-8959.

Glazebrook, J., Rogers, E.E., and Ausubel, F.M. (1996). Isolation of Arabidopsis mutants with enhanced disease susceptibility by direct screening. *Genetics* **143,** 973-982.

Glazebrook, J., Zook, M., Mert, F., Kagan, I., Rogers, E.E., Crute, I.R., Holub, E.B., Hammerschmidt, R., and Ausubel, F.M. (1997). Phytoalexin-deficient mutants of Arabidopsis reveal that PAD4 encodes a regulatory factor and that four PAD genes contribute to downy mildew resistance. *Genetics* **146,** 381-392.

Gohre, V., Spallek, T., Haweker, H., Mersmann, S., Mentzel, T., Boller, T., de Torres, M., Mansfield, J.W., and Robatzek, S. (2008). Plant pattern-recognition receptor FLS2 is directed for degradation by the bacterial ubiquitin ligase AvrPtoB. *Curr Biol* **18,** 1824-1832.

Gomez-Gomez, L., and Boller, T. (2000). FLS2: an LRR receptor-like kinase involved in the perception of the bacterial elicitor flagellin in Arabidopsis. *Mol Cell* **5,** 1003-1011.

Goodstein, D.M., Shu, S., Howson, R., Neupane, R., Hayes, R.D., Fazo, J., Mitros, T., Dirks, W., Hellsten, U., Putnam, N., and Rokhsar, D.S. (2012). Phytozome: a comparative platform for green plant genomics. *Nucleic Acids Res* **40,** D1178-1186.

Goritschnig, S., Zhang, Y., and Li, X. (2007). The ubiquitin pathway is required for innate immunity in Arabidopsis. *Plant J* **49,** 540-551.

Goritschnig, S., Weihmann, T., Zhang, Y., Fobert, P., McCourt, P., and Li, X. (2008). A novel role for protein farnesylation in plant innate immunity. *Plant Physiol* **148,** 348-357.

Gou, M., Shi, Z., Zhu, Y., Bao, Z., Wang, G., and Hua, J. (2012). The F-box protein CPR1/CPR30 negatively regulates R protein SNC1 accumulation. *Plant J* **69,** 411-420.

Grant, J.J., Chini, A., Basu, D., and Loake, G.J. (2003). Targeted activation tagging of the Arabidopsis NBS-LRR gene, ADR1, conveys resistance to virulent pathogens. *Mol Plant Microbe Interact* **16,** 669-680.

Gray, W.M., Kepinski, S., Rouse, D., Leyser, O., and Estelle, M. (2001). Auxin regulates SCF(TIR1)-dependent degradation of AUX/IAA proteins. *Nature* **414,** 271-276.

Gray, W.M., del Pozo, J.C., Walker, L., Hobbie, L., Risseeuw, E., Banks, T., Crosby, W.L., Yang, M., Ma, H., and Estelle, M. (1999). Identification of an SCF ubiquitin-ligase complex required for auxin response in Arabidopsis thaliana. *Genes Dev* **13,** 1678-1691.

Griebel, T., Maekawa, T., and Parker, J.E. (2014). NOD-like receptor cooperativity in effector-triggered immunity. *Trends Immunol* **35,** 562-570.

Haglund, K., and Dikic, I. (2005). Ubiquitylation and cell signaling. *EMBO J* **24,** 3353-3359.

Handford, C.E., Elliott, C.T., and Campbell, K. (2015). A review of the global pesticide legislation and the scale of challenge in reaching the global harmonization of food safety standards. *Integr Environ Assess Manag* **11,** 525-536.

Heidrich, K., Wirthmueller, L., Tasset, C., Pouzet, C., Deslandes, L., and Parker, J.E. (2011). Arabidopsis EDS1 connects pathogen effector recognition to cell compartment-specific immune responses. *Science* **334,** 1401-1404.

Hershko, A., and Ciechanover, A. (1998). The ubiquitin system. *Annu Rev Biochem* **67,** 425-479.

Hicke, L. (2001). Protein regulation by monoubiquitin. *Nat Rev Mol Cell Biol* **2,** 195-201.

Hua, J., Grisafi, P., Cheng, S.H., and Fink, G.R. (2001). Plant growth homeostasis is controlled by the Arabidopsis BON1 and BAP1 genes. *Genes Dev* **15,** 2263-2272.

Hua, Z., and Vierstra, R.D. (2011). The cullin-RING ubiquitin-protein ligases. *Annu Rev Plant Biol* **62,** 299-334.

Huang, S., Monaghan, J., Zhong, X., Lin, L., Sun, T., Dong, O.X., and Li, X. (2014a). HSP90s are required for NLR immune receptor accumulation in Arabidopsis. *Plant J* **79,** 427-439.

Huang, S., Chen, X., Zhong, X., Li, M., Ao, K., Huang, J., and Li, X. (2016). Plant TRAF Proteins Regulate NLR Immune Receptor Turnover. *Cell Host Microbe* **19,** 204-215.

Huang, X., Li, J., Bao, F., Zhang, X., and Yang, S. (2010). A gain-of-function mutation in the Arabidopsis disease resistance gene RPP4 confers sensitivity to low temperature. *Plant Physiol* **154,** 796-809.

Huang, Y., Minaker, S., Roth, C., Huang, S., Hieter, P., Lipka, V., Wiermer, M., and Li, X. (2014b). An E4 ligase facilitates polyubiquitination of plant immune receptor resistance proteins in Arabidopsis. *Plant Cell* **26,** 485-496.

Huang, Y., Chen, X., Liu, Y., Roth, C., Copeland, C., McFarlane, H.E., Huang, S., Lipka, V., Wiermer, M., and Li, X. (2013). Mitochondrial AtPAM16 is required for plant survival and the negative regulation of plant immunity. *Nat Commun* **4,** 2558.

Igari, K., Endo, S., Hibara, K., Aida, M., Sakakibara, H., Kawasaki, T., and Tasaka, M. (2008). Constitutive activation of a CC-NB-LRR protein alters morphogenesis through the cytokinin pathway in Arabidopsis. *Plant J* **55,** 14-27.

Jabs, T., Dietrich, R.A., and Dangl, J.L. (1996). Initiation of runaway cell death in an Arabidopsis mutant by extracellular superoxide. *Science* **273,** 1853-1856.

Jacobs, A.K., Lipka, V., Burton, R.A., Panstruga, R., Strizhov, N., Schulze-Lefert, P., and Fincher, G.B. (2003). An Arabidopsis Callose Synthase, GSL5, Is Required for Wound and Papillary Callose Formation. *Plant Cell* **15,** 2503-2513.

Jander, G., Norris, S.R., Rounsley, S.D., Bush, D.F., Levin, I.M., and Last, R.L. (2002). Arabidopsis map-based cloning in the post-genome era. *Plant Physiol* **129,** 440-450.

Jia, Y., McAdams, S.A., Bryan, G.T., Hershey, H.P., and Valent, B. (2000). Direct interaction of resistance gene and avirulence gene products confers rice blast resistance. *EMBO J* **19,** 4004-4014.

Johnson, K.C., Dong, O.X., Huang, Y., and Li, X. (2012). A rolling stone gathers no moss, but resistant plants must gather their moses. *Cold Spring Harb Symp Quant Biol* **77,** 259-268.

Johnson, K.C., Xia, S., Feng, X., and Li, X. (2015). The Chromatin Remodeler SPLAYED Negatively Regulates SNC1-Mediated Immunity. *Plant Cell Physiol* **56,** 1616-1623.

Johnson, K.C., Yu, Y., Gao, L., Eng, R.C., Wasteneys, G.O., Chen, X., and Li, X. (2016). A partial loss-of-function mutation in an Arabidopsis RNA polymerase III subunit leads to pleiotropic defects. *J Exp Bot*.

Jones, J.D., and Dangl, J.L. (2006). The plant immune system. *Nature* **444,** 323-329.

Kaku, H., Nishizawa, Y., Ishii-Minami, N., Akimoto-Tomiyama, C., Dohmae, N., Takio, K., Minami, E., and Shibuya, N. (2006). Plant cells recognize chitin fragments for defense signaling through a plasma membrane receptor. *Proc Natl Acad Sci U S A* **103,** 11086-11091.

Kamoun, S. (2007). Groovy times: filamentous pathogen effectors revealed. *Curr Opin Plant Biol* **10,** 358-365.

Kong, L., Cheng, J., Zhu, Y., Ding, Y., Meng, J., Chen, Z., Xie, Q., Guo, Y., Li, J., Yang, S., and Gong, Z. (2015). Degradation of the ABA co-receptor ABI1 by PUB12/13 U-box E3 ligases. *Nat Commun* **6,** 8630.

Kosugi, S., Hasebe, M., Tomita, M., and Yanagawa, H. (2009). Systematic identification of cell cycle-dependent yeast nucleocytoplasmic shuttling proteins by prediction of composite motifs. *Proc Natl Acad Sci U S A* **106,** 10171-10176.

Kraft, E., Stone, S.L., Ma, L., Su, N., Gao, Y., Lau, O.S., Deng, X.W., and Callis, J. (2005). Genome analysis and functional characterization of the E2 and RING-type E3 ligase ubiquitination enzymes of Arabidopsis. *Plant Physiol* **139,** 1597-1611.

Kravtsova-Ivantsiv, Y., and Ciechanover, A. (2012). Non-canonical ubiquitin-based signals for proteasomal degradation. *J Cell Sci* **125,** 539-548.

Kravtsova-Ivantsiv, Y., Sommer, T., and Ciechanover, A. (2013). The lysine48-based polyubiquitin chain proteasomal signal: not a single child anymore. *Angew Chem Int Ed Engl* **52,** 192-198.

Kulathu, Y., and Komander, D. (2012). Atypical ubiquitylation - the unexplored world of polyubiquitin beyond Lys48 and Lys63 linkages. *Nat Rev Mol Cell Biol* **13,** 508-523.

Kwon, C., Neu, C., Pajonk, S., Yun, H.S., Lipka, U., Humphry, M., Bau, S., Straus, M., Kwaaitaal, M., Rampelt, H., El Kasmi, F., Jurgens, G., Parker, J., Panstruga, R., Lipka, V., and Schulze-Lefert, P. (2008). Co-option of a default secretory pathway for plant immune responses. *Nature* **451,** 835-840.

Lee, D.H., Choi, H.W., and Hwang, B.K. (2011). The pepper E3 ubiquitin ligase RING1 gene, CaRING1, is required for cell death and the salicylic acid-dependent defense response. *Plant Physiol* **156,** 2011-2025.

Lee, J., Nam, J., Park, H.C., Na, G., Miura, K., Jin, J.B., Yoo, C.Y., Baek, D., Kim, D.H., Jeong, J.C., Kim, D., Lee, S.Y., Salt, D.E., Mengiste, T., Gong, Q., Ma, S., Bohnert, H.J., Kwak, S.S., Bressan, R.A., Hasegawa, P.M., and Yun, D.J. (2007). Salicylic acid-mediated innate immunity in Arabidopsis is regulated by SIZ1 SUMO E3 ligase. *Plant J* **49,** 79-90.

Leitner, J., Petrasek, J., Tomanov, K., Retzer, K., Parezova, M., Korbei, B., Bachmair, A., Zazimalova, E., and Luschnig, C. (2012). Lysine63-linked ubiquitylation of PIN2 auxin carrier protein governs hormonally controlled adaptation of Arabidopsis root growth. *Proc Natl Acad Sci U S A* **109,** 8322-8327.

Li, W., Bengtson, M.H., Ulbrich, A., Matsuda, A., Reddy, V.A., Orth, A., Chanda, S.K., Batalov, S., and Joazeiro, C.A. (2008). Genome-wide and functional annotation of human E3 ubiquitin ligases identifies MULAN, a mitochondrial E3 that regulates the organelle's dynamics and signaling. *PLoS One* **3,** e1487.

Li, X., Kapos, P., and Zhang, Y. (2015). NLRs in plants. *Curr Opin Immunol* **32,** 114-121.

Li, X., Clarke, J.D., Zhang, Y., and Dong, X. (2001). Activation of an EDS1-mediated R-gene pathway in the snc1 mutant leads to constitutive, NPR1-independent pathogen resistance. *Mol Plant Microbe Interact* **14,** 1131-1139.

Li, X., Zhang, Y., Clarke, J.D., Li, Y., and Dong, X. (1999). Identification and cloning of a negative regulator of systemic acquired resistance, SNI1, through a screen for suppressors of npr1-1. *Cell* **98,** 329-339.

Li, Y., Tessaro, M.J., Li, X., and Zhang, Y. (2010a). Regulation of the expression of plant resistance gene SNC1 by a protein with a conserved BAT2 domain. *Plant Physiol* **153,** 1425-1434.

Li, Y., Li, S., Bi, D., Cheng, Y.T., Li, X., and Zhang, Y. (2010b). SRFR1 negatively regulates plant NB-LRR resistance protein accumulation to prevent autoimmunity. *PLoS Pathog* **6,** e1001111.

Lin, S.S., Martin, R., Mongrand, S., Vandenabeele, S., Chen, K.C., Jang, I.C., and Chua, N.H. (2008). RING1 E3 ligase localizes to plasma membrane lipid rafts to trigger FB1-induced programmed cell death in Arabidopsis. *Plant J* **56,** 550-561.

Lozano-Duran, R., Bourdais, G., He, S.Y., and Robatzek, S. (2014). The bacterial effector HopM1 suppresses PAMP-triggered oxidative burst and stomatal immunity. *New Phytol* **202,** 259-269.

Lu, D., Lin, W., Gao, X., Wu, S., Cheng, C., Avila, J., Heese, A., Devarenne, T.P., He, P., and Shan, L. (2011). Direct ubiquitination of pattern recognition receptor FLS2 attenuates plant innate immunity. *Science* **332,** 1439-1442.

Lu, Y., Song, S., Wang, R., Liu, Z., Meng, J., Sweetman, A.J., Jenkins, A., Ferrier, R.C., Li, H., Luo, W., and Wang, T. (2015). Impacts of soil and water pollution on food safety and health risks in China. *Environ Int* **77,** 5-15.

Macho, A.P., and Zipfel, C. (2014). Plant PRRs and the activation of innate immune signaling. *Mol Cell* **54,** 263-272.

Mackey, D., Holt, B.F., 3rd, Wiig, A., and Dangl, J.L. (2002). RIN4 interacts with Pseudomonas syringae type III effector molecules and is required for RPM1-mediated resistance in Arabidopsis. *Cell* **108,** 743-754.

Maekawa, T., Kufer, T.A., and Schulze-Lefert, P. (2011a). NLR functions in plant and animal immune systems: so far and yet so close. *Nat Immunol* **12,** 817-826.

Maekawa, T., Cheng, W., Spiridon, L.N., Toller, A., Lukasik, E., Saijo, Y., Liu, P., Shen, Q.H., Micluta, M.A., Somssich, I.E., Takken, F.L., Petrescu, A.J., Chai, J., and Schulze-Lefert, P. (2011b). Coiled-coil domain-dependent homodimerization of intracellular barley immune receptors defines a minimal functional module for triggering cell death. *Cell Host Microbe* **9,** 187-199.

Mendgen, K., and Hahn, M. (2002). Plant infection and the establishment of fungal biotrophy. *Trends Plant Sci* **7,** 352-356.

Meyers, B.C., Kozik, A., Griego, A., Kuang, H., and Michelmore, R.W. (2003). Genome-wide analysis of NBS-LRR-encoding genes in Arabidopsis. *Plant Cell* **15,** 809-834.

Minkoff, R., Bales, E.S., Kerr, C.A., and Struss, W.E. (1999). Antisense oligonucleotide blockade of connexin expression during embryonic bone formation: evidence of functional compensation within a multigene family. *Dev Genet* **24,** 43-56.

Monaghan, J., and Zipfel, C. (2012). Plant pattern recognition receptor complexes at the plasma membrane. *Curr Opin Plant Biol* **15,** 349-357.

Mulligan, G.J., Wong, J., and Jacks, T. (1998). p130 is dispensable in peripheral T lymphocytes: evidence for functional compensation by p107 and pRB. *Mol Cell Biol* **18,** 206-220.

Narusaka, M., Shirasu, K., Noutoshi, Y., Kubo, Y., Shiraishi, T., Iwabuchi, M., and Narusaka, Y. (2009). RRS1 and RPS4 provide a dual Resistance-gene system against fungal and bacterial pathogens. *Plant J* **60,** 218-226.

Nawrath, C., and Metraux, J.P. (1999). Salicylic acid induction-deficient mutants of Arabidopsis express PR-2 and PR-5 and accumulate high levels of camalexin after pathogen inoculation. *Plant Cell* **11,** 1393-1404.

Neutzner, M., and Neutzner, A. (2012). Enzymes of ubiquitination and deubiquitination. *Essays Biochem* **52,** 37-50.

Nicaise, V., Roux, M., and Zipfel, C. (2009). Recent advances in PAMP-triggered immunity against bacteria: pattern recognition receptors watch over and raise the alarm. *Plant Physiol* **150,** 1638-1647.

Padmanabhan, M.S., and Dinesh-Kumar, S.P. (2014). The conformational and subcellular compartmental dance of plant NLRs during viral recognition and defense signaling. *Curr Opin Microbiol* **20,** 55-61.

Palma, K., Zhang, Y., and Li, X. (2005). An importin alpha homolog, MOS6, plays an important role in plant innate immunity. *Curr Biol* **15,** 1129-1135.

Palma, K., Zhao, Q., Cheng, Y.T., Bi, D., Monaghan, J., Cheng, W., Zhang, Y., and Li, X. (2007). Regulation of plant innate immunity by three proteins in a complex conserved across the plant and animal kingdoms. *Genes Dev* **21,** 1484-1493.

Pandey, S.P., and Somssich, I.E. (2009). The role of WRKY transcription factors in plant immunity. *Plant Physiol* **150,** 1648-1655.

Park, B.S., Eo, H.J., Jang, I.C., Kang, H.G., Song, J.T., and Seo, H.S. (2010). Ubiquitination of LHY by SINAT5 regulates flowering time and is inhibited by DET1. *Biochem Biophys Res Commun* **398,** 242-246.

Peart, J.R., Mestre, P., Lu, R., Malcuit, I., and Baulcombe, D.C. (2005). NRG1, a CC-NB-LRR protein, together with N, a TIR-NB-LRR protein, mediates resistance against tobacco mosaic virus. *Curr Biol* **15,** 968-973.

Peng, Y.J., Shih, C.F., Yang, J.Y., Tan, C.M., Hsu, W.H., Huang, Y.P., Liao, P.C., and Yang, C.H. (2013). A RING-type E3 ligase controls anther dehiscence by activating the jasmonate biosynthetic pathway gene DEFECTIVE IN ANTHER DEHISCENCE1 in Arabidopsis. *Plant J* **74,** 310-327.

Pham, A.D., and Sauer, F. (2000). Ubiquitin-activating/conjugating activity of TAFII250, a mediator of activation of gene expression in Drosophila. *Science* **289,** 2357-2360.

Pickart, C.M. (2001). Mechanisms underlying ubiquitination. *Annu Rev Biochem* **70,** 503-533.

Proost, S., Van Bel, M., Vaneechoutte, D., Van de Peer, Y., Inze, D., Mueller-Roeber, B., and Vandepoele, K. (2015). PLAZA 3.0: an access point for plant comparative genomics. *Nucleic Acids Res* **43,** D974-981.

Qi, S., Lin, Q., Zhu, H., Gao, F., Zhang, W., and Hua, X. (2016). The RING Finger E3 Ligase SpRing is a Positive Regulator of Salt Stress Signaling in Salt-Tolerant Wild Tomato Species. *Plant Cell Physiol*.

Rairdan, G.J., and Moffett, P. (2006). Distinct domains in the ARC region of the potato resistance protein Rx mediate LRR binding and inhibition of activation. *Plant Cell* **18,** 2082-2093.

Rairdan, G.J., Collier, S.M., Sacco, M.A., Baldwin, T.T., Boettrich, T., and Moffett, P. (2008). The coiled-coil and nucleotide binding domains of the Potato Rx disease resistance protein function in pathogen recognition and signaling. *Plant Cell* **20,** 739-751.

Riederer, B.M., Leuba, G., Vernay, A., and Riederer, I.M. (2011). The role of the ubiquitin proteasome system in Alzheimer's disease. *Exp Biol Med (Maywood)* **236,** 268-276.

Roberts, M., Tang, S., Stallmann, A., Dangl, J.L., and Bonardi, V. (2013). Genetic requirements for signaling from an autoactive plant NB-LRR intracellular innate immune receptor. *PLoS Genet* **9,** e1003465.

Robzyk, K., Recht, J., and Osley, M.A. (2000). Rad6-dependent ubiquitination of histone H2B in yeast. *Science* **287,** 501-504.

Rotin, D., and Kumar, S. (2009). Physiological functions of the HECT family of ubiquitin ligases. *Nat Rev Mol Cell Biol* **10,** 398-409.

Sadanandom, A., Bailey, M., Ewan, R., Lee, J., and Nelis, S. (2012). The ubiquitin-proteasome system: central modifier of plant signalling. *New Phytol* **196,** 13-28.

Schmid, M., Davison, T.S., Henz, S.R., Pape, U.J., Demar, M., Vingron, M., Scholkopf, B., Weigel, D., and Lohmann, J.U. (2005). A gene expression map of Arabidopsis thaliana development. *Nat Genet* **37,** 501-506.

Serrano, M., Coluccia, F., Torres, M., L'Haridon, F., and Metraux, J.P. (2014). The cuticle and plant defense to pathogens. *Front Plant Sci* **5,** 274.

Shao, F., Golstein, C., Ade, J., Stoutemyer, M., Dixon, J.E., and Innes, R.W. (2003). Cleavage of Arabidopsis PBS1 by a bacterial type III effector. *Science* **301,** 1230-1233.

Shimizu, T., Nakano, T., Takamizawa, D., Desaki, Y., Ishii-Minami, N., Nishizawa, Y., Minami, E., Okada, K., Yamane, H., Kaku, H., and Shibuya, N. (2010). Two LysM receptor molecules, CEBiP and OsCERK1, cooperatively regulate chitin elicitor signaling in rice. *Plant J* **64,** 204-214.

Shirasu, K. (2009). The HSP90-SGT1 chaperone complex for NLR immune sensors. *Annu Rev Plant Biol* **60,** 139-164.

Smalle, J., and Vierstra, R.D. (2004). The ubiquitin 26S proteasome proteolytic pathway. *Annu Rev Plant Biol* **55,** 555-590.

Somers, D.E., and Fujiwara, S. (2009). Thinking outside the F-box: novel ligands for novel receptors. *Trends Plant Sci* **14,** 206-213.

Stamatakis, A. (2014). RAxML version 8: a tool for phylogenetic analysis and post-analysis of large phylogenies. *Bioinformatics* **30,** 1312-1313.

Stegmann, M., Anderson, R.G., Ichimura, K., Pecenkova, T., Reuter, P., Zarsky, V., McDowell, J.M., Shirasu, K., and Trujillo, M. (2012). The ubiquitin ligase PUB22 targets a subunit of the exocyst complex required for PAMP-triggered responses in Arabidopsis. *Plant Cell* **24,** 4703-4716.

Stokes, T.L., Kunkel, B.N., and Richards, E.J. (2002). Epigenetic variation in Arabidopsis disease resistance. *Genes Dev* **16,** 171-182.

Sun, T., Zhang, Y., Li, Y., Zhang, Q., Ding, Y., and Zhang, Y. (2015). ChIP-seq reveals broad roles of SARD1 and CBP60g in regulating plant immunity. *Nat Commun* **6,** 10159.

Tang, X., Xie, M., Kim, Y.J., Zhou, J., Klessig, D.F., and Martin, G.B. (1999). Overexpression of Pto activates defense responses and confers broad resistance. *Plant Cell* **11,** 15-29.

Tao, Y., Yuan, F., Leister, R.T., Ausubel, F.M., and Katagiri, F. (2000). Mutational analysis of the Arabidopsis nucleotide binding site-leucine-rich repeat resistance gene RPS2. *Plant Cell* **12,** 2541-2554.

Tena, G., Asai, T., Chiu, W.L., and Sheen, J. (2001). Plant mitogen-activated protein kinase signaling cascades. *Curr Opin Plant Biol* **4,** 392-400.

Thines, B., Katsir, L., Melotto, M., Niu, Y., Mandaokar, A., Liu, G., Nomura, K., He, S.Y., Howe, G.A., and Browse, J. (2007). JAZ repressor proteins are targets of the SCF(COI1) complex during jasmonate signalling. *Nature* **448,** 661-665.

Tian, M., and Xie, Q. (2013). Non-26S proteasome proteolytic role of ubiquitin in plant endocytosis and endosomal trafficking(F). *J Integr Plant Biol* **55,** 54-63.

Tieman, D.M., Taylor, M.G., Ciardi, J.A., and Klee, H.J. (2000). The tomato ethylene receptors NR and LeETR4 are negative regulators of ethylene response and exhibit functional compensation within a multigene family. *Proc Natl Acad Sci U S A* **97,** 5663-5668.

Trujillo, M., and Shirasu, K. (2010). Ubiquitination in plant immunity. *Curr Opin Plant Biol* **13,** 402-408.

Trujillo, M., Ichimura, K., Casais, C., and Shirasu, K. (2008). Negative regulation of PAMP-triggered immunity by an E3 ubiquitin ligase triplet in Arabidopsis. *Curr Biol* **18,** 1396-1401.

Underwood, W. (2012). The plant cell wall: a dynamic barrier against pathogen invasion. *Front Plant Sci* **3,** 85.

van den Burg, H.A., Harrison, S.J., Joosten, M.H., Vervoort, J., and de Wit, P.J. (2006). Cladosporium fulvum Avr4 protects fungal cell walls against hydrolysis by plant chitinases accumulating during infection. *Mol Plant Microbe Interact* **19,** 1420-1430.

Vierstra, R.D. (2009). The ubiquitin-26S proteasome system at the nexus of plant biology. *Nat Rev Mol Cell Biol* **10,** 385-397.

Walsh, C.K., and Sadanandom, A. (2014). Ubiquitin chain topology in plant cell signaling: a new facet to an evergreen story. *Front Plant Sci* **5,** 122.

Wang, F., Zhu, D., Huang, X., Li, S., Gong, Y., Yao, Q., Fu, X., Fan, L.M., and Deng, X.W. (2009). Biochemical insights on degradation of Arabidopsis DELLA proteins gained from a cell-free assay system. *Plant Cell* **21,** 2378-2390.

Wang, Y., Zhang, Y., Wang, Z., Zhang, X., and Yang, S. (2013). A missense mutation in CHS1, a TIR-NB protein, induces chilling sensitivity in Arabidopsis. *Plant J* **75,** 553-565.

Williams, S.J., Sohn, K.H., Wan, L., Bernoux, M., Sarris, P.F., Segonzac, C., Ve, T., Ma, Y., Saucet, S.B., Ericsson, D.J., Casey, L.W., Lonhienne, T., Winzor, D.J., Zhang, X., Coerdt, A., Parker, J.E., Dodds, P.N., Kobe, B., and Jones, J.D. (2014). Structural basis for assembly and function of a heterodimeric plant immune receptor. *Science* **344,** 299-303.

Winter, D., Vinegar, B., Nahal, H., Ammar, R., Wilson, G.V., and Provart, N.J. (2007). An "Electronic Fluorescent Pictograph" browser for exploring and analyzing large-scale biological data sets. *PLoS One* **2,** e718.

Xia, S., Cheng, Y.T., Huang, S., Win, J., Soards, A., Jinn, T.L., Jones, J.D., Kamoun, S., Chen, S., Zhang, Y., and Li, X. (2013). Regulation of transcription of nucleotide-binding leucine-rich repeat-encoding genes SNC1 and RPP4 via H3K4 trimethylation. *Plant Physiol* **162,** 1694-1705.

Xie, Q., Guo, H.S., Dallman, G., Fang, S., Weissman, A.M., and Chua, N.H. (2002). SINAT5 promotes ubiquitin-related degradation of NAC1 to attenuate auxin signals. *Nature* **419,** 167-170.

Xin, X.F., and He, S.Y. (2013). Pseudomonas syringae pv. tomato DC3000: a model pathogen for probing disease susceptibility and hormone signaling in plants. *Annu Rev Phytopathol* **51,** 473-498.

Xu, F., Xu, S., Wiermer, M., Zhang, Y., and Li, X. (2012). The cyclin L homolog MOS12 and the MOS4-associated complex are required for the proper splicing of plant resistance genes. *Plant J* **70,** 916-928.

Xu, F., Cheng, Y.T., Kapos, P., Huang, Y., and Li, X. (2014a). P-loop-dependent NLR SNC1 can oligomerize and activate immunity in the nucleus. *Mol Plant* **7,** 1801-1804.

Xu, F., Kapos, P., Cheng, Y.T., Li, M., Zhang, Y., and Li, X. (2014b). NLR-associating transcription factor bHLH84 and its paralogs function redundantly in plant immunity. *PLoS Pathog* **10,** e1004312.

Xu, F., Zhu, C., Cevik, V., Johnson, K., Liu, Y., Sohn, K., Jones, J.D., Holub, E.B., and Li, X. (2015a). Autoimmunity conferred by chs3-2D relies on CSA1, its adjacent TNL-encoding neighbour. *Sci Rep* **5,** 8792.

Xu, F., Huang, Y., Li, L., Gannon, P., Linster, E., Huber, M., Kapos, P., Bienvenut, W., Polevoda, B., Meinnel, T., Hell, R., Giglione, C., Zhang, Y., Wirtz, M., Chen, S., and Li, X. (2015b). Two N-terminal acetyltransferases antagonistically regulate the stability of a nod-like receptor in Arabidopsis. *Plant Cell* **27,** 1547-1562.

Xu, S., Zhang, Z., Jing, B., Gannon, P., Ding, J., Xu, F., Li, X., and Zhang, Y. (2011). Transportin-SR is required for proper splicing of resistance genes and plant immunity. *PLoS Genet* **7,** e1002159.

Yamaguchi, K., Yamada, K., Ishikawa, K., Yoshimura, S., Hayashi, N., Uchihashi, K., Ishihama, N., Kishi-Kaboshi, M., Takahashi, A., Tsuge, S., Ochiai, H., Tada, Y., Shimamoto, K., Yoshioka, H., and Kawasaki, T. (2013). A receptor-like cytoplasmic kinase targeted by a plant pathogen effector is directly phosphorylated by the chitin receptor and mediates rice immunity. *Cell Host Microbe* **13,** 347-357.

Yang, C.W., Gonzalez-Lamothe, R., Ewan, R.A., Rowland, O., Yoshioka, H., Shenton, M., Ye, H., O'Donnell, E., Jones, J.D., and Sadanandom, A. (2006). The E3 ubiquitin ligase activity of arabidopsis PLANT U-BOX17 and its functional tobacco homolog ACRE276 are required for cell death and defense. *Plant Cell* **18,** 1084-1098.

Yang, H., Shi, Y., Liu, J., Guo, L., Zhang, X., and Yang, S. (2010). A mutant CHS3 protein with TIR-NB-LRR-LIM domains modulates growth, cell death and freezing tolerance in a temperature-dependent manner in Arabidopsis. *Plant J* **63,** 283-296.

Yang, Y., Zhang, Y., Ding, P., Johnson, K., Li, X., and Zhang, Y. (2012). The ankyrin-repeat transmembrane protein BDA1 functions downstream of the receptor-like protein SNC2 to regulate plant immunity. *Plant Physiol* **159,** 1857-1865.

Ye, Y., and Rape, M. (2009). Building ubiquitin chains: E2 enzymes at work. *Nat Rev Mol Cell Biol* **10,** 755-764.

Yi, H., and Richards, E.J. (2009). Gene duplication and hypermutation of the pathogen Resistance gene SNC1 in the Arabidopsis bal variant. *Genetics* **183,** 1227-1234.

Zhang, Y., and Li, X. (2005). A putative nucleoporin 96 Is required for both basal defense and constitutive resistance responses mediated by suppressor of npr1-1,constitutive 1. *Plant Cell* **17,** 1306-1316.

Zhang, Y., Glazebrook, J., and Li, X. (2007a). Identification of components in disease-resistance signaling in Arabidopsis by map-based cloning. *Methods Mol Biol* **354,** 69-78.

Zhang, Y., Goritschnig, S., Dong, X., and Li, X. (2003). A gain-of-function mutation in a plant disease resistance gene leads to constitutive activation of downstream signal transduction pathways in suppressor of npr1-1, constitutive 1. *Plant Cell* **15,** 2636-2646.

Zhang, Y., Cheng, Y.T., Bi, D., Palma, K., and Li, X. (2005). MOS2, a protein containing G-patch and KOW motifs, is essential for innate immunity in Arabidopsis thaliana. *Curr Biol* **15,** 1936-1942.

Zhang, Y., Yang, Y., Fang, B., Gannon, P., Ding, P., Li, X., and Zhang, Y. (2010). Arabidopsis snc2-1D activates receptor-like protein-mediated immunity transduced through WRKY70. *Plant Cell* **22,** 3153-3163.

Zhang, Y., Yang, C., Li, Y., Zheng, N., Chen, H., Zhao, Q., Gao, T., Guo, H., and Xie, Q. (2007b). SDIR1 is a RING finger E3 ligase that positively regulates stress-responsive abscisic acid signaling in Arabidopsis. *Plant Cell* **19,** 1912-1929.

Zhang, Z., Wu, Y., Gao, M., Zhang, J., Kong, Q., Liu, Y., Ba, H., Zhou, J., and Zhang, Y. (2012). Disruption of PAMP-induced MAP kinase cascade by a Pseudomonas syringae effector activates plant immunity mediated by the NB-LRR protein SUMM2. *Cell Host Microbe* **11,** 253-263.

Zhao, Q., Tian, M., Li, Q., Cui, F., Liu, L., Yin, B., and Xie, Q. (2013). A plant-specific in vitro ubiquitination analysis system. *Plant J* **74,** 524-533.

Zhu, Z., Xu, F., Zhang, Y., Cheng, Y.T., Wiermer, M., and Li, X. (2010). Arabidopsis resistance protein SNC1 activates immune responses through association with a transcriptional corepressor. *Proc Natl Acad Sci U S A* **107,** 13960-13965.